November 2020

Modeling Early Life: Ontogenetic Growth and Behavior Affect Population Connectivity in Gulf of Mexico Marine Fish

Kelly Vasbinder
University of South Florida

Scholar Commons Citation
Vasbinder, Kelly, "Modeling Early Life: Ontogenetic Growth and Behavior Affect Population Connectivity in Gulf of Mexico Marine Fish" (2020). *USF Tampa Graduate Theses and Dissertations.*
https://digitalcommons.usf.edu/etd/8598

Modeling Early Life: Ontogenetic Growth and Behavior Affect Population Connectivity in Gulf of Mexico Marine Fish

by

Kelly Vasbinder

A dissertation submitted in partial fulfillment
of the requirements for the degree of
Doctor of Philosophy in Marine Science
with a concentration in Marine Resource Assessment
College of Marine Science
University of South Florida

Major Professor: Cameron Ainsworth, Ph.D.
Kendra Daly, Ph.D.
Mandy Karnauskas, Ph.D.
Ernst Peebles, Ph.D.
Robert Weisberg, Ph.D.

Date of Approval:
November 12, 2020

Key Words: Early-life history, trade-offs, larval transport, larval migration, connectivity, fisheries management

This work is dedicated to my parents,

Leslie and Richard Vasbinder

and to my earliest mentors,

Angela Lodge, Teresa Greely, and Andrea Sanders

for inspiring my love of the ocean and a deep sense of wonder at the beauty of creation

Acknowledgments

I would like to thank my funding sources, including the Presidential Doctoral Fellowship from the University of South Florida and the William and Elsie Knight Endowed Fellowship from the University of South Florida College of Marine Science for funding me during my time here at USF.

I would like to extend many thanks to my advisor Cameron Ainsworth, from whom I have learned so many technical, research, and life skills, and who has been a steadfast source of mentorship and encouragement. I am so thankful to have worked with such a wonderful advisor. I would also like to thank my committee: Dr. Kendra Daly, Dr. Mandy Karnauskas, Dr. Ernst Peebles and Dr. Robert Weisberg for providing advice and support throughout this project. Thank you for all for helping me to become a better researcher.

I would also like to thank Fish Florida and the Association for the Sciences of Limnology and Oceanography for travel scholarships that allowed me to present portions of this dissertation at national and international conferences. Thank you to the Ocean Circulation Group at University of South Florida and the SEAMAP icthyoplankton survey for providing data for this dissertation. Specifically, thank you to Dr. Robert Weisberg, Dr. Yonggang Liu, and Glenn Zapfe for facilitating the sharing of this data and providing advice on its use in this dissertation.

I would like to thank all of my mentors, friends, and family for your encouragement and inspiration. Thank you to Dr. Angela Lodge and Dr. Teresa Greely, for inspiring me to pursue a

career in marine science at Oceanography Camp for Girls, and all of the wonderful OCG staff, students, and mentors I've had the chance to know along the way. Thank you to the everyone at the College of Marine Science for supporting me through this process, especially those students and staff in the Marine Resource Assessment Program and my labmates. Thank you to Dr. Gary Mitchum, Dr. Mya Breitbart, Dr. Jonathan Cohen, Dr. Darren Dunlap, Dr. Christopher Chambers, Dr. Will Ryan, and Dr. Kendra Daly for seeing the scientist in me as a high school and undergraduate student, and for your mentorship that led me to graduate school. Thank you to Alex I., Julie V., Natalie S., Makenna M., Jared K., Dana N., Ryan V., Imogen B., Jon S., Shaniqua G., Megan F., Natalia L., Theresa K., Becky S., Kara D., and Shahd A. for all of the amazing encouragement, conversations, and brainstorming times, and for making my time in graduate school memorable and fun. Finally, I would like to thank my family, all of whom have been tremendously supportive. I would like to especially thank my parents, Richard and Leslie Vasbinder, and my sister Kimberly Vasbinder, for always believing in me and being my anchors.

Table of Contents

List of Tables

List of Figures

Abstract

This dissertation is an examination of growth, behavior, and dispersal during the early life stages of marine fishes in the Gulf of Mexico. Understanding movements of early life stages is a key part of managing exploited fish populations. Position in the water column can impact larval dispersal, since it determines those currents to which larvae are exposed. First, I investigated the relationship between length and age in early life stages of marine fishes. I found that demersal fish taxa tend to be represented by exponential models, while pelagic fish tend to be represented by linear models. I suggest this may be indicative of risk-taking strategies associated with a consumption/predation risk trade-off. Using some of the age models from this study to estimate the ages of sampled larvae, generalized additive models (GAM) were built using a suite of environmental variables. The GAMs were then used to predict the ontogenetic vertical migration patterns for a range of age classes and taxa of major commercial and recreational fishes in the Gulf of Mexico. These ontogenetic vertical migration patterns are used in combination with circulation data from the West Florida Coastal Ocean Model (WFCOM) to predict larval trajectories in the Gulf of Mexico. These trajectories are then used to identify spawning and settlement habitats. This creates a source/sink matrix, which can help support realistic modeling of population connectivity within ecosystem models such as Atlantis. This project lies at the intersection of predictive statistical modeling, hydrodynamic modeling, and ecosystem modeling, and represents an interdisciplinary approach to understanding larval dynamics and the impacts that they have on ecosystems and fish production.

Chapter 1: Introduction

A substantial body of literature has demonstrated that the use of spatial information in fisheries management, particularly in regard to larval connectivity, has the potential to enhance fishery yields, profits, and sustainability (Costelloa et al. 2010). Self-connectivity and local retention, as well as remote connectivity (the ability of larvae to recruit to remote locations), can be used to influence Marine Protected Area (MPA) design, and can lower the overall fishing effort in an area and increase the abundance of fish (Watson et al. 2010, Costelloa et al. 2010). We now have in hand both the biophysical modeling capacity to accurately estimate larval movements between areas and the "end-to-end" ecosystem models that allow us to understand the biological and socioeconomic impacts of spatial management actions (Zheng and Weisberg 2012, Weisberg et al. 2014a, Ainsworth et al. 2015). This project seeks to combine these tools to study the importance of larval dispersal in the Gulf of Mexico.

"Solving the recruitment problem" has often been called the "Holy Grail" of fisheries science (Houde 2008). Two hypotheses dominated recruitment research for most of the 20th century (Houde 2008, Hjort 1914). Hjort's critical period hypothesis posits that year class strength is predicated on the ability of newly post-yolk sac larvae to find food, and the aberrant drift hypothesis posits that year-class strength varies based on the number of larvae swept into unfavorable habitat by current-driven dispersal, (Houde 2008, Hjort 1914). These seminal ideas led to additional, related hypotheses, including Cushing's match-mismatch hypothesis and Lasker's stable ocean hypothesis (Cushing 1978, Cushing 1990, Laser 1978, Lasker 1981). At present, it is understood that a myriad of factors contribute to recruitment variability, including temperature, maternal and larval health, predator-prey interactions, growth, the degree of density dependence, and the hydrodynamic environment (Houde 2008). Some of these factors can be experienced differently by different types of larvae, depending on behavior. Thus, the incorporation of larval behavior into models of processes occurring during early life has been identified as a critical research need for better understanding recruitment (Houde 2008).

One behavior that larvae exhibit which can impact dispersal is ontogenetic vertical migration. Ontogenetic vertical migration of reef larvae in the Caribbean has been shown to impact connectivity, where deep vertical migration patterns increased the exchange of larvae and shallow vertical migration patterns increased the numbers of recruits, leading larval behavior to have just as high of an impact on self-recruitment as eddies (Paris et al. 2007). Damselfish larvae on reefs off the coast of Barbados have been shown to use a downward vertical ontogenetic migration to take advantage of stratified currents in order to achieve retention on their natal reef (Paris and Cowen 2004). This vertical migration is important because larvae that change depth throughout their early life history will encounter different biophysical environments at different depths (Leis 2010). This dissertation seeks to define both the patterns and impact of ontogenetic depth migration during early life for a range of fisheries taxa in the Gulf of Mexico (GOM).

As our understanding of recruitment processes has changed with time, so have the tools that we use to study these processes. The recognition that both biological and physical factors impact recruitment is reflected in the shift in recruitment-related papers in the literature. A 2007 review of recruitment literature revealed that from 1989 to 2007, sixty-nine recruitment-related papers were published using coupled biophysical models, the majority of which contained a Lagrangian dispersal component (Miller et al. 2007). The coupled biophysical modeling of recruitment processes in these years was focused mainly on gadoid (cod or cod-like) species due to economic interest (Miller et al. 2007). In the decade since this review, biophysical modeling of the early life history of reef-associated marine fish taxa has ramped up in the GOM, an ecosystem that had previously been understudied (Karnauskas et al. 2013a, Karnauskas et al. 2013b, Weisberg et al. 2014, Vaz et al. 2016).

We are now in a position where our computational abilities allow us to consider dispersal and recruitment within a whole ecosystem framework of biogeophysical interactions and spatially resolved habitats. Ecosystem Based Fishery Management (EBFM) is a directive that shifts the focus from management of a single fishery to a whole -ecosystem approach (Pikitch et al. 2004). EBFM, and its broader relatives Ecosystem Based Management (EBM) and Ecosystem Approach to Management (EAM) are not just proposed ideas, but are governmentally mandated and integrated into the principles of U.S. resource policy (Levin et al. 2009, USGA 1994, NOAA 2006). As Link (2002) points out in his essay on the topic, EBFM is not an attempt to manage an entire ecosystem, but rather to manage fisheries in an ecosystem context, moving the goal from something next to impossible under our current management structure to something that can be attained with defined goals, indicators, sampling surveys, models, terminology, and management plans (Link 2002). While EBFM can be difficult due to the vast amounts of data needed for implementation, there has been a recent shift from using a reductionist approach to using an approach of synthesis and integration, in which biological, physical and socio-economic information are united into decision making frameworks (Levin et al. 2009). Ecosystem models have the potential to play an important role in this framework as they integrate large swaths of information into a tool usable for hypothesis testing and scenario comparison.

This dissertation makes use of the GOM Atlantis ecosystem model. Atlantis is a spatial biogeochemical food web model with a structure based on the management strategy evaluation cycle, which has modules representing biophysical, oceanographic, human, and policy factors (Fulton et al. 2004, 2007). Atlantis is an end-to-end model, which means that it encompasses not only biological processes, but also biogeochemical processes and biophysical modeling (Ainsworth et al. 2012, Ainsworth et al. 2015). An irregular polygon structure represents ecosystems in three-dimensional space within Atlantis, and species are aggregated into functional groups based on shared traits, while species with dedicated management or key functional or commercial importance are designated as their own functional groups (Ainsworth et al. 2015). The Gulf of Mexico Atlantis Ecosystem Model contains 66 spatial polygons, up to 7 depth layers, 91 functional groups (taxa that share similar traits, are taxonomically related, or have similar trophic relationships to potential prey and predators), and fishing fleet dynamics for the major countries around the Gulf (Ainsworth et al. 2015). Within Atlantis, framework is in place to represent primary producer dynamics, nutrients, consumer biomass dynamics, natural mortality, waste production and removal, population dynamics of dinoflagellates and bacteria, sediment chemistry, animal movement, and vertebrate reproduction (Ainsworth et al 2015). Reproduction for all fish species is represented by the Beverton-Holt recruitment relationship. Seasonal movement is accounted for, as well as movement patterns for highly migratory pelagic species (Ainsworth et al. 2015). Although Atlantis does not explicitly incorporate larval transport, it can partition new recruits according to a larval transport matrix. Since Atlantis does not explicitly incorporate larval transport, outsourcing these calculations to a dedicated larval dispersal model is an advantageous and novel approach to improving realism through model coupling (Drexler 2018).

In this dissertation, I examine three distinct, yet intrinsically connected, aspects of early life in fishes: growth, vertical migration, and dispersal. The impetus behind choosing these three aspects of early life was a backwards journey from ecosystem considerations down to the individual fish level. In order to investigate the impact of larval processes on the distribution of production in the GOM ecosystem using the GOM Atlantis model, I first needed to know the larval connectivity among the Atlantis polygons. In order to determine the polygon connectivity in Atlantis, I needed to know the dispersal trajectories of a range of functional groups in the GOM and track them from their spawning sites to their settlement sites. Therefore, I built a Lagrangian dispersal model. In order to determine the depth-inhabitance of the larvae for the Lagrangian dispersal model, I needed to know the vertical larval behavioral shifts throughout early ontogeny. I built generalized additive models that predict the concentration of larvae at depth based on a diversity of environmental variables. In order to construct these predictive models through pelagic larval duration, the length of time that larvae stay in the water column before settling or metamorphosing into juveniles, I needed to assign ages to the larvae from the sampling survey data. This meant that in order to solve the wider ecosystem question of larval connectivity, I first needed to look at age and growth at the individual fish level. Thus, my dissertation builds from an analysis of the relationship between larval length and age, to the relationship between larval age and depth, to the relationship between larval depth and dispersal trajectory, to the impact of adding dispersal to an ecosystem model.

Chapter 2 is entitled “Early life history growth in fish reflects consumption-mortality tradeoffs” and is an investigation into the relationship between length and age in early life stages of marine fishes and was published in Fisheries Research (Vasbinder and Ainsworth 2020). I fit growth models to twelve grouper and snapper larval data sets from literature in the Gulf of Mexico and similar climatological regions to determine the relationship between length and growth. I fit five types of growth model for each species and then determined the most parsimonious model using a modified version of the Akaike Information Criterion. Exponential growth patterns best represented grouper and snapper species (Vasbinder and Ainsworth 2020). I also surveyed published early life growth models globally to explore growth pattern differences between taxonomic groups. In the meta-analysis of the growth models from this literature survey, I uncovered a pattern in which early life stages of demersal fish were most often represented using exponential growth, while early life stages of pelagic fish were most often characterized using linear growth. These results indicate that early life growth patterns could be related to the risk abatement strategies of young marine fishes (Vasbinder and Ainsworth 2020).

Throughout chapters 3 and 4, I reference several fish taxa. The identification of these taxa is based on the resolution of identification in the SEAMAP surveys. Scaridae, commonly known as parrot fish, are a bio-eroding reef fish family. Lutjanidae, the snapper family, is also a reef fish family and contains several economically valuable fisheries species. *Hemanthias* is a genus of groupers from the family Serranidae. Ophichthidae and Ophidiidae, snake eels and cusk eels, are two large reef fish families and are interesting for dispersal explorations because they have very long larval dispersal compared to most other fish groups. Labridae are another reef fish family that include the wrasse. I have species level resolution data for the species *Trachurus lathami* and *Decapterus punctatus*, both of which are in the Jack family, and

Katsuwonus pelamis, and *Euthynnus alleteratus*, two large pelagic fish.

In Chapter 3, “Using Generalized Additive Modeling to Predict Larval Depth at Age”, I built Generalized Additive Models (GAMs) to predict the concentration of larvae at depth for a range of age classes and ten taxa of major commercial and recreational fishes in the Gulf of Mexico, based on a range of environmental variables using larval sampling and environmental data from the SEAMAP ichthyoplankton survey, archived runs of the GOM HYCOM, and averaged data from the NOAA National Data Buoy Center. Taxa showed different patterns of vertical migration by age. I suggest that these differences in depth at age may be related to differing life history strategies between taxa and life stages. Leptokurtic distributions in water column occupancy reflect taxa that show high fidelity to their chosen depth ranges, indicating that these taxa may utilize specific currents for transport. Taxa with a more uniform water column distribution may be employing a more risk-averse dispersal strategy.

Chapter 4, "Gulf of Mexico Larval Dispersal", contains the Lagrangian model that uses the ontogenetic depth occupancy predictions from Chapter 3 to determine which depths to pull current vectors from the outputs of the West Florida Coastal Ocean Model (WFCOM). The dispersal model uses a fourth-order Runge-Kutta algorithm to iterate the larvae forward in time to their settling sites and backwards in time to their spawning sites. The WFCOM current data constitutes a time series from 2006-2012 and includes all sampling events used to build the Chapter 3 depth occupancy models. Thus, as I use forward and backward integration from the sampling time, I am using the actual currents from those days to track the larval particles to their spawning and settling sites. I then use these spawning and settling sites to calculate the connectivity of polygons in the GOM Atlantis model. I used these results to build a connectivity matrix which parameterizes the GOM Atlantis model larval dispersal. Finally, I compare the distribution of production with and without the use of larval dispersion in Atlantis to assess the impacts of including larval data in an ecosystem modeling framework. Overall, this dissertation is an investigation of early life history movement in fish and its relevance to the productivity of stocks.

References

Ainsworth, C.H., Schirripa, M.J., Morzaria -Luna, H. (eds.) 2015. An Atlantis ecosystem model for the Gulf of Mexico supporting integrated ecosystem assessment. NOAA Technical Memorandum. NMFS-SEFSC-676, 149 p. doi: 10.7289/V5X63JVH.

Ainsworth, C.H., Morzaria-Luna, H., Kaplan, I.C., Levin, P.S., Fulton, E.A., Cudney-Bueno, R., Turk-Boyer, P., Torre, J., Danemann, G.D., Pfister, T. 2012. Effective ecosystem-based management must encourage regulatory compliance: A Gulf of California case study. Mar. Policy 36:1275–1283.

Costelloa, C., Rassweilerb, A., Siegelc, D., De Leod, G., Michelie, F., and Rosenbergf, A. 2010. The value of spatial information in MPA network design. PNAS 107(43):18294-18299.

Cushing, D.H. 1974. The natural regulation of fish populations. In: F. R. Harden-Jones, Ed. Sea fisheries research. John Wiley and Sons, New York, p. 399–412. 1975. Marine ecology and fisheries. Cambridge University Press, Cambridge, 278 p.

Cushing, D.H. 1990. Plankton production and year-class strength in fish populations: an update of the match/mismatch hypothesis. Adv. Mar. Biol., 26: 250–93.

Drexler, M. 2018. Evaluating the use of larval connectivity information in fisheries models and management in the Gulf of Mexico. Graduate Theses and Dissertations. https://scholarcommons.usf.edu/etd/7499

Fulton, E.A., Parslow, J.S., Smith, A.D.M., Johnson, C.R. 2004. Biogeochemical marine ecosystem models. 2. The effect of physiological data on model performance. Ecol. Model., 173, 371-406.

Fulton, E.A., Smith, A.D.M. & Smith, D.C. 2007. Alternative management strategies for Southeast Australian CommonwealthfFisheries: Stage 2: Quantitative management strategy evaluation. Australian Fisheries Management Authority. Fisheries Research and Development Corporation.

Houde, E. D. 2008. Emerging from Hjort’s Shadow. J. Northw. Atl. Fish. Sci., 41: 53–70. doi:10.2960/J.v41.m634

Hjort, J. 1914. Fluctuations in the great fisheries of northern Europe viewed in the light of biological research. Rapp. P.-V. Reun. Cons. Int. Explo. Mer., 20: 1–228.

Lasker, R. 1978. The relation between oceanographic conditions, and larval anchovy food in the California Current: identification of factors contributing to recruitment failure. Rapp. P. V. Reun. Cons. Int. Explo. Mer., 173: 212–230.

Lasker, R. 1981. Factors contributing to variable recruitment of the northern anchovy (*Engraulis mordax*) in the California Current: contrasting years, 1975 through 1978. Rapp.P.-V. Reun. Cons. Int. Explo. Mer., 178: 375–388.

Lasker, R. 1987. Use of fish eggs and larvae in probing some major problems in fisheries and aquaculture. Am. Fish. Soc. Symp., 2: 1–16.

Leis, J.M. 2010. Ontogeny of behaviour in larvae of marine demersal fishes. Ichthyol. Res. 57:325–342

Leis, J.M., Hay, A.C., Lockett, M.M., Chen, J., and Fang, L. 2007. Ontogeny of swimming speed in larvae of pelagic-spawning, tropical, marine fishes. Mar. Ecol. Prog. Ser. Vol. 349: 255–267.

Link, J. 2002. What does ecosystem based fisheries management mean? Fisheries 27(4): 18-21.

Miller, T.J. 2007. Contribution of individual-based coupled physical–biological models to understanding recruitment in marine fish populations. Marine Ecol. Prog. Ser. Vol. 347: 127–138.

National Oceanic and Atmospheric Administration (2006) Evolving an ecosystem approach to science and management through NOAA and its partners. Available: http://www.sab.noaa.gov/Reports/eETT_Final_1006.pdf.

Paris, C.B., Che'rubin, L. M. and R. K. Cowen. 2007. Surfing, spinning, or diving from reef to reef: effects on population connectivity. Mar. Ecol. Prog. Ser. Vol. 347: 285–300.

Paris, C.B., Cowen, R.K. 2004**.** Direct evidence of a biophysical retention mechanism for coral reef fish larvae. Limnol. Oceanogr. 49(6): 1964–1979.

Pikitch, E.K., Santora, C., Babcock, E.A., Bakun, A., Bonfil, R., Conover, D.O., Dayton, P., Doukakis, P., Fluharty, D., Heneman, B., Houde, D., Link, J., Livingston, P.A., Mangel, M. McAllister, M.K., Pope, J., Sainsbury, K.J. 2004. Ecosytem based fishery management. Science 305: 346-347.

United States Government Accounting Office (1994) Ecosystem management: Additional actions needed to adequately test a promising approach. Available: http://archive.gao.gov/

Watson, J.R., Mitarai1, S., Siegel, D.A., Caselle, J.E., Dong, C., McWilliams, J.C. 2010. Realized and potential larval connectivity in the Southern California Bight. Mar. Ecol. Prog. Ser., 401:31-28.

Weisberg, R.H., Zheng, L., Liu, Y., Murawski, S., Hu, C., Paul, J. Did Deepwater Horizon hydrocarbons transit to the west Florida continental

shelf? Deep-Sea Res. II http://dx.doi.org/10.1016/j.dsr2.2014.02.002i.

Zheng, L., Weisberg, R. (2012). Modeling the west Florida coastal ocean by downscaling from the deep ocean, across the continental shelf and into the estuaries. Ocean Model. 48:10 -29. DOI: 10.1016/j.ocemod.2012.02.002.

Chapter 2: Early life history growth in fish reflects consumption-mortality tradeoffs

This chapter was published in the July 2020 issue of Fisheries Research with co-author Cameron Ainsworth, Ph.D. and is included in this dissertation under the author permissions guidelines of Elsevier publishers, which includes a release to authors to include their publication in their dissertation. This article is included as Appendix 3 in this dissertation, and its corresponding online supplement is included as Appendix 1 in this dissertation.

Reference:

Vasbinder, K and C. Ainsworth. 2020. Early Life History Growth in Fish Reflects Consumption-Mortality Tradeoffs. Fish. Res. 227:105538.

To access this article through the publisher:

https://doi.org/10.1016/j.fishres.2020.105538

Supplementary material related to this article can be found in the online version at doi:https://doi.org/10.1016/j.fishres.2020.105538.

Chapter 3: Using Generalized Additive Modeling to Predict Larval Depth at Age

This chapter is in preparation as a manuscript with the following co-authors:

Kelly Vasbinder[1], Cameron Ainsworth[1], Yonggang Liu[1], Robert Weisberg[1], Glenn Zapfe[2]

Corresponding author: kmvasbinder@mail.usf.edu

[1]University of South Florida College of Marine Science, 830 1st St S, St. Petersburg, FL 33701

[2]National Oceanic and Atmospheric Administration, Pascagoula, MS Laboratory: Southeast Fisheries Science Center, 3209 Frederic Street Pascagoula, MS 39567, United States

Abstract

Generalized Additive Models (GAMs) were built to predict the concentration of larvae at depth for ten taxa of major commercial and recreational fishes, for a range of age classes in the Gulf of Mexico. A training data set of larval data from the Southeast Area Monitoring and Assessment Program (SEAMAP) ichthyoplankton survey MOCNESS (Multiple Opening/Closing Net and Environmental Sensing System) tows was used to parameterize the model. Validation of all models were conducted utilizing a reserved subset of the overall SEAMAP dataset. Differences in the depth at age may reflect differing life history strategies between taxa and life stages. Taxa that show high fidelity to their chosen depth ranges produce leptokurtic distributions in water column occupancy and may utilize specific currents for transport. Other taxa are distributed throughout the water column more uniformly. This may reflect a more risk-averse dispersal strategy. These depth-at-age predictions are useful for Lagrangian transport calculations and developing a matrix of larval spawning and settlement sites for the Gulf of Mexico.

Introduction

Vertical Migration of Larvae

A substantial body of literature has demonstrated that the use of spatial information in fisheries management, particularly about larval connectivity, has the potential to enhance fishery yields, profits, and sustainability (Costelloa et al. 2010). Larval connectivity and dispersal can be impacted by a wide variety of factors, including the depth at which larvae are traveling (Weisberg et al. 2014b). Fish larvae can inhabit different depth strata during different life stages and this affects how they interact with ocean currents and their transport to rearing areas (Huebert et al. 2010). Depth stratification of larvae in the Gulf of Mexico (GOM) has been investigated in a handful of instances (Dagg and Govoni 1996, Carrasou et al. 2012, Govoni et al. 1986, Govoni et al. 1992, Ortner 1989, Raynie and Shaw 1993), but these instances are mostly restricted to discreet areas of the northern Gulf and many only report data for a few species. Carrasou et al. (2012) investigated ichthyoplankton assemblages off the coast of Alabama and found structure in the assemblages based on distance from shore, season of the year, and depth. The authors suggested that the input of water from the Alabama River played a key role in the spatial distribution of ichthyoplankton. During studies of ichthyoplankton predation on copepods, Dagg and Govoni (1996) and Govoni et al. (1986) performed some MOCNESS (Multiple Opening/Closing Net and Environmental Sensing System) sampling of larvae at discrete depths near the surface. Govoni et al. (1986) reported a depth table for Spot (*Leiostomus xanthurus*) and Atlantic Croaker (*Micropogonias undulatus*) larvae, which indicated that most of the Spot larvae identified in the samples were found in the uppermost meter of the water column. In an investigation of surface accumulations of larvae at the Mississippi River plume front, larval concentrations were found to be higher in surface layers associated with the frontal zone, than in other areas due to frontal convergence (Govoni 1992).

Larvae vertically migrate for a variety of reasons. Larvae need to choose water column depth occupancies that balance different fitness factors such as growth, survival, potential drift trajectories, and the potential to reach suitable habitat (Fiksen et al. 2007). Larvae feed on other plankton, and on a diel scale, zooplankton migrate in response to kairomones from predators which activate vertical migration behaviors using light as a proximate control (Pers. Communication Kendra Daly, Cohen and Forward 2009). Larvae need to balance the need for food with predation risk, and this choice is reflected in short term larval vertical migration strategies such as diel migration (Fiksen et al. 2007). Longer term changes in depth occupancy such as those associated with ontogenetic vertical migration affect drift trajectories and future habitat suitability (Fiksen et al. 2007). Ontogenetic vertical migration can be on a fixed schedule that allow larvae to return to specific habitat (Pineda and Reyns 2018). Migration can be facilitated by environmental cues (Pineda and Reyns 2018). Larvae can also exhibit adaptive behavior related to vertical migration as a response to changes in their physical environment; for example, larvae change their vertical position to either take advantage of or avoid certain hydrodynamic features (Pineda and Reyns 2018). One highly studied example of this is in selective tidal stream transport, in which larvae move up or down in the water column to take advantage of ebb and flow tides coming in and out of estuaries to reach habitat with specific characteristics, such as suitable nursery habitat (Forward and Tankersley 2001). The focus of my dissertation is on longer term choices associated with ontogenetic vertical migration strategies that would have an impact on transport to settlement habitat.

Little information on the vertical movements of reef fish larvae in the GOM is available, but a few laboratory and modeling investigations into the early life history of reef larvae and their vertical distributions have been done for small areas of the GOM. Using tows of a MOCNESS and statistical modeling of the Straits of Florida, Huebert et al. (2010) found different vertical distributions for several families of reef fish larvae, with depth as the most predictive factor for larval density in four of the families. Larvae of deep-dwelling snapper species traveled deeper as they aged, indicating an ontogenetic shift in depth ranges over larval ages and active maintenance of depth (D'Allesandro et al. 2010).

The aforementioned studies suggest some vertical structure to larval assemblages is present. An ideal data set to use for the investigation of larval organization by depth would be a data set that spanned large regions of the GOM and contained samples of a range of taxa at depth intervals throughout the water column. The Southeast Area Monitoring and Assessment Program (SEAMAP) icthyoplankton survey data provides this ideal data set.

Importance of Modeling Larval Depth

Recent studies have explored the relationship between ontogenetic vertical migration and larval transport for reef fish species. One key study investigated the transport of Gag larvae from offshore spawning sites to inshore settlement habitat on the West Florida Shelf (Weisberg et al. 2014b). The authors used a stable isotope analysis to determine larval origin and ran particle trajectory simulations in the West Florida Coastal Ocean Model, WFCOM (Zheng and Weisberg 2012, Weisberg et al. 2014a, Weisberg et al. 2014b). By comparing surface transport and transport in the bottom Ekman layer, they found that the near-bottom transport hypothesis provided a mechanism for Gag larval transport from spawning areas to known settlement areas, as near-bottom particles reached near-shore areas, while surface particles did not (Weisberg et al.

2014b). Thus, the near-bottom transport pathway was consistent with Gag spawning and settlement patterns, emphasizing the importance of including larval depth stratification in modeling scenarios investigating larval trajectories.

In addition to larval depth, vertical migration has been investigated using the Connectivity Modeling System, CMS, as a part of the Southeast Data Assessment and Review (SEDAR) workshops for Gag and Red Snapper (Karnauskas et al. 2013a, Karnauskas et al. 2013b). For Gag, the total number of larvae was split into depth bins according to age, based on data from Serranid larvae found during SEAMAP surveys and MOCNESS data collections (Karnasukas et al. 2013a). This was used to represent vertical migration by moving a percentage of the particles at each age into different depth bins (Karnauskas et al. 2013a). CMS was used to identify strong recruitment years and recruitment areas (Karnauskas et al. 2013a). For Red Snapper, a probability matrix similar to that used for Gag was employed, based on a congeneric species, which was estimated to have similar vertical migration behaviors to Red Snapper (Karnauskas et al. 2013b). This model was also used to investigate recruitment, and the authors found that changing the vertical distribution of larvae changed the recruitment index (Karnauskas et al. 2013b). A sensitivity analysis in which the standard deviation around the depth estimate was increased and the mean was slightly raised or lowered in the water column resulted in differences in recruitment index in the same year, but maintained the general between-year trends and found that the same general trends were evident between runs (Karnauskas et al. 2013b). Although vertical distribution and vertical migration information is important for estimating larval trajectories, depth stratification of larval populations for major fish functional groups in the GOM is still largely unknown.

GAM Modeling for Ecological Problems

One way to investigate the vertical distribution of larvae in the water column is to use statistical modeling to examine the relationship between larval depth, environmental variables, and ontogenetic measures, such as length and age. The Generalized Additive Model (GAM) is a class of models that allows covariates in a regression to take non-linear forms using smoothing functions (Hastie and Tibshirani 1986). GAMs are considered a good choice for investigating environmental effects on organisms, because they are non-parametric and flexible due to the presence of smoothers, so the type of relationship between a predictor variable and the response variable does not need to be known (Shih et al. 2014, Yee and Wild 1996). GAMs take a step away from some of the biases of traditional linear models, because unlike linear regression, GAMs allow the data to drive the shape of the relationship between predictor and response variables (Guisan et al. 2002). While GAMs must be built within a certain distribution family, the smooth terms can be chosen in a way that allows predictor variables to drive their own response shapes. GAMs are data driven models, and are useful in situations in which there is little information available about the relationships being modeled (Guisan et al. 2002, Shih et al. 2014).

GAMs have become a common tool for investigating ecological questions related to species distributions, and have been used in the field of marine modeling to investigate scales of temporal variability in squid abundances in the Pacific, predict shrimp distribution and abundance in the Tampa Bay estuary, and to predict species abundances and distribution maps for use in ecosystem models in the Gulf of Mexico (Wei et al 2016, Rubec et al. 2016, Gruss et al 2014, Drexler and Ainsworth 2013). GAMs were chosen for this study due to their flexibility and their ability to draw out patterns in responses to environmental predictors. When compared to linear, logistic, and residuals regression techniques, GAMs were not only better able to predict water temperature based on other environmental variables, but also able to capture non-linear patterns (Laanaya et al. 2017). GAMs have been found to provide better fits than generalized linear models, when used to model the relationship between environmental factors and recruitment due to the presence of non-linear environmental predictors (Shih et al. 2014). Finally, GAMs have been suggested as a useful solution in studies with a large number of predictors (Moisen and Fescino 2002). In this paper, GAMs are used to explore the relationship between larvae and environmental variables and to predict larval depth at age for ten taxa of fish from the Gulf of Mexico.

Methods

Data

The National Oceanic and Atmospheric Administration (NOAA) conducts several yearly ichthyoplankton surveys in the northern GOM throughout the year as part of the Southeast Area Monitoring and Assessment Program (SEAMAP). The surveys cover the continental shelf in the late summer months (August and September), deeper GOM waters in Spring (April and May), and the continental shelf break in winter months (January – March). Starting in 2007, a 1 m^2 MOCNESS was implemented as supplemental sampling gear during the surveys when time allows. The MOCNESS is equipped with nine, 0.505 mm mesh with one net used in the oblique tow (Net 0) from the surface to the bottom or a maximum depth of 130 m. Each of the remaining 8 nets (Nets 1-8) sample a discrete depth bins depending on the area and water depth sampled during each of the different surveys. In shallower areas, the depth bins may be set at 10 m, while the deeper waters may have depth bins set at 20 m. A minimum target volume of 250-300 m^3 of water filtered for each depth bin is set to ensure ample sampling. Temperature, salinity, dissolved oxygen concentration, wind speed, and wind direction were measured using sensors on the MOCNESS, survey vessel, and corresponding CTD. The overall goal of the MOCNESS tows is to provide detailed descriptions of the vertical distribution of larval fish in the GOM.

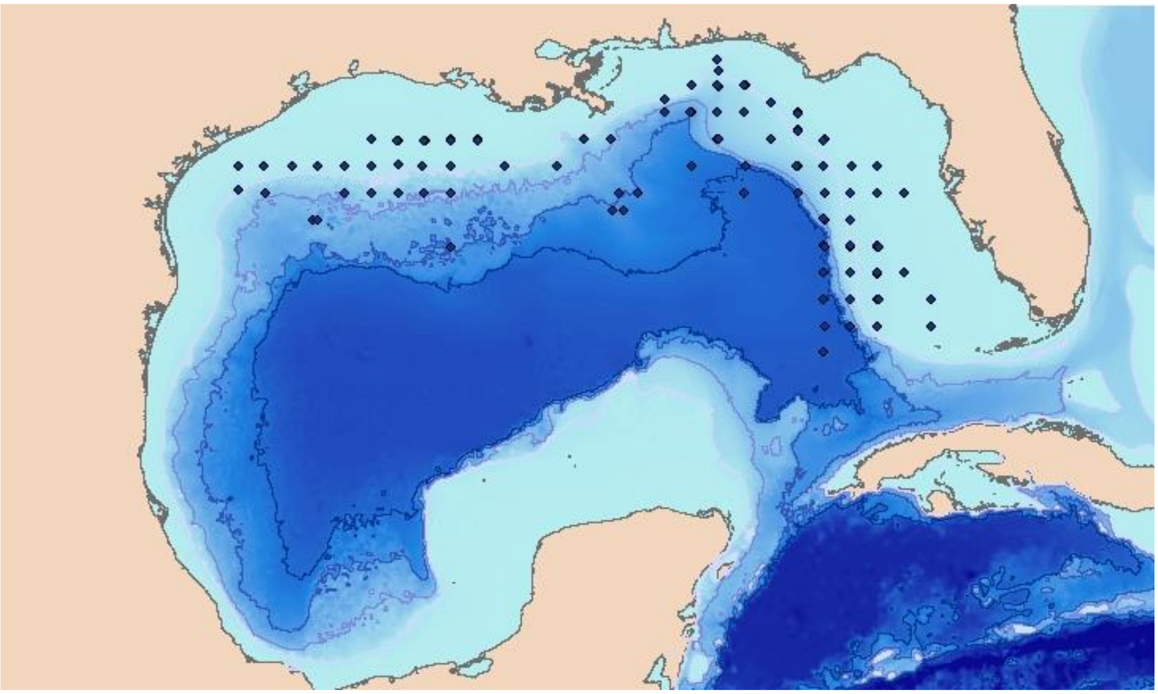

Figure 3.1: SEAMAP MOCNESS sampling sites from all surveys (2007 – 2012)

Larval vertical depth distribution data from 2007 through 2012 was analyzed from the SEAMAP MOCNESS tows as the concentration of larvae per unit of volume (larvae/cubic meter) at depth. The dataset comprises over 4000 individual larval observations (Figure 3.1). Lengths of larvae were measured as part of the SEAMAP ichthyoplankton sorting protocols. However, in some instances, only a subset of the larvae were measured due to the large numbers found in the sample. Depth at age models were made at family level resolution for Scaridae, Lutjanidae, Scombridae, Ophichthidae, and Ophidiidae, at the genus level of resolution for *Hemanthias*, and at species level resolution for the species *Trachurus lathami*, *Decapterus punctatus*, *Katsuwonus* *pelamis*, and *Euthynnus alleteratus*. The reason for the disparity in the taxonomic resolution is due to the difficulty in separating taxa within some of these families. For each taxon, a GAM was built with 14 predictor variables (Equation 2). Mixed-layer depth was obtained from archived runs of the Gulf of Mexico HYbrid Coordinate Ocean Model (HYCOM) from 2007-2012 (Yonggang Liu, USF, Pers. Comm.; Chassignet et al. 2009). The HYCOM is a global ocean prediction system used by a consortium of institutions and is currently run by the U.S. Navy and National Oceanic Atmospheric Administration (Chassignet et al. 2009). The Gulf of Mexico HYCOM is based on the U.S. Navy's nowcast/forecast system, with a 1/25° resolution and 36 vertical layers that assimilates deep ocean observations, allowing it to represent the impact of circulation on the West Florida Shelf by correctly placing the GoM's Loop Current and eddies (Chassignet et al. 2009, Weisberg et al. 2014a). Up to twelve-hour average wind speed and direction was calculated using archived data from the National Data Buoy Center by triangulating the closest buoy to each of our sampling locations (NDBC: these data were collected and made freely available by NOAA/NDBC). Finally, age was calculated by fitting age models to length at age data in the larval literature and by comparing and combining published larval age models by family (Vasbinder and Ainsworth, 2020).

Statistical Modeling Methods

GAMs were built according to the general equation for a GAM adapted from Yee and Wild (1996) and Hastie and Tibshirani (1990) (Equation 1).

$$g(\mu) = \beta_0 + s_1(x_1) + \cdots etc \qquad \text{Eq. 1}$$

Where "g" is the link function, "μ" is the response variable, "β_0" is the intercept, "x" is the predictor(s), and "s" represents the smoothers applied to the predictor variables.

GAMs were built for each taxon in R using the mgcv package with a gamma distribution and log link (Wood 2016). Thin plate splines, which are low rank isotropic smoothers, were chosen as the smoothing functions (Wood 2003, Wood 2016). Smoothers were specified with 2 basis dimensions and an REML (Restricted Maximum Likelihood) selection method was used for fitting smoothing functions (Wood 2003, Wood 2016, Marra and Wood 2011). Environmental variables and length were included in the model as smoothed terms, while age, time, date, and location were included as terms without smoothers (Equation 2).

$$g(\mu(X)) = \beta_0 + s_1(\text{Depth of Sample}) + \text{Time of Day} + s_2(\text{Length}) + \text{Latitude} + \text{Longitude} +$$

$$s_3(\text{Instantaneous Wind Speed}) + s_4(\text{Instantaneous Wind Direction}) + s_5(\text{Average Wind Speed}) + s_6(\text{Average Wind Direction}) + s_7(\text{Mid-Depth Oxygen Layer}) + s_8(\text{Temperature}) + s_9(\text{Salinity}) + s_{10}(\text{Mixed-layer depth}) \qquad \text{Eq. 2}$$

Instead of AIC, a double penalty approach was used for variable selection recommended by Marra and Wood (2011). This method penalizes the null and range space of a smoother and can shrink them to zero, so it functions as a one-step shrinkage variable selection method instead of an iterative knock out method. Instead of knocking out the insignificant variables, this method shrinks their smoother coefficients so that they are essentially down-weighted in the model. Thus, variables showing a high p-value (for example $p>0.05$) have had their importance in the model shrunk by this selection method. This is known as "shrinkage" selection, because instead of iteratively fitting models and dropping terms each time, this shrinkage method fits the model in one step and by penalizing the smoothers, variables that are less significant to the model are down-weighted or removed from the model completely (Marra and Wood 2011).

A series of model diagnostics was generated for examination of the model fit. Quantile-quantile plots (QQ-plots) are a tool to compare two data sets and determine whether they came from the same distribution (Wang et al. 2016). QQ-plots can be used to assess the model skill by checking the distribution of points around a line comparing two sets of quantiles. Typically, sample quantiles from one data set are plotted against quantiles from another data set, with a straight line indicating a match between the distributions of the two data sets (Wang et al. 2016). Typically, this is done between theoretical quantiles of the desired distribution and sample quantiles from the model distribution, however, for generalized linear models, it is instead suggested that deviance residuals be compared to the theoretical quantiles (Wang et al. 2016, Augustin et al. 2012). For GAMs, this can be done using the qq.gam function in the mgcv package, which creates reference quantiles by simulating a data set from the fitted GAM and calculating the residuals of that simulated data set, repeating this process over and over to simulate a specified replicate number of data sets (Augustin et al. 2012, MGCV Documentation). A total of 100 replicate simulated data sets were used to generate the theoretical quantiles. These residuals were then plotted against the model residuals using qq.gam (R doc mgcv). Models were considered valid when there was a spread of data along the 1:1 line between deviance residuals and theoretical quantiles. Validation of the model was accomplished using 10% of the original dataset not utilized in the model build. The validated data set was used to determine the Pearson correlation coefficient. The variables from the withheld validation data set were run in the GAMs to generate predictions, and then these predictions were compared to the actual known values. Pearson’s correlation coefficient was calculated between these observed and predicted values.

Two taxa, Scombridae (a family of tuna and large pelagic fish) and Scaridae (a reef-associated family of bioeroding fish) were chosen for in-depth analysis as they provide examples of contrasting patterns in larval depth distributions and so may represent different life history strategies. Depth at age profiles for Lutjanidae, Ophichthidae, and Ophidiidae at the family level, *Hemanthias* at the genus level, and *Trachurus lathami, Decapterus punctatus, Katsuwonus pelamis,* and *Euthynnus alleteratus* at the species level are included in Appendix 2.

The final GAM for each family can be used in a predictive way to generate a concentration gradient indicating how larvae are distributed throughout the water column. GAMs with a large number of predictors require data sets of a certain size, so that each data set contains more data points than the number of coefficients in the model. Because smoothed variables can have multiple coefficients for each smooth function, small data sets were insufficient to fit GAMs in this scenario. In order to alleviate this problem, datasets for each taxa were split into two or three age classes, each with a large enough amount of data to fit a GAM model. This results in each taxa having different age class splits based on how much data was available for each age.

Results

Depth at age plots for all ten taxa (Appendix 2) showed a range of ontogenetic vertical migration patterns. Scombridae, *Trachurus lathami*, Ophidiidae, *Hemanthias*, and Lutjanidae larvae remained at the surface for the entire larval duration. *Euthynnus alleteratus* larvae began at the surface then moved deeper as they aged. Scaridae and Ophichthidae taxa had larvae that began on the surface, then traveled deeper, and then moved to the surface again. Finally, *Katsuwonus pelamis* and *Decapterus punctatus* larvae occupied deeper depths during early stages and surface depths during later stages. Table 3.1 shows the depth with the maximum concentration of larvae and the standard deviation of depth at age predictions for all taxa.

Two examples of age profiles and their associated smooth plots and diagnostics are presented for comparison in greater detail. Scaridae vertical distribution appears to fluctuate from surface water to deeper waters as the larvae grows. (Figure 3.2, Table 3.1). Early age larvae (< 12.48 days) are located in surface waters, but move to deeper waters with a high concentration at 28 m until 22 days when they return back to the surface waters. In contrast, all three age classes of Scombridae are located in surface waters from age zero all the way to age forty-five days (Figure 3.2, Table 3.1).

Pearson's correlation coefficients between training and validation data sets indicate model skill. For Scaridae, the Pearson's coefficient for the first and third age classes are high (Table 3.2), while the Pearson's coefficient for the second age class is lower and negative, indicating that models for the first and third age groups are more skilled than the one for the second age class. Scombrids have consistently high values of Pearson's coefficient, ranging from 0.78 to 0.85 for all three age classes, indicating high model skill. QQ-plots for both species (Figure 3.4 for Scaridae and Figure 3.5 for Scombridae) show an even spread of data along the 1:1 line between deviance residuals and theoretical quantiles to consider the models valid. Among the rest of the taxa, Pearson’s coefficients are generally high with a few exceptions. *Hemanthias*, the second age class of *Katsuwonus pelamis*, Ophidiidae, and *Trachurus lathami*, and the third age class of Ophichtidae had Pearson’s values below 0.4, indicating lower model skill.

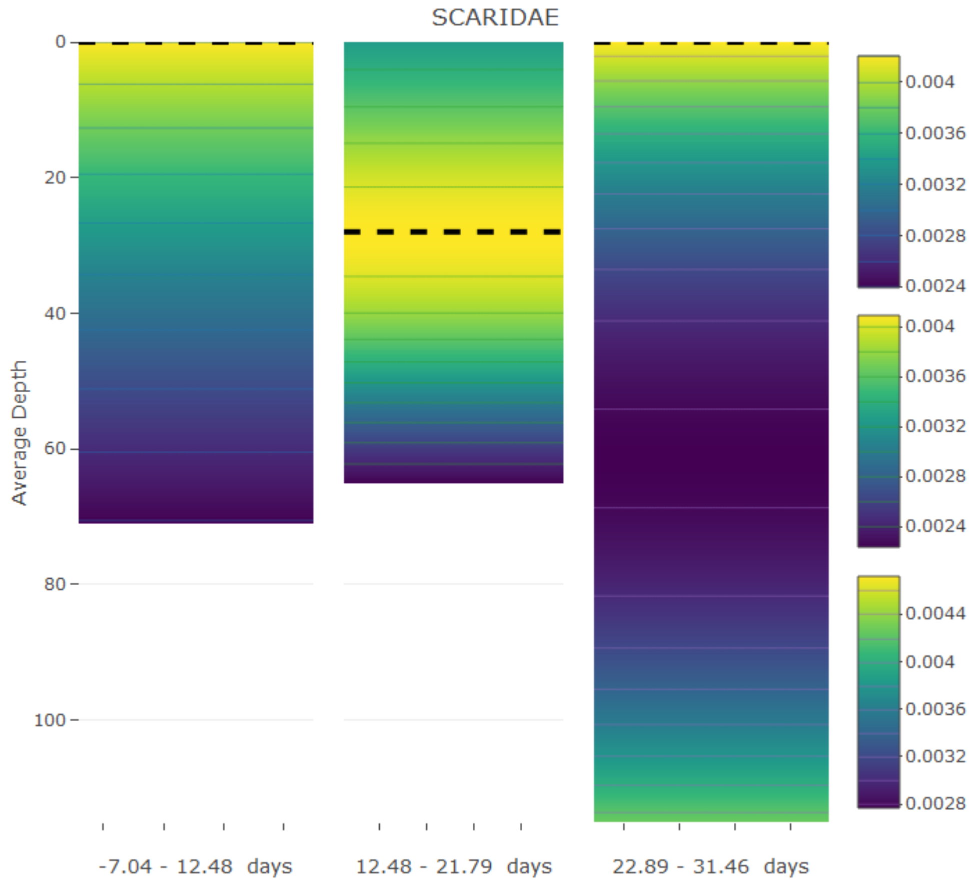

Figure 3.2: Depth at age for Scaridae

Color gradient refers to the concentration of larvae per cubic meter predicted in the water column at each depth from purple (low) to yellow (high). Each age class has its own corresponding gradient, ranging from youngest (at top) to oldest (at bottom) on the right side of each plot.

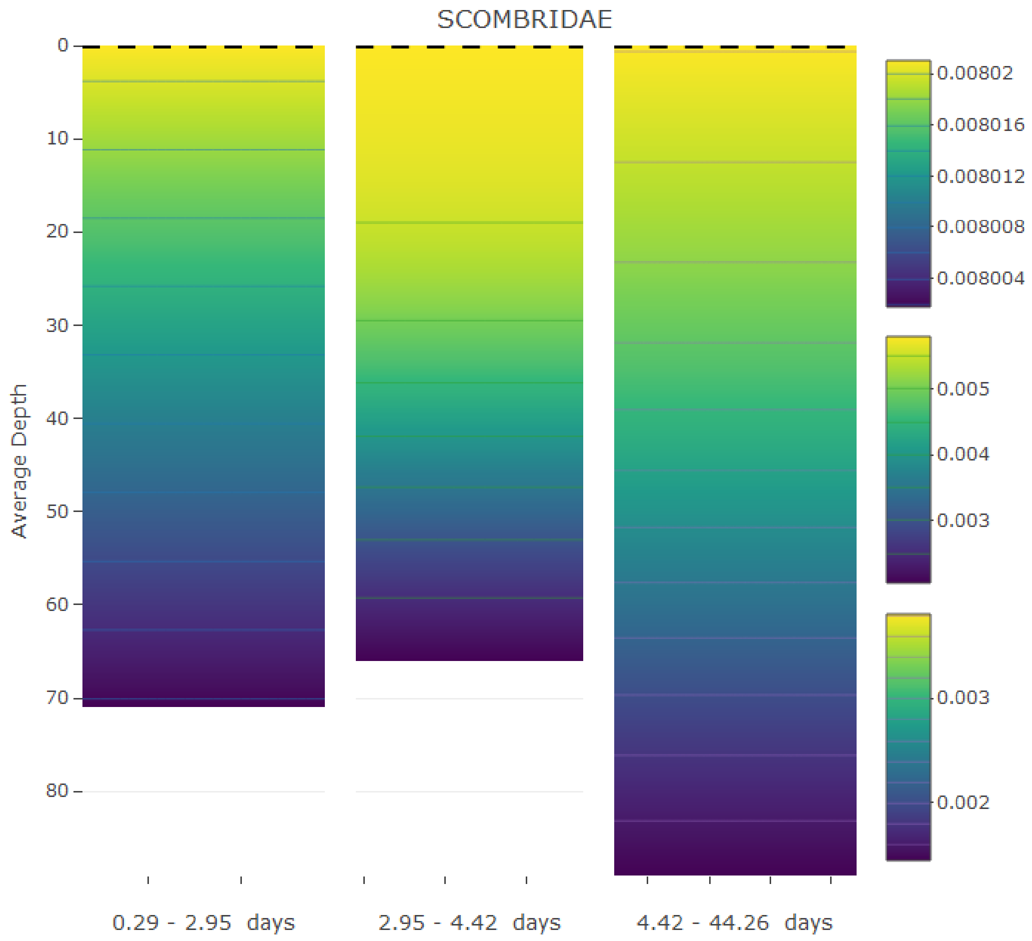

Figure 3.3: Depth at age for Scombridae

Color gradient refers to the concentration of larvae per cubic meter predicted in the water column at each depth from purple (low) to yellow (high). Each age class has its own corresponding gradient, ranging from youngest to oldest on the right side of each plot.

Table 3.1: Depth at Age predictions for all taxa and age classes

Taxa	**Age Class**	**Depth**	**Predicted Maximum Larval Concentration (Mode)** **(larvae/cubic meter)**	**Standard Deviation on the Mean of Predictions** **(larvae/cubic meter)**
Scaridae	1	0	0.00420	0.000529
Scaridae	2	28	0.00409	0.000525
Scaridae	3	0	0.00472	0.000544
Hemanthias	1	0	0.0151	0.00327
Hemanthias	2	0	0.00280	0.000193
Trachurus lathami	1	0	0.00438	0.000659
Trachurus lathami	2	0	0.0122	0.00324
Trachurus lathami	3	0	0.0177	0.00432
Decapterus punctatus	1	20	0.00382	0.000423
Decapterus punctatus	2	0	0.00536	0.00102
Decapterus punctatus	3	0	0.00524	0.000568
Katsuwonus pelamis	1	65	0.0104	0.00178
Katsuwonus pelamis	2	13	0.00345	0.000487
Ophichthidae	1	0	0.00378	8.08E-05
Ophichthidae	2	28	0.00526	0.000436
Ophichthidae	3	0	0.00401	0.000403
Ophidiidae	1	0	0.00499	0.000637
Ophidiidae	2	0	0.00409	3.33E-09
Ophidiidae	3	0	0.00614	0.000711
Euthynnus alleteratus	1	0	0.0138	0.00173
Euthynnus alleteratus	2	0	0.0103	0.00151
Euthynnus alleteratus	3	20	0.00763	0.00138

Table 3.1 (continued): Depth at Age predictions for all taxa and age classes

Taxa	**Age Class**	**Depth**	**Predicted Maximum Larval Concentration (Mode) (larvae/cubic meter)**	**Standard Deviation on the Mean of Predictions (larvae/cubic meter)**
Lutjanidae	1	0	0.00931	0.00139
Lutjanidae	2	0	0.00834	0.00126
Lutjanidae	3	0	0.00474	0.000596
Scombridae	1	0	0.00802	5.66E-06
Scombridae	2	0	0.00580	0.00124
Scombridae	3	0	0.00381	0.000733

Scaridae and Scombridae also showed differences in which environmental variables were most significant. For Scaridae's oldest age class, depth, instantaneous wind direction, and mid-depth oxygen all had significant p-values, while for Scrombridae's oldest age class, depth, instantaneous wind speed, instantaneous wind direction, daily averaged wind direction, mid-depth-oxygen, salinity, and mixed-layer depth had significant p-values. GAM smoothing function relationships are shown in Figures 3.6 and 3.7 for Scaridae and Scombridae, respectively and each taxa shows different smoothing relationships to each variable. For example, the Scaridae smoothing function shows a strong inverse relationship with salinity, while the Scombridae function shows a less pronounced and non-linear relationship.

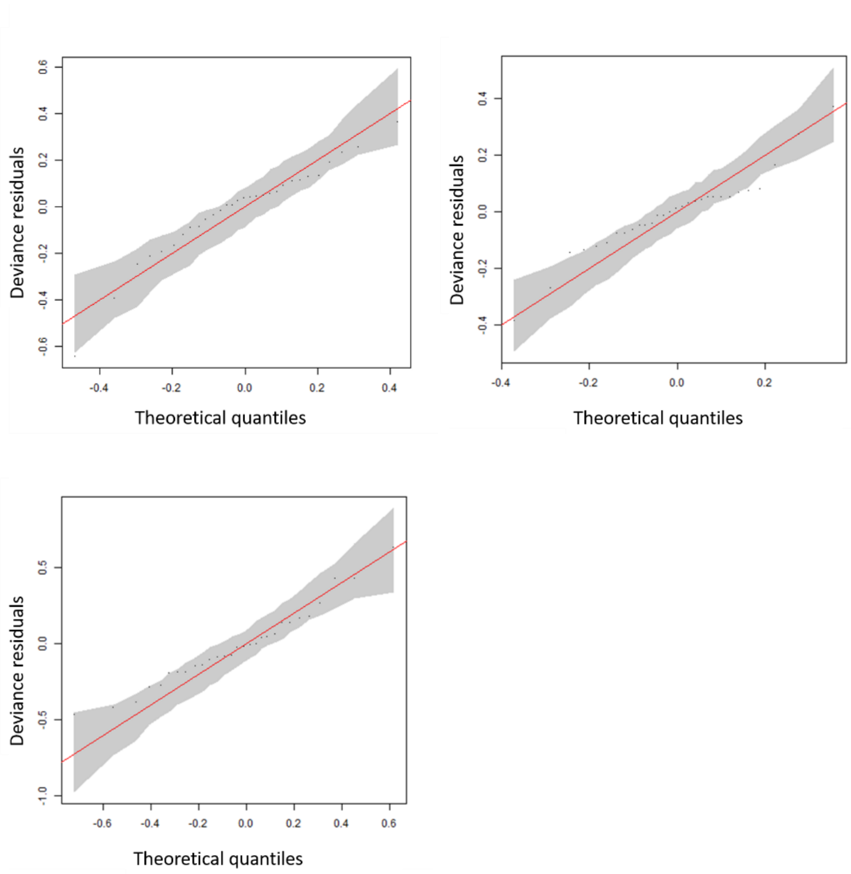

Figure 3.4: QQ-plots for the three age classes of Scaridae (youngest to oldest) showing residuals from theoretical quantiles plotted against model residuals. An even spread of data along the red 1:1 line between deviance residuals (y-axis) and theoretical quantiles (x-axis) is considered a valid model.

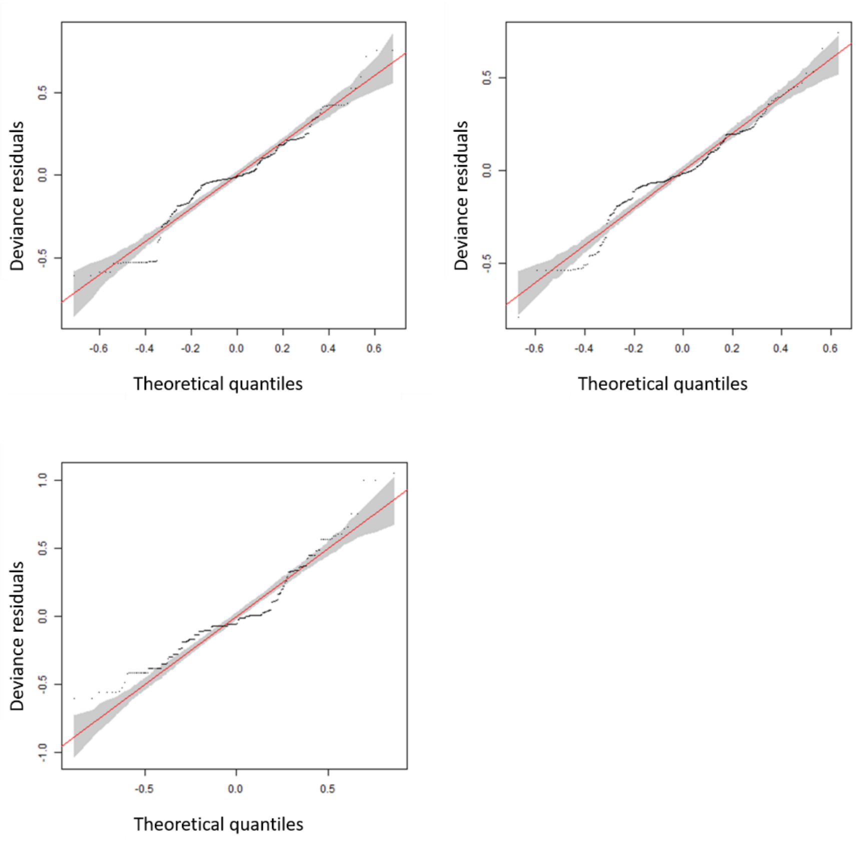

Figure 3.5: QQ-plots for the three age classes of Scombridae (youngest to oldest) showing residuals from theoretical quantiles plotted against model residuals. An even spread of data along the red 1:1 line between deviance residuals (y-axis) and theoretical quantiles (x-axis) is considered a valid model.

Table 3.2: Model diagnostic information for each taxa and age class

Taxa	**Age Class**	**R-squared Value**	**Deviance explained**	**(-)REML**	**Number of Observations**	**Pearson's Correlation for Observed vs Predicted in Test Data**	**p-value of Pear-son's**
Decapterus punctatus	1	0.985	98.10%	-413.17	58	0.994	4.87E-06
	2	0.987	98.60%	-373.87	58	0.991	1.31E-05
	3	0.829	92.40%	-328.17	56	0.916	0.0102
Euthynnus alleteratus	1	0.679	75.50%	-697.88	141	0.475	0.0542
	2	0.681	77.90%	-700.5	141	0.971	6.98E-07
	3	0.688	80.90%	-729.19	141	0.937	1.21E-09
Hemanthias	1	0.873	96%	-158.65	28	-0.00888	0.989
	2	0.699	88.40%	-144.59	27		
Katswonus pelamis	1	0.994	99.4%	-349.15	52	1.00	6.386e-08
	2	0.827	82.5%	-309.12	52	-0.0401	0.940
Lutjanidae	1	0.79	88.70%	-2037	367	0.851	2.52E-13
	2	0.678	77.60%	-1904.4	367	0.840	6.54E-09
	3	0.689	72.20%	-1908.7	366	0.891	< 2.2e-16

Table 3.2 (continued): Model diagnostic information for each taxa and age class

Taxa	**Age Class**	**R-squared Value**	**Deviance explained**	**(-)REML**	**Number of Observations**	**Pearson's Correlation for Observed vs Predicted in Test Data**	**p-value of Pear-son's**
Ophicthidae	1	0.759	84.10%	-366.93	70	0.555	0.0761
	2	0.535	72%	-347.94	70	0.635	0.250
	3	0.658	72.50%	-351.91	70	0.273	0.513
Ophidiidae	1	0.61	70.30%	-251.16	48	-0.454	0.700
	2	0.55	50.90%	-229.98	48	-0.193	0.714
	3	0.253	45.50%	-239.39	48	0.413	0.357
Scaridae	1	0.603	62.6%	-163.1	30	0.845	0.155
	2	0.732	85.8%	-165.2	30	-0.470	0.688
	3	0.518	71.5%	-150.88	29	0.979	0.132
Scombridae	1	0.662	77.70%	-2111.3	405	0.832	1.96E-15
	2	0.726	82.20%	-2148.3	405	0.781	1.65E-09
	3	0.705	75.30%	-2155.1	403	0.853	1.10E-11
Trachurus lathami	1	0.573	53.90%	-316.39	62	0.934	0.0662
	2	0.68	83.10%	-335.7	62	-0.264	0.493
	3	0.827	90.90%	-342.93	62	-0.598	0.117

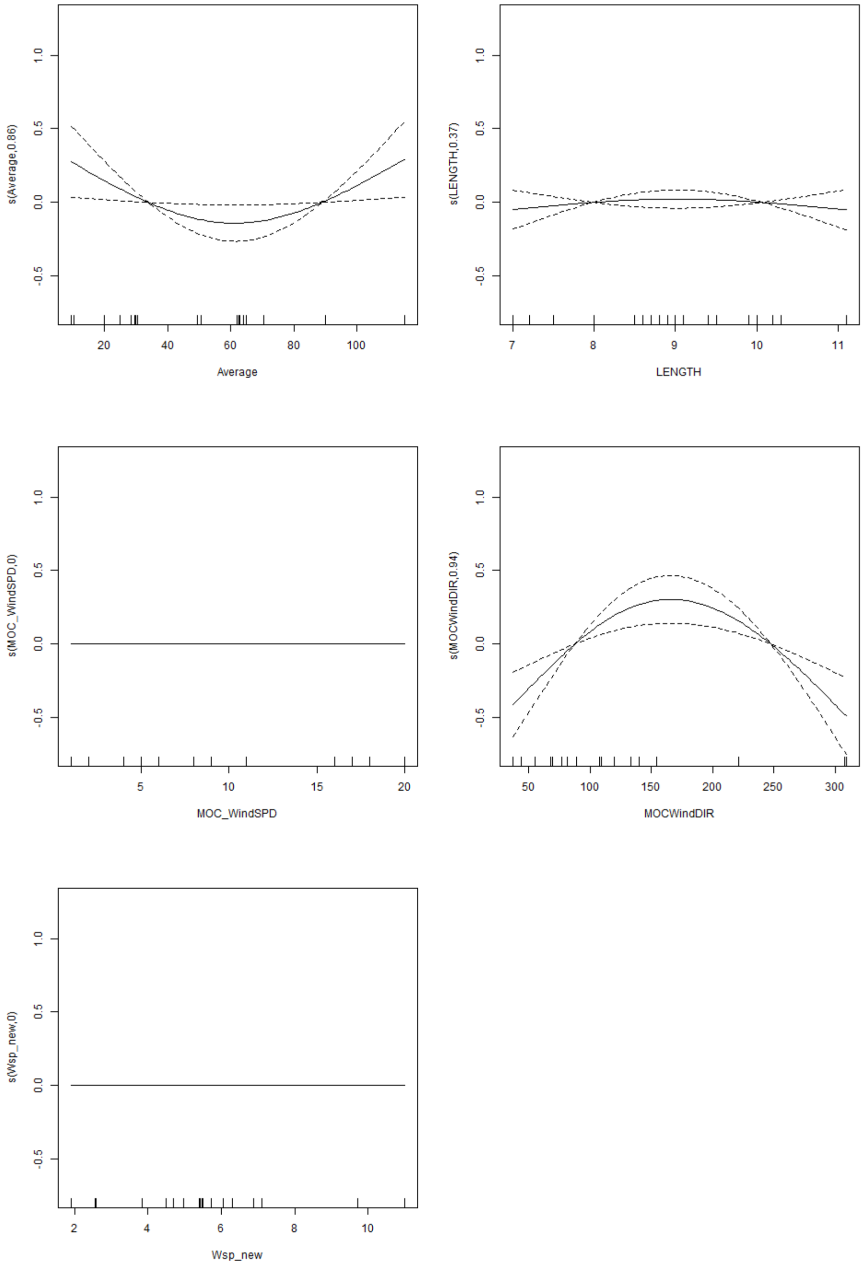

Figure 3.6: Smooth terms for the GAM of the oldest age class of Scaridae. The x-axis is the values of the covariate, while the y axis is the smooth and the edf, (estimated degrees of freedom). Standard error bounds are indicated with the dashed lines. Smooth terms are in the following order: depth of sample, length, instantaneous wind speed, instantaneous wind direction, and average wind speed

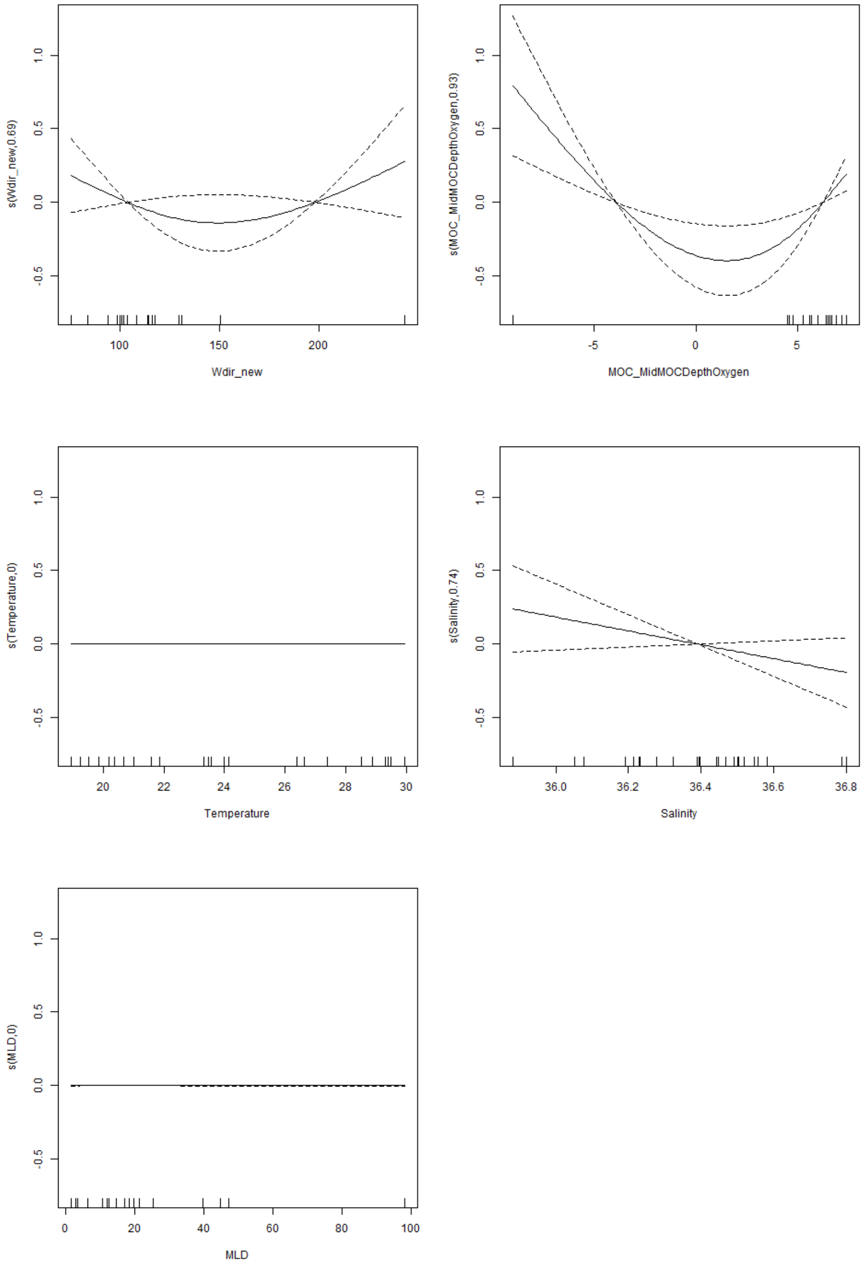

Figure 3.6 (continued): Smooth terms for the GAM of the oldest age class of Scaridae. The x-axis is the values of the covariate, while the y axis is the smooth and the edf, (estimated degrees of freedom). Standard error bounds are indicated with the dashed lines. Smooth terms are in the following order: average wind direction, mid-depth oxygen layer, temperature, salinity, and mixed-layer depth.

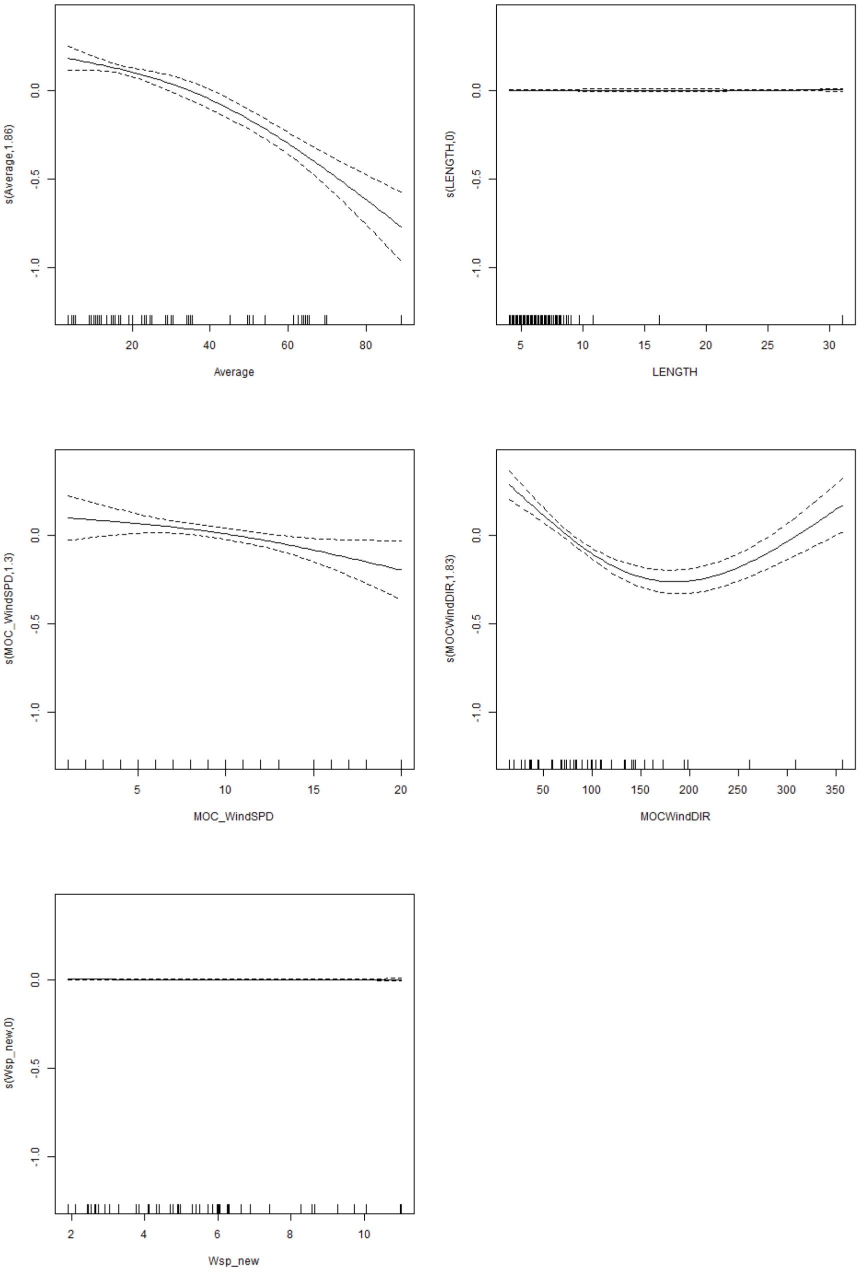

Figure 3.7: Smooth terms for the GAM of the oldest age class of Scombridae. The x-axis is the values of the covariate, while the y axis is the smooth and the edf, (estimated degrees of freedom). Standard error bounds are indicated with the dashed lines. Smooth terms are in the following order: depth of sample, length, instantaneous wind speed, instantaneous wind direction, and average wind speed,

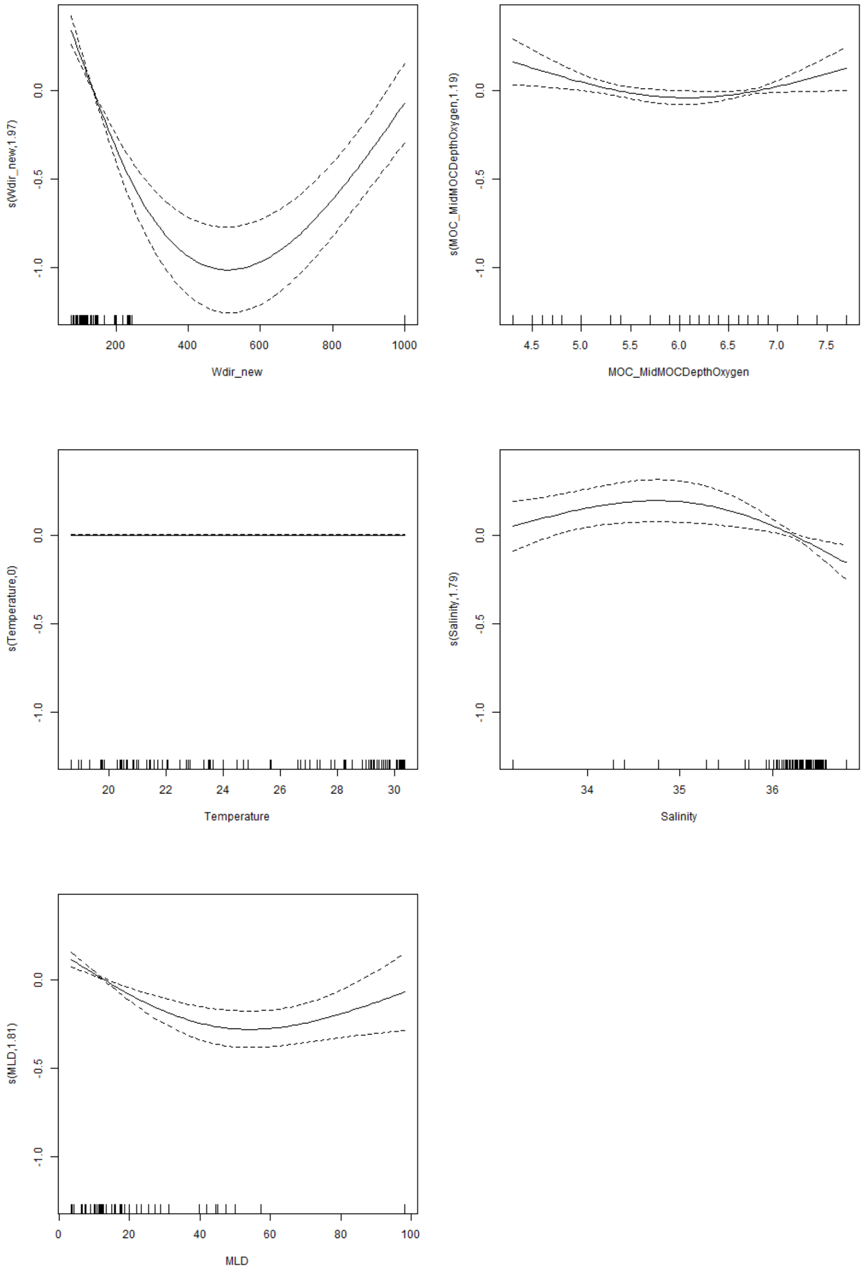

Figure 3.7 (continued): Smooth terms for the GAM of the oldest age class of Scombridae. The x-axis is the values of the covariate, while the y axis is the smooth and the edf, (estimated degrees of freedom). Standard error bounds are indicated with the dashed lines. Smooth terms are in the following order: average wind direction, mid-depth oxygen layer, temperature, salinity, and mixed-layer depth.

While each taxon has its own unique set of environmental predictors, some variables regularly showed high significance. Out of the linear predictor variables, longitude was highly significant values for close to two-thirds of the ten taxa ($p<0.001$) for all three age classes (Figure 3.8 and 3.9). Latitude was significant at the $p<0.05$ level or higher for close to two-thirds of the ten taxa for the first two age classes, but was less important in the third age class. The intercept was also significant in two thirds of the taxa for all age classes. The intercept is not an ecological predictor variable, but rather is a drive parameter. Out of the smoothed predictor variables, depth was the most common highly significant variable among the ten taxa for all age classes at the $p<0.001$ level for half of the ten taxa or more for each age class, and at the $p<0.05$ level for two thirds or more of the taxa at each age class. Wind speed was also a highly important predictor variable at the $p<0.001$ level for five out of the ten taxa at every age class, and at the $p<0.05$ level for close to two thirds of the taxa (Figure 3.8 and 3.9). The other two variables that were significant at the $p<0.05$ level or lower for half or more taxa at every age class were wind direction and mid-depth oxygen (Figure 3.8 and 3.9).

In addition to those trends, the first and second age classes also showed some additional significant variables. In the first age class, average wind direction and salinity were significant ($p<0.05$) for two thirds or more of the taxa, average wind speed was highly significant ($p<0.001$) for half of the taxa, and temperature was significant ($p<0.05$) for half of the taxa. In the second age class, average wind speed, average wind direction, and the mixed-layer depth were significant predictors at the $p<0.05$ level or above for at least half of the taxa (Figure 3.8 and 3.9).

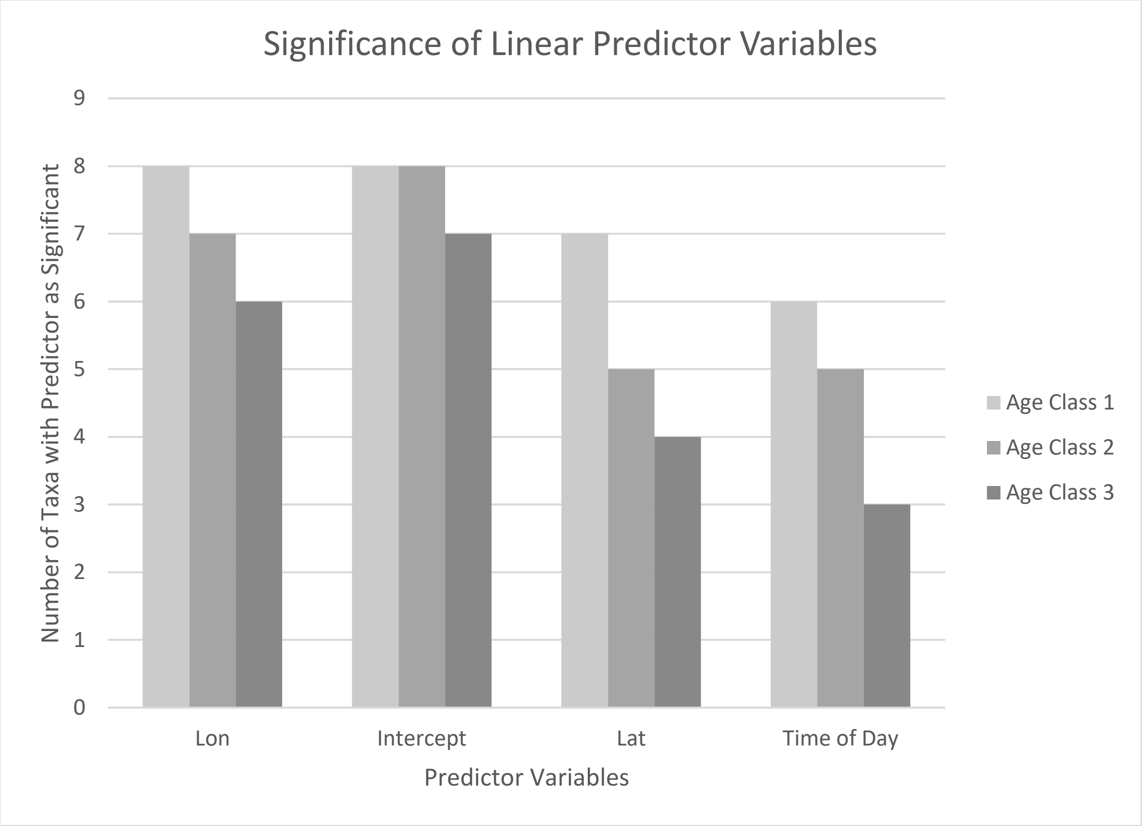

Figure 3.8: Importance of linear variables among all taxa by age class

Standard deviations typically remain within one order of magnitude of the predicted concentrations with a few exceptions (Table 3.1). The first age classes of Scombrids and Ophicthidae and the second age class of Ophididae had very low standard deviations, indicating a leptokurtic distribution. Early ages of Lutjanids, the last age class of *Euthynnus alleteratus*, and the second age class of Scombrids had standard deviations on the same order of magnitude as the predictions, indicating platykurtic distribution. This shift from a leptokurtic distribution in the first age class to a platykurtic distribution in the second age class of Scombrids is also reflected in the depth at age plot, as the higher concentrations of larvae, represented by yellow in the figure, are all condensed around the depth of the maximum in the first age class but spread out throughout the upper water column in the second and third age classes (Figure 3.3).

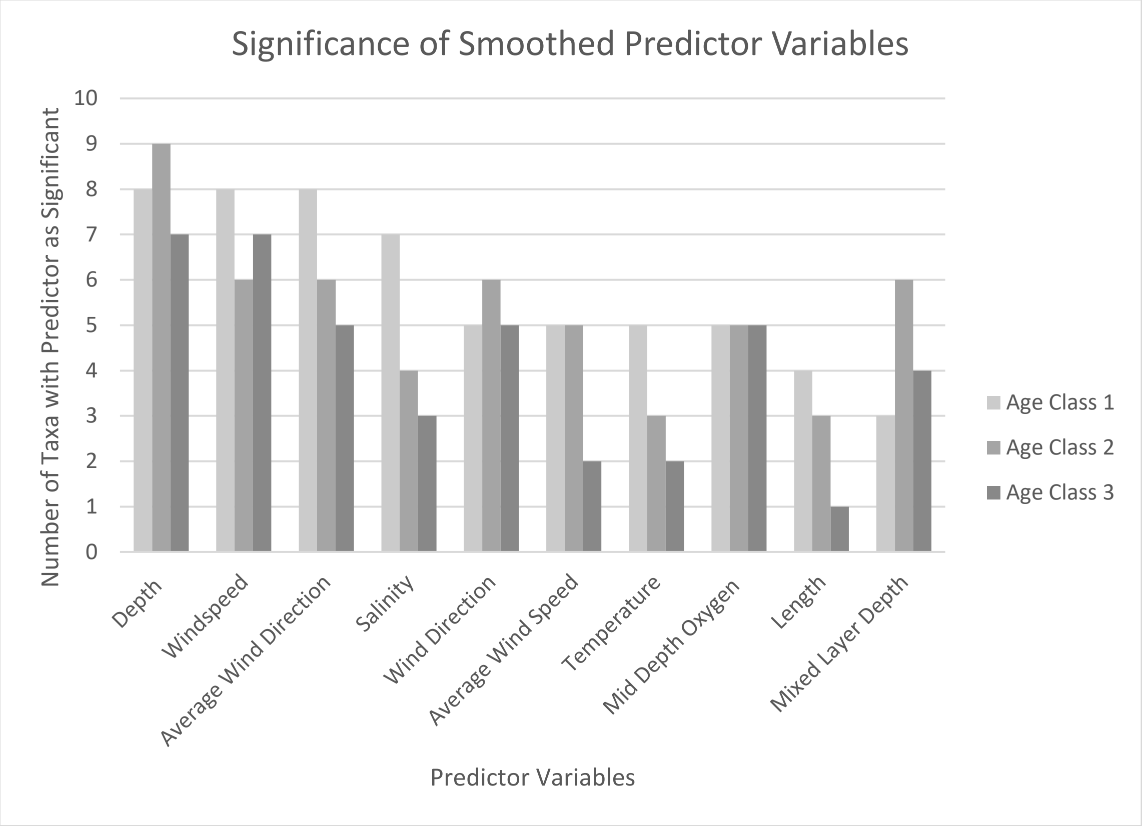

Figure 3.9: Importance of smooth variables among all taxa by age class

Discussion

Depth at age plots for the 10 chosen taxa indicate that there is not one universal ontogenetic pattern for larval vertical distribution in the GOM (Appendix 2). Using larval depth at age in conjunction with hydrodynamic or ecosystem models is one way of including larval behavior in modeling. Faillettaz et al. (2018) compared passive larval tracking modeling scenarios with models where directional orientation in larval swimming behavior were parameterized and found that larval settlement success was better when swimming behavior was added, but also parameterized their model so that swimming behavior was unimportant before flexion. Other studies have shown that larvae demonstrate ontogenetic shifts in vertical distribution and swimming capabilities, that the ability to orient develops early on, and that they may even be able to orient using magnetic fields (Leis et al. 2010, O'Connor and Muheim 2017). Including ontogenetic vertical depth shifts in dispersal modeling allows larval movement to be represented.

Both the importance of wind related variables for most taxa and the suggestion that some taxa are following different depth fidelity strategies point to the importance of wind in the process of larval dispersal. Upwelling and downwelling patterns on the West Florida Shelf (WFS) show synoptic and seasonal variability and current patterns change in response to forcing by winds (Weisberg et al. 2001, Liu and Weisberg 2007). Winds are usually upwelling favorable from fall through spring, downwelling favorable in the summer time, and favor upwelling in the long-term average (Weisberg et al. 2009, Liu and Weisberg 2012). There is also inter-annual variability in the Loop Current and variability in its interaction with waters on the West Florida Shelf. Anomalous upwelling has also been found to occur on the WFS (Liu et al. 2016, Weisberg et al. 2016). Variability in hydrodynamic patterns would impact larval dispersal if larvae were highly concentrated in a particular layer of the water column. For example, larvae travelling in the bottom layers would be transported towards shore during an upwelling event, but transported away from shore during a downwelling event, potentially pushing them into oceanic areas and away from suitable habitat. If instead larvae were scattered throughout the water column, some larvae would be transported towards shore no matter which hydrodynamic pattern was dominant. Taxa employing this technique would thereby have a moderate year class strength, but would be protected against anomalous wind forcing or variability, whereas larvae highly concentrated at a specific depth might ensure strong year classes in years when the hydrodynamic conditions are favorable to transport to nursery habitat, but risk having the entire year class lost at sea if an anomalous, aberrant-drift event occurs. Variability in wind can also influence other environmental factors that impact larval dispersal through the impacts of currents. Wei et al. (2015) compared changes in environmental variables that were shown to impact squid using GAM models to average geostrophic currents from the same time frames and posited that these currents were driving the variability in the environmental factors being modeled. Thus, wind may be driving other variables that are not included in our models, but are impacting the depth distribution of larvae in our study.

These GAM results also further elucidate the relationship between environmental variables and larval depth distribution. While wind and mixed-layer depth are important predictors regardless of taxon, other environmental predictors such as temperature, salinity, and mid-depth dissolved oxygen concentration differ greatly in their impact depending on the taxonomic group. This indicates that a suite of environmental variables is needed to accurately model larval depth distribution at age. The flexibility of the smoothing functions is desirable for representing common domed relationships between environmental predictors and the response variables. A dome could represent an optimal temperature range, for example. The significance of the environmental variables in predicting depth distribution at age may be related to their relationship to factors impacting larval dispersal. For example, latitude and longitude may be important linear predictors, because the geographic position of the larvae is directly related to which currents they will be exposed. Likewise, water depth could be an important smoothed variable for the same reason: different currents occur at different depths. Instantaneous wind speed and instantaneous wind direction were important for all ages, and average wind speed and average wind direction were important for the first and second age classes, potentially due to the relationship between wind and currents. Wind is a primary driver for currents, including upwelling and downwelling patterns on the West Florida shelf (Weisberg et al. 2001, Liu and

Weisberg 2007). The impact of average wind speed and direction tapering off during the last age class, while instantaneous wind speed and direction remain important, could be due to enhanced swimming behavior by older larvae. Older, more developed larvae may be able to better select their depth distribution regardless of synoptic scale patterns, while still needing to adjust to gusts and storms. Temperature and salinity were often only important predictors in the first age class, which could indicate that buoyancy is playing a larger role in this age class due to the lack of swimming behavior in younger larvae; young larvae could be using buoyancy to regulate depth instead. Mixed-layer depth is only an important predictor in the second age class, which could be due to the onset of feeding.

Two factors that are important to larval migration but which are not explicitly included in these predictions are diel vertical migration and food availability. The first, diel vertical migration, is related to the timescale of sampling. In addition to occupying diverse depths during different ages, some species' distribution changes based on the time of day. For example, damselfish larvae have been found to migrate to shallower depths at night (Huebert et al. 2010). The diel vertical migration of the larvae of Gulf of Mexico commercial and recreational fisheries species is largely unstudied. These models include both day and night values, because there was not have enough data to build separate models for different times of day. The sampling protocols of SEAMAP surveys do not support investigations of changes in larval diel vertical distribution. Samples are collected from each station no matter what time of day, without repeat sampling at the other side of the diel period (i.e., no sampling at night for a day sample). Time of day was one of the least important linear predictors in the GAMs, and in the case that there was a large difference between day and night values, this would be captured in our methodology as a wider distribution in the predictions. Another possible driver for distribution that was not captured explicitly in these models was food availability. Feeding is an important factor for decisions made by larvae during early life and was even originally thought to be the driver for recruitment in Hjort's Critical Period Hypothesis, which posits that year class strength is predicated on the ability of newly post-yolk sac larvae to find food (Houde 2008, Hjort 1914). While we now know that the drivers for recruitment are more complex, food is still important for growth and survival after the depletion of the yolk sac.   We represented food availability in the GAMs only indirectly via the proxy of Mixed Layer Depth (MLD) . Unfortunately, it is not practical to represent food density explicitly since plankton blooms can be transient and ephemeral, moving in a matter of hours. Including bloom presence in a model would not lend itself well to predictive ability in other areas. MLD and other environmental variables included here can impact food availability.   Models with Pearson's correlation coefficients under 0.4 are all models that were built with less than 100 data points. *Hemanthias*, which had the lowest Pearson's value, also had the least number of data points out of all of the models. Some taxa with higher variance require larger data sets to accurately represent the distribution of larvae in the water column.

The kurtosis of the predictions for an age class may indicate differing levels of fidelity to their preferred depths. Leptokurtic distributions such as that of the early ages of Scombridae, Ophicthidae, and Ophidiidae may point to a high fidelity for the depths at which they are transported during their larval period. In other cases, such as early ages of Lutjanids, uniform distributions could indicate that larvae are scattered throughout the water column. This could be due to well mixed water or it could be that our sampling depth bins are too large to discern the fine scale distribution patterns and the models are unable to predict the patterns here. It is possible that the difference in apparent fidelity between taxa could be indicative of two differing life history strategies: one in which larvae concentrate at a specific depth and one in which larvae are scattered throughout the water column. Larvae with high kurtosis, or high fidelity to certain depth layers, may be adapted to rely on the hydrodynamic features of these depth layers to find suitable habitat. Further research (Chapter 4) uses these depth-at-age relationships in a Lagrangian trajectory model to help determine what currents influence larvae at different life stages and identify potential spawning and settlement areas, adding a realistic expression of vertical migration behaviors to the dispersal model.

While the knowledge of larval depth at age is useful in understanding early life history strategies and behavior for a variety of taxa, it also has important applications in management. These depth-at-age predictions were developed for use in future work with circulation data from a model are useful for Lagrangian transport calculations and developing hydrodynamic model, with the aim of developing larval trajectories and a matrix of larval spawning and settlement sites for the Gulf of Mexico. These depth at age profiles will be used in conjunction with the hydrodynamic model WFCOM (Weisberg et al. 2014b) to track the larval trajectory of all ten taxa and identify larval sources and sinks for the Gulf of Mexico. Identifying larval sources and sinks has management implications for Marine Protected Area siting, increasing understanding of recruitment dynamics, improving conservation and restoration efforts, and determining differences in transport strategies between taxa. By categorizing sources and sinks, it may be possible to identify potential spawning and nursery habitats for these taxa, which would aid in stock assessment and fisheries management.

Acknowledgements

I would like to thank the South East Area Monitoring and Assessment Program (SEAMAP) ichtyoplankton surveys and the Ocean Circulation Group at University of South Florida for providing data for these models. Funding for K. Vasbinder was provided by the Presidential Doctoral Fellowship from the University of South Florida, Office of Graduate Studies. Partial funding for C. Ainsworth was provided by the Gulf of Mexico Research Initiative through the C-IMAGE III consortium (GRI2001-I-072) and by NOAA through the Marine Resource Assessment Program at USF (95-NA10OAR4320143).

References

Ainsworth, C.H., Schirripa, M.J., and Morzaria -Luna, H. (eds.) 2015. An Atlantis ecosystem model for the Gulf of Mexico supporting integrated ecosystem assessment. NOAA Technical Memorandum. NMFS-SEFSC-676, 149 p. doi: 10.7289/V5X63JVH.

Ainsworth, C.H., Morzaria-Luna, H., Kaplan, I.C., Levin, P.S., Fulton, E.A., Cudney-Bueno, R., Turk-Boyer, P., Torre, J., Danemann, G.D., Pfister, T.2012. Effective ecosystem-based management must encourage regulatory compliance: A Gulf of California case study. Mar. Policy 36:1275–1283.

Arnold, D., P. Wagner, Baayen, R.H. 2013. Using generalized additive models and random forest to model prosodic prominence in German. Interspeech Conference, Lyon, France: 272-276.

Augustin, N., Sauleau, E-A., Wood, S. 2012. On quantile-quantile plots for generalized linear models. Comput. Stat. Data An. 56(8):2404-2409.

Bennett, N.J., Dearden, P. 2014. From measuring outcomes to providing inputs: governance, management, and local development for more effective marine protected areas. Mar. Policy 50:96–110.

Chassignet, E.P, Hurlburt, H.E., Metzger, E.J., Smedstad, O.M., Cummings, J.,Halliwell, G.R., Bleck, R., Baraille, R., Wallcraft, A.J., Lozano, C., Tolman, H.,Srinivasan, A., Hankin, S., Cornillon, P., Weisberg, R., Barth, A., He, R., Werner, C.,Wilkin, J., 2009. U.S. GODAE: global ocean prediction with the Hybrid Coordinate Ocean Model (HYCOM). Oceanography 22, 48–59.

Chen, C.S., Liu, H., Breadsley, R.C., 2003. An unstructured, finite-volume, three dimensional primitive equation ocean model: application to coastal ocean and estuaries. J. Atmos. Oceanic Technol. 20, 159–186.

Cohen, J.H., and Forward, R.B. 2009. Zooplankton Diel Vertical Migration — A Review of Proximate Control. In: R. N. Gibson, R. J. A. Atkinson, and J. D. M. Gordon, Ed. Oceanography and Marine Biology: An Annual Review 47: 77-110 © Taylor & Francis.

Colin, P.L., Koenig, C.C., Laroche, W.A. 1996. Development from egg to juvenile of the Red Grouper (*Epinephelus morio*) (Pisces: Serranidea) in the Laboratory. Pp 399-414. In F. Arreguin-Sanchez, J.L. Munroe, M.C. Balgos, and D. Pauly (eds.) Biology, fisheries, and culture of tropical groupers and snappers. ICLARM Conf. Proc. 48, 449p.

Costelloa, C., Rassweilerb, A., Siegelc, D., De Leod , G., Michelie, F., Rosenbergf, A.. 2010. The value of spatial information in MPA network design. Proc. Natl. Acad. Sci. 107(43):18294-18299.

Dagg, M.J., Govoni, J.J. 1996. Is ichthyoplankton predation an important source of copepod mortality in subtropical coastal waters? Mar: Freshwater Res.47:37-44

D'Allessandro, E.K., Sponaugle, S., Serafy. J.E. 2010. Larval ecology of a suite of snappers (family:Lutjanidae) in the Straits of Florida, western Atlantic Ocean. Mar. Ecol. Prog. Ser. 410: 159–175.

Donahue, M.J., Karnauskas, M., Toews, C., Paris, C.B. 2015. Location isn't everything: timing of spawning aggregations optimizes larval replenishment. PLoS ONE 10(6): e0130694.

Drexler M., Ainsworth, C.H. 2013. Generalized additive models used to predict species abundance in the Gulf of Mexico: An ecosystem modeling tool. PLoS ONE 8(5): e64458. doi:10.1371/journal.pone.0064458

Faillettaz R., Paris, C.B., Irisson, J-O. 2018. Larval Fish Swimming Behavior Alters Dispersal Patterns From Marine Protected Areas in the North-Western Mediterranean Sea. Front. Mar. Sci. 5:97. doi: 10.3389/fmars.2018.00097

Fiksen, O., Jørgensen, C., Kristiansen, T., Vikebø, F., and Huse, G. 2007. Linking behavioural ecology and oceanography: larval behaviour determines growth, mortality and dispersal. Mar. Ecol. Prog. Ser. 347: 195–205.

Forward, R.B. and Tankersley, R.A. 2001. Selective Tidal-Steam Transport of Marine Animals. In: Oceanography and Marine Biology: an Annual Review 39:305–353 © R.N.Gibson, Margaret Barnes and R.J.A.Atkinson, Editors Taylor & Francis

Fulton, E.A., Parslow, J.S., Smith, A.D.M., Johnson, C.R. 2004. Biogeochemical marine ecosystem models. 2. The effect of physiological data on model performance. Ecol. Model., 173, 371-406.

Fulton, E.A., Smith, A.D.M., Smith, D.C. 2007. Alternative management strategies for Southeast Australian Commonwealth fisheries: Stage 2: Quantitative management strategy evaluation. Australian fisheries management authority. Fisheries Research and Development Corporation.

Gruss, A., Drexler, M., Ainsworth, C. 2014. Using delta generalized additive models to produce distribution maps for spatially explicit ecosystem models. Fish. Res. 159 (2014) 11–24

Guisan, A., Edwards Jr., T., Hastie, T. 2002. Generalized linear and generalized additive models in studies of species distributions: setting the scene. Ecol. Model. 157: 89-100.

Govoni, J.J., Ortner, P.B., Al-Yamani, F., Hill, L.C. 1986. Selective feeding of spot, *Leiostomus xanthurus*, and Atlantic croaker, *Micropogonias undulatus*, larvae in the northern Gulf of Mexico. Mar. Ecol. Prog. Ser. 28: 175-183

Govnoni, J.J., Churchill, B.G. 1992. The surface accumulation of larval fishes by hydrodynamic convergence within the Mississippi River plume front. Cont. Shelf Res. 12(11):1265 1276

Hastie, T., Tibshirani, R. 1986. Generalized additive models. Statistical Science 1(3): 297-310.

Hastie, T., Tibshirani, R. 1990. Generalized additive models. London: Chapman and Hall.

Hastie, T., Tibshirani. R. 1995. Generalized additive models for medical research. Stat. Med. Res. 4(3):187-196.

Heppell, S. S., Heppell, S.A., Coleman, F.C., Koenig, C.C. 2006. Models to compare management options for a protogynous fish. Ecol. Appl. 16(1): 238–249.

Hjort, J. 1926. Fluctuations in the year classes of important food fishes. J. Cons. Int. Explor. Mer., 1: 5-39.

Houde, E. D. 2008. Emerging from Hjort's Shadow. J. Northw. Atl. Fish. Sci., 41: 53–70. doi:10.2960/J.v41.m634

Huebert, K.B., Sponaugle, S., Cowen, R.K. 2010. Predicting the vertical distributions of reef fish larvae in the Straits of Florida from environmental factors. Can. J. Fish. Aquat. Sci. 67: 1755–1767. doi:10.1139/F10-116.

Karnauskas, M., Paris, C.B. Zapfe, G., Gruss, A., Walter, J.F., Schirripa, M.J. 2013. Use of the Connectivity Modeling System to estimate movements of Gag Grouper (*Mycteroperca microlepis*) recruits in the northern Gulf of Mexico. SEDAR33-DW18.SEDAR, North Charleston, SC. 12 pp.

Karnauskas, M., Walter, J.F., Paris, C.B. 2013. Use of the Connectivity Modeling System to estimate movements of Red Snapper (*Lutjanus campechanus*) recruits in the northern Gulf of Mexico. SEDAR31-AW10.SEDAR, North Charleston, SC. 20 pp.

Lanaaya, F., St-Hilaire, A., Gloaguen, E. 2017. Water temperature modelling: comparison between the generalized additive model, logistic, residuals regression and linear regression models, Hydro. Sci. J., 62:7, 1078-1093, DOI: 10.1080/02626667.2016.1246799

Leis, J. M. 2010. Ontogeny of behavior in larvae of marine demersal fishes. Ichthyol. Res. 57:325–342 DOI 10.1007/s10228-010-0177-z

Liu, Y., Weisberg, R.H. 2007. Current Patterns on the west Florida shelf from joint self -organizing map analyses of HF radar and ADCP data. J. Atmos. Oceanic Technol. 24:702-712.

Liu, Y., Weisberg, R.H. 2012. Seasonal variability on the West Florida Shelf, Prog. Oceanogr. 104:80-98, doi:10.1016/j.pocean.2012.06.001.

Liu, Y., Weisberg, R.H., Vignudelli, S., Mitchum, G. 2016. Patterns of the loop current system and regions of sea surface height variability in the eastern Gulf of Mexico revealed by the self-organizing maps. J. Geophys. Res-Oceans 121:2347-2366.

Marra, G., Wood, S. N. 2011. Practical variable selection for generalized additive models. Comput. Stat. Data An. 55(7):2372-2387

Moisen, G., Fresino, T. 2002. Comparing five modelling techniques for predicting forest characteristics. Ecol. Modell. 157: 209-225.

National Marine Fisheries Service. 2014. 3rd Quarter 2014 Update Table A. Summary of Stock Status for FSSI Stocks. Web. Accessed Jan 28 2015. http://www.nmfs.noaa.gov/sfa/fisheries_eco/status_of_fisheries/archive/2014/third/q3_stock_status_tables.pdf .

NOAA Fisheries. 2013. Status of Stocks 2013: Annual Report to Congress on the Status of U.S. Fisheries. A publication of the U.S. Department of Commerce, Penny Pritzker, Secretary of Commerce National Oceanic and Atmospheric Administration, Kathryn D. Sullivan, Ph.D., Under Secretary of Commerce for Oceans and Atmosphere, National Marine Fisheries Service, Eileen Sobeck, Assistant Administrator for Fisheries. Web. Accessed Jan 28 2015. http://www.nmfs.noaa.gov/sfa/fisheries_eco/status_of_fisheries/archive/2013/status_of_stocks_2013_web.pdf.

O’Connor, M.I., Bruno, J.F., Gaines, S.D., Halpern, B. S., Lester, S.E., Kinlan, B. P., Weiss, J.M. 2007. Temperature Control of Larval Dispersal and the Implications for Marine Ecology, Evolution, and Conservation. Proc. Natl. Acad. Sci. 104(4):1266-1271.

O'Connor, J., Muheim, R. 2017. Pre-settlement coral-reef fish larvae respond to magnetic field changes during the day. J. Exp. Biol. 220: 2874-2877 doi:10.1242/jeb.159491

Pineda, J. and Reyns, N. 2018. Larval transport in the coastal zone: biological and physical processes. In. Evolutionary Ecology of Marine Invertebrate Larvae. Edited by Carrier, T.J., Reitzel, A.M., Heyland, A. : Oxford University Press. © Oxford University Press. DOI: 10.1093/oso/9780198786962.003.0011

Porch, C.E., Fitzhugh, G.R., Land, E.T., Lyon, H.M., Linton, B.C. 2015. Estimating the dependence of spawning frequency on size and age in the Gulf of Mexico red snapper. Mar. Coast. Fish. 7:233-245.

Powell, A.B., Tucker, J.W., Jr. 1992. Egg and larval development of laboratory-reared Nassau grouper, *Epinephelus striatus* (Pisces, Serranidae). Bull. Mar. Sci., *50*(1), 171-185.

Rubec, P.J., Kiltie, R., Leone, E., Flamm, R.O., McEachron, L. Santi, C.. 2016. Using Delta generalized additive models to predict spatial distributions and population abundance of juvenile pink shrimp in Tampa Bay, Florida. Mar. Coast. Fish 8:1, 232 243, DOI: 10.1080/19425120.2015.1084408

Savina, M., Condie, S.A., Fulton, E.A. 2013. The Role of Pre-Existing Disturbances in the Effect of Marine Reserves on Coastal Ecosystems: a Modeling approach. PLoS One, DOI: 10.1371/journal.pone.0061207.

Shih, C-L, Chen, Y-H., Hsu, C-C. 2014. Modeling the Effect of Environmental Factors on the Ricker Stock-Recruitment Relationship for North Pacific Albacore Using Generalized Additive Models. Terr. Atmos. Ocean. Sci. (25): 581-590.

SEDAR. 2013. SEDAR 31 – Gulf of Mexico Red Snapper Stock Assessment Report. SEDAR, North Charleston SC. 1103 pp. Available online at: http://www.sefsc.noaa.gov/sedar/Sedar_Workshops.jsp?WorkshopNum=31

Tanskanen, J., Taipale, S., Antilla, T. 2016. Revealing Hidden Curvilinear Relations Between Work Engagement and Its Predictors: Demonstrating the Added Value of Generalized Additive Model (GAM). J. Happiness Stud. 17:367-387.

Vasbinder, K., Ainsworth, C. 2020. Early Life History Growth in Fish Reflects Consumption -Mortality Tradeoffs. Fish. Res. 227:105538.

Von Bertalanffy, l. 1938. A Quantitative Theory of Organic Growth (Inquiries on Growth Laws II). Hum. Biol. 10(2):181-213.

Watson, J. R., S. Mitarai1, D. A. Siegel, J. E. Caselle , C. Dong, J. C. McWilliams. 2010. Realized and Potential Larval Connectivity in the Southern California Bight. Mar. Ecol. Prog. Ser. 401:31-28.

Wei, Y., Xinjun, C., Yong, C., Qian, Y., Yang, Z. 2015. Effects of environmental variations on the abundance of western winter-spring cohort of neon flying squid(*Ommastrephes bartramii*) in the Northwest Pacific Ocean. Acta. Oceanol. Sin., 2015,34(8):43–5. doi: 10.1007/s13131-015-0707-7

Wei, Y., Xinjun, C., Qian, Y. 2016. Inerannual and Seasonal Variability of Winter-SpringCohort of Neon Flying Squid Abundance in the Northwest Pacific Ocean During 1995-2011. J. Ocean Univ. China (Oceanic and Coastal Sea Research) 15(3):480-488.

Weijerman M., Fulton E.A., Brainard, R.E. 2016. Management strategy evaluation applied to coral reef ecosystems in support of ecosystem-based management. PLoS ONE 11(3): e0152577. doi:10.1371/journal.pone.0152577.

Weisberg, R. H., Li, Z., Muller-Karger, F. 2001. West Florida shelf response to local wind forcing: April 1998. J. of Geophys. Res. 106(12):31239-31,236.

Weisberg, R.H., Liu, Y., Mayer, D.A. 2009. Mean circulation on the west Florida continental shelf observed with long-term moorings, Geophys. Res. Lett. 36:L19610, doi:10.1029/2009GL040028.

Weisberg, R.H., Zheng, L. Liu, Y., Murawski, S., Hu, C., Paul, J. 2014. Did Deepwater Horizon hydrocarbons transit to the west Florida continental shelf? Deep-Sea Res. II http://dx.doi.org/10.1016/j.dsr2.2014.02.002i.

Weisberg, R. H., Zheng, L., Peebles, E.. 2014. Gag grouper larvae pathways on the West Florida Shelf. Cont. Shelf Res. *88* :11–23. doi: http://dx.doi.org/10.1016/j.csr.2014.06.003

Weisberg, R. H., Zheng, L. Liu, Y. 2016. West Florida Shelf upwelling pathways. J. of Geophys. Res.: Oceans 121:5672-5681.

Weninger, Q., Water, J. R. 2003. Economic benefits of management reform in the northern Gulf of Mexico reef fish fishery. J. Environ Econ. and Manage. 46:207–230.

Wood, S.N. 2003. Thin plate regression splines. J. R. Statist. Soc. B 65(1):95-114.

Wood, S.N. 2016. Mixed GAM Computation Vehicle with GCV/AIC/REML smoothness estimation. From: https://stat.ethz.ch/R-manual/R-devel/library/mgcv/html/gam.html

Yee, T.W., Wild, C.J. 1996. Vector Generalized Additive Models. J. R. Statist. Soc. B (Methodological). Vol. 58, No. 3. Pp. 481-493.

Zheng, L., Weisberg, R.H. 2012. Modeling the West Florida coastal ocean by downscaling from the deep ocean, across the continental shelf and estuaries. Ocean Model. 48:10 -29.

Chapter 4: Gulf of Mexico Larval Dispersal

Abstract

This chapter makes use of a custom-made Lagrangian larval dispersal model and two published modeling systems: the West Florida Coastal Ocean Model (WFCOM) hydrodynamic model and the Atlantis biogeochemical end-to-end ecosystem model. Depth occupancy at age by larval taxon has been previously modeled and was used to draw WFCOM current field data. These current data inform the dispersal model that uses numerical time step integration. Dispersal models can be done at family level resolution for Scaridae, Lutjanidae, Scombridae, Labridae, Ophichthidae, and Ophidiidae, at the genus level for *Hemanthias,* and at species level resolution for the species *Trachurus lathami, Decapterus punctatus, Katsuwonus pelamis,* and *Euthynnus alleteratus.* These spawning and settlement sites were then used to update the connectivity matrix in the Atlantis GOM model, which is used to apportion the young of year spatially. I compare dispersal and non-dispersal scenarios in Atlantis and find differences in production, indicating the importance of including dispersal in our model. This project lies at the intersection of predictive statistical modeling, hydrodynamic modeling, and ecosystem modeling. It represents an interdisciplinary approach to understanding larval dynamics and their impacts on ecosystems.

Introduction

Coupling Hydrodynamic Models to Investigations of Lagrangian Dispersal

There is a rich history in the use of numerical and hydrodynamic models for the study of larval dispersal. Several of these studies have occurred in the southern United States. A numerical model incorporating Lagrangian drift, based on currents and turbulence with larval horizontal swimming behavior, was used in 1997 to simulate larval settling and identify hydrodynamic processes which would allow larvae to be retained on the southeast coast of Florida (Porch 1997). A circulation model with wind and tidal forcing was used to study the accuracy of Lagrangian trajectory modeling along the southeastern U.S. continental shelf, and found that modeled tracks agreed well with the tracks of released drifters, with both showing the potential for larval retention on the shelf (Edwards 2006). The Florida Keys Regional Oceanic Modeling System (FK-ROMS) has been used in conjunction with a Lagrangian dispersal model to investigate larval dispersal in the Florida Keys (Fiechter et al. 2008). Despite these studies in the southern Atlantic Ocean and Florida Keys, an extensive 2007 review of the use of coupled physical and biological models in investigations of recruitment found only one study in the GOM (Miller et al. 2007). This number has increased over the last decade to include several gag grouper and red snapper studies in the GOM as well as several studies on the connectivity of reef fish populations using the Connectivity Modeling System (CMS) and the West Florida Coastal Ocean Model (WFCOM) (Karnauskas et al. 2013a, Karnauskas et al. 2013b, Weisberg et al. 2014, Vaz et al. 2016).

The majority of the studies covered by the Miller et al. (2007) review employ an offline approach in which the hydrodynamic model is run first, and then outputs are stored and used in an offline particle tracking model. This is the method that I employ in my dissertation. One challenge of using hydrodynamic modeling to track larvae is that larval behavior is often characterized through laboratory studies that may not represent real world processes, so even complex hydrodynamic models may be unable to accurately predict ichthyoplankton distributions (Miller et al. 2007). My dissertation addresses this concern in the GOM by resolving larval depth at age outside of the dispersal model using a series of predictive models, based on empirical, *in situ* data to parameterize ontogenetic depth changes for a range of taxa (Chapter 3, Vasbinder et al. 2020 in prep). This allows me to include larval depth occupancy and access vertically stratified currents within the hydrodynamic model that would not be resolved if larvae were only seeded at the surface.

Larval Behavior

Hydrodynamic models continue to advance in popularity and usage, but their application in predicting larval dispersal patterns is limited by information on larval behavior. In particular, species or family-level vertical migration behavior are not well documented in the Gulf of Mexico (GOM). Weisberg et al. (2014b) found that Gag larvae travel in the near bottom Ekman layer from their spawning sites to their settlement areas, indicating that larval depth is important to larval transport, as larvae traveling in the near-bottom Ekman layers ended in verifiable Gag settling habitat. Larvae make use of currents at different depths to guide their transport horizontally, making depth at age a key piece to understanding larval dynamics (Pineda et al. 2007). Hydrodynamic studies have shown that larvae traveling in different depth layers would be advected to different locations or in different directions (Werner et al. 1993, Weisberg et al. 2014b). The default assumption that many authors make is that of Lagrangian, or passive, drift transport for larvae (Siegel et al. 2003, Pineda et al. 2007, Gawarkiewicz et al. 2007, Lett et al. 2008).

In the first half of the 20th century, estuarine and coastal biologists working on intertidal and mollusk species began to accept that larvae were not passive drifters and were instead capable of vertical migration and behavior that could change their movement tracks (Pineda et al. 2007). Studies as early as 1971 explored the concept that oyster larval transport was not completely passive, but explicit knowledge of larval fish behavior and vertical migration is still lacking for most species (Woods and Hargis 1971). There are a small number of studies in which taxon-specific information on larval migration and behavior has been incorporated into trajectory modeling, but these efforts need to be expanded in order to incorporate larval behavior into ecosystem management (Karnaukas et al. 2013a and 2013b, Weisberg et al. 2014, Hare et al. 1999, Paris et al. 2005). The goal of our depth at age and dispersal models is to expand the use of larval depth occupancy behaviors to a wider range of taxa for use with the GOM Atlantis model.

WFS Circulation

I used outputs from the West Florida Coastal Ocean Model (WFCOM) to build a larval dispersal model. WFCOM is a model that nests the FVCOM inside the GOM HYCOM. Nested models have previously been used in particle tracking studies in the West Florida Shelf (WFS) and the GOM (Weisberg et al. 2009, Weisberg et al. 2014b). Weisberg et al. (2009) made the case for a coordinated observing and modeling system for the WFS. The WFS is not just impacted by local forcing, but also depends on interactions between the shelf and its two main sources of nutrients, the deep ocean and estuaries, to define circulation and water properties in coastal areas (Weisberg et al. 2009). The deep ocean inputs to circulation on the West Florida Shelf are typically from Loop Current interactions with the shelf. Tides are a dominant circulation feature in estuaries, and they are included in FVCOM to account for estuarine influences so that downscaling into estuaries can be achieved (Zheng and Weisberg 2012).

Circulation is heterogeneous, thus larval connectivity cannot be modeled without accounting for circulation in the specific area of interest. In order to accurately study connectivity on the WFS and in the GOM, I needed to build a dispersal model based on the hydrodynamics in our area, which is why the dispersal model is based on current outputs from WFCOM. All continental shelves are not structured uniformly, and even circulation on a single shelf is heterogeneous. The Burger number (the Rossby radius at the shelf break divided by the shelf width and squared) indicates whether the inner and outer shelves are overlapping or isolated, with smaller numbers indicating isolated inner and outer shelves, as is the case for the WFS (Weisberg et al. 2009). Circulation on the WFS is fully three-dimensional, meaning that along-shelf, across-shelf, and vertical transport all play roles in WFS circulation patterns, even in shallow areas of the shelf (Li and Weisberg 1999a, Li and Weisberg 1999b, Weisberg et al. 2001, Weisberg et al. 2009). Modeling production and connectivity processes on the shelf requires resolution of the shelf environment into at least the inner, mid, and outer shelf regions, based on the dominant terms in the momentum balance (Li and Weisberg 1999b, Weisberg et al. 2009). The outer shelf is where topographic waves occur, due to constraints on the across-isobath flow and the shelf transitions to deep ocean at the shelf break (Weisberg et al. 2001, Li and Weisberg 1999b, Weisberg et al. 2009). The inner shelf is a region where divergence bridges surface and bottom Ekman layers, the mid-shelf is the area between the inner and outer shelf, and the innermost region of the inner shelf, which can be called the nearshore region, is where the inner shelf and estuaries interact (Weisberg et al. 2009). This heterogeneity emphasizes the need for my dispersal model to be based on localized current values with high resolution, such as those produced by WFCOM.

A coordinated observing and modeling system using a WFS hydrodynamic model has been used in previous studies to investigate red tide, because red tide is reliant on both on physical circulation and biological processes (Weisberg et al. 2009). Lagrangian particle modeling of the red tide organism, *Karenia brevis*, revealed that *K. brevis* red-tide events were largely driven not by what occurred at the surface, but by what occurred at depth (Weisberg et al. 2009). The bottom Ekman layer was found to be a major pathway to the near-shore areas for biological materials (Weisberg et al. 2009). Offshore traveling particles occurred in the surface layers, whereas onshore traveling particles came from deep layers and upwelled to the surface once they were closer to shore (Weisberg et al. 2009). Stratification changes where upwelling occurs and produces an asymmetry between upwelling and downwelling responses, where upwelling responses are much stronger (Weisberg et al. 2001, Weisberg et al. 2009). The complex nature of hydrodynamics in the WFS region and the importance of a vertical component in shelf circulation and previous transport studies emphasize the need for larval transport models to be based on well-resolved current data and include a vertical migration component. The newest version of the WFCOM model is a good candidate for use in a larval dispersal model for several reasons, (1) it includes both deep ocean and estuarine influences on the shelf, (2) it has a nested structure, and (3) it has the ability to resolve smaller-scale hydrodynamic processes that impact larvae, due to its high resolution and unstructured nature of the grid in areas closer to shore (Zheng and Weisberg 2012, Weisberg et al 2014b). HYCOM can provide properties that are important for the deep ocean and can impact the shelf, whereas FVCOM’s unstructured grid allows increased horizontal resolution as the domain moves toward shore into estuaries and river mouths, allowing both the deep ocean and inshore features, such as estuaries, to impact the shelf (Zheng and Weisberg 2012).

Project Impacts on Dispersal Modeling

The use of larval connectivity and spatial information in models and management has the potential to increase the reliability of model results and enhance fishery yields, profits, and sustainability (Costelloa et al. 2010, Berger et a. 2017, Goethal et al. 2015, Punt et al. 2015). We now have in hand both the biophysical modeling capacity to accurately estimate larval flows between areas, and the "end to-end" ecosystem models, which allow us to understand the biological and socioeconomic impacts of spatial management actions. Ecosystem models can be used to guide habitat restoration efforts and account for the use of habitat by different life stages (Gruss et al. 2017, O'Farell et al. 2017). This project combines statistical, numerical, and end-to-end ecosystem modeling to identify potential spawning and settlement locations for GOM taxa, through the development of a Lagrangian particle transport model that can simulate the movement of larval particles from spawning to settlement.

For this chapter, I built an original Lagrangian model. I integrate particle trajectories backwards from the larval sampling events to the spawning event, with the age of the particles informed by the growth models in Chapter 2, and the currents drawn from WFCOM at the depths specified by the depth occupancy models in Chapter 3. I also integrate forwards to the settlement event using the estimated larval durations from the GOM Atlantis model (Ainsworth et al. 2015). This modeling effort produces a map of spawning and settlement areas for GOM larvae, which I then use to build a larval connectivity matrix for the GOM Atlantis model polygons. I compare Atlantis scenarios with and without dispersal to demonstrate that the biophysical coupling is necessary to address productivity, distribution, and connectivity questions. By outsourcing the larval transport from Atlantis to my dispersal model, I am able to produce spatial patterns of productivity in Atlantis that are more precise and reflect the present and unique oceanographic conditions in its calculations.

Methods

Overview

The larval dispersal model was built in R using current outputs from WFCOM and the results of a larval depth at age model based on SEAMAP ichthyoplankton sampling from Chapter 3 (Vasbinder et al. in prep, Zheng and Weisberg 2012, Weisberg et al. 2014a). The dispersal model can be run at family level resolution for Scaridae, Lutjanidae, Scombridae, Labridae, Ophichthidae, and Ophidiidae, at genus level resolution for the genus *Hemanthias*, and at species level resolution for the species *Trachurus lathami*, *Decapterus punctatus*, *Katswonus pelamis*, and *Euthynnus alleteratus*.. Currents are computed in a three-dimensional domain and larval movement depends on vertical migration behavior of each taxon, which determines the depth of currents for transport. This dispersal model can be used to track larvae both deterministically and probabilistically in order to identify both the start and end points for specific larvae deterministically and the probabilistic distribution of start and end points. In this chapter, I use the deterministic tracking capabilities.

Characterizing Spawning and Settlement Areas

Using MOCNESS (Multiple Opening/Closing Net and Environmental Sensing System) MOCNESS trawl data from the SEAMAP ichthyoplankton survey data, which gives larval depth and a range of environmental predictors, a set of generalized additive models was constructed to predict larval depth at age with a suite of environmental variables (Chapter 3). By combining knowledge of ontogenetic shifts in depth occupancy with the current direction at those depths, a dispersal model was constructed that tracked larvae iteratively through time to trace their trajectories. Currents used in this dispersal model are from the West Florida Shelf Connectivity Model (WFCOM) (Zheng and Weisberg 2012, Weisberg et al. 2014a). WFCOM downscales from the deep ocean into the continental shelf and estuaries by nesting the unstructured grid of the Finite Volume Coastal Ocean Model known as FVCOM (Chen et al. 2003) inside the structured grid of the GOM HYCOM (Chassignet et al. 2009, Weisberg et al. 2014a). The nesting of these two models allows the grid sizes to be finer on the shelf than in the center of the GOM, allowing for better representation of small-scale processes closer to shore. The original implementation of WFCOM was by Zheng and Weisberg (2012). Water properties are used as state variables and this system has a structure that can integrate local and remote inputs impacting state variables.

FVCOM is nested in HYCOM using one-way nesting, in which the outer model provides boundary values to the inner model. The models fit together using something called a "buffer zone", in which the outer model directly impacts the inner model. Forcing is applied at the open boundary (Weisberg et al. 2009). A weight factor is also defined to indicate what the influence of the outer model is on a specific variable from the inner model inside this buffer zone. This is in contrast to two-way nesting, in which both models draw from each other (Zheng and Weisberg 2012). Weisberg et al. (2014b) extended the domain to directly include Mississippi River outflow and Weisberg et al. (2014a) updated the nested model to place FVCOM inside the Gulf of Mexico HYCOM (GOM HYCOM), instead of the Global HYCOM. The most recent version of WFCOM has 31 sigma layers and a higher resolution of surface boundaries (Weisberg et al 2014b). The model domain of WFCOM can be seen in Figure 4.1.

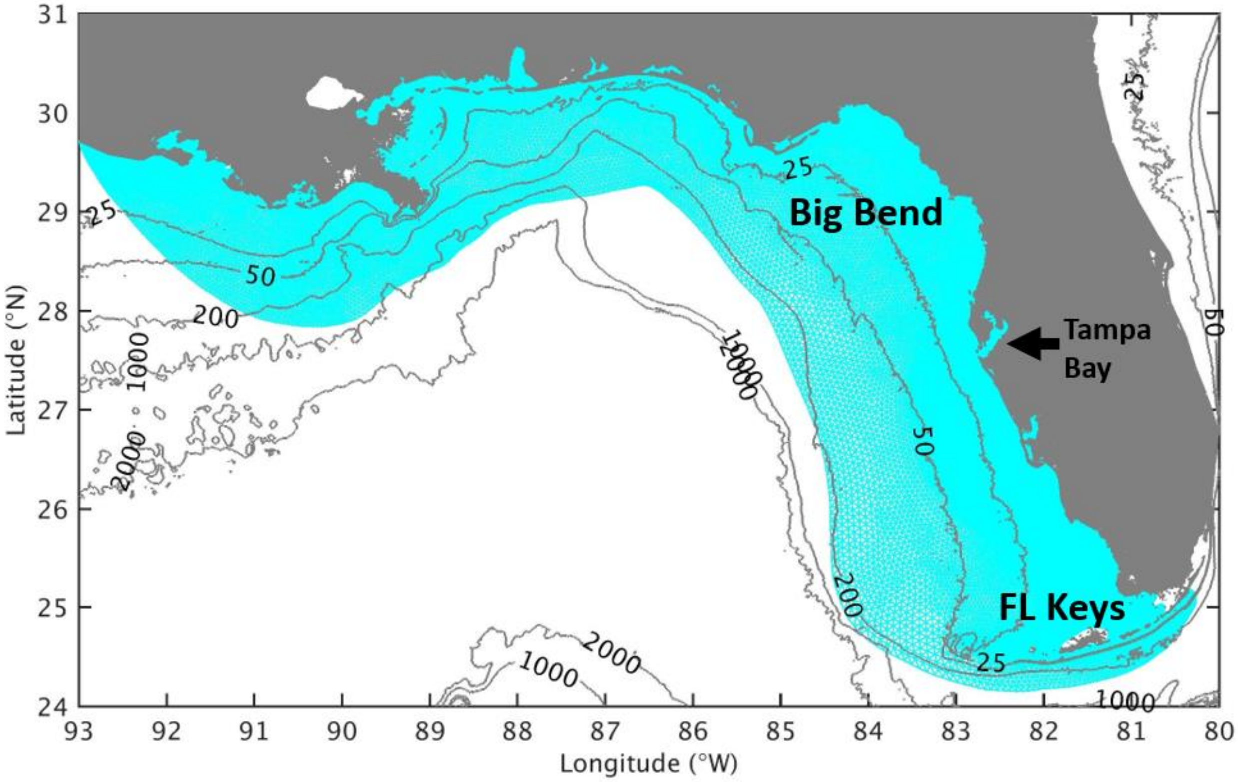

Figure 4.1: WFCOM model domain (adapted from Liu et al. 2020 with permission from author, labels added to denote several locations)

The dispersal model moves larvae through time and space using a fourth order Runge-Kutta (RK4) algorithm. The RK4 algorithm is used to solve ordinary differential equations by evaluating a derivative once at the starting location, twice at mid-point locations, and once at an end-point location, for a total of four derivatives. In particle tracking, this means that a particle is advanced through time by evaluating predictor current trajectories at four different points and solving for a final slope in both the U and V directions using the following equation (Joy 1999):

$$p_{i+1} = p_i + \frac{1}{6}\Delta t({\vec{v}}_i + 2{\vec{v}^1}_{i+1} + 2{\vec{v}^2}_{i+1} + {\vec{v}^3}_{i+1})$$

The current is evaluated at the initial point and several mid-points, then weighted to calculate a final end-point. In the dispersal model, timesteps encompass two hours so that the currents can be evaluated at midpoints of one hour. Larvae are seeded into the model in the closest WFCOM grid location to the SEAMAP sampling location. The RK4 is run forward every two hours from the initial seeding location to the end of the larvae's pelagic larval duration, and run backwards from the initial seeding location to the beginning of the larvae's pelagic larval duration, giving a start and end point for every measured larvae in the SEAMAP ichthyoplankton survey over the course of a six year period. The starting points were used to identify potential spawning locations and the end points were used to determine possible settlement locations. "Settling" is used in this case to refer to a larvae reaching the end of the pelagic larval duration, not the physical act of settling. Larvae are allowed to approach or hit the boundary of the model; they are not explicitly re-directed and are not removed from the model. The ages for the starting points were informed by my Chapter 2 length-at-age models and the ages for the end points were informed by the GOM Atlantis larval durations, which came from a literature review of pelagic durations (Vasbinder and Ainsworth 2020, Ainsworth et al., 2015). I determined the larval duration by comparing the value from the Atlantis review with the age of the oldest larvae from our sample and taking the larger of the two. Larval groups with long larval durations were tracked forward into the following year or backwards into the previous year. Results are designated in this paper by sampling year. The WFCOM current data constitutes a time series from 2006-2012 and includes all sampling events used to build the Chapter 3 depth occupancy models. Thus, as I use forward and backward integration from the sampling time, I am using the actual currents from those days to track the larval particles to their spawning and settling sites.

Atlantis Gulf of Mexico Ecosystem Model

I used the settling and spawning sites determined from the dispersal model to update the larval dispersal matrices for the Gulf of Mexico Atlantis ecosystem model. Atlantis is a spatial biogeochemical food web model (Fulton et al. 2004). Atlantis has modules representing biophysical, oceanographic, human, and policy factors (Fulton et al. 2004, 2007). The GOM Atlantis model is divided into 66 polygons, based on a range of factors including physical features and processes, habitat, and patterns in fishing and resource use (Ainsworth et al. 2015). Most published applications of Atlantis do not employ the larval dispersion mechanisms, and instead distribute Age-1 recruits in proportion to the breeding population of adults. Hereafter, I will refer to this common assumption as the parent-location model. Outsourcing larval transport calculations to a dedicated larval dispersal model is an advantageous approach to improving realism through model coupling (Drexler 2018). Dispersal model results were used to calculate a dispersal matrix between Atlantis polygons for each functional group that was included in my dispersal model. Atlantis can use a 2D matrix of donor and recipient polygons to apportion the new young of year, though it is not used in the determination of the recruit numbers.

Atlantis simulations were then run using the updated larval dynamics. I assessed two scenarios: an experimental scenario with larval dispersal included and a control scenario using the parent-location model.

The GOM Atlantis model was most recently tuned by Morzaria-Luna et al. (2018) to produce an appropriate amount of recruitment under the parent-location assumption. However, when larval dispersal is modeled explicitly, as in the current paper, a much smaller fraction of the entire pool of propagules finds itself in premium habitat. Ocean currents are likely to deliver a portion of the larvae to poor habitat, where there are fewer feeding opportunities and higher risk of predation. Thus, recruitment must be increased in Atlantis to maintain a similar amount of group production relative to the parent-location control simulation. This was achieved by increasing the steepness parameter of the recruitment relationship. All groups use Beverton-Holt recruitment (Ainsworth et al. 2015). The scenarios were run for 10 years to a near-equilibrium state. The change in production in each polygon between the dispersal and control scenarios was calculated and scaled by dividing by the median so that the relative change in production can be observed.

Results

Spawning Locations

The most common area in both spawning and settlement of larvae was the West Florida Shelf (WFS) (Table 4.1, Figures 4.2-4.12). I refer to the area stretching between Mississippi, Alabama, and FL Pan handle/Big Bend as the northeastern Gulf, and the area around and past the Louisiana peninsula as the northwestern Gulf. The spawning areas found from backwards integration are in Figures 4.2-4.12. Bioeroding fish in the Scaridae family spawn along the WFS and in the northern GOM area in all years (Figure 4.2). In 2011, backwards tracking shows most of the larvae originating in the southern WFS and the southern tip of the Florida Keys reef tract (Figure 4.2). *Hemanthias*, a deep-water grouper genus, spawned along the WFS as well as in the northern GOM (Figure 4.3). No *Hemanthias* were present in the 2011 data set (Figure 4.3). In 2007, *Trachurus lathami*, a member of the Jack family, spawned off of the WFS edge and along the FL panhandle (Figure 4.4). In 2009, the spawning shifted northward and reached the Louisiana coastline. In 2010 and 2011, only one data point was available for this species, but both backtracked to waters near the Louisiana coast (Figure 4.4). Another member of the jack family, *Decapterus punctatus*, showed very similar patterns in 2009 and 2010, but was also found along the WFS edge in 2007, 2010, and 2011 and inward towards the coast of central Florida in 2011 (Figure 4.5). *Katsuwunous pelamis*, a large pelagic fish called the skipjack tuna, showed a range of spawning areas (Figure 4.6). In both 2009 and 2011, spawning was in the northwestern GOM, while 2007 and 2010 show spawning in an area off of southern Florida and in the northeastern GOM (Figure 4.6). Eel families Ophicthidae and Ophidiidae also show these clusters of northwestern spawning sites for 2009 and 2011, and both of these families show a mix of northern and northwestern spawners in 2010 (Figures 4.7, 4.8). In 2009, only Ophidiidae shows spawning along the WFS (Figure 4.8). In 2007, both eel families show spawning along the entire WFS and in 2011, both show spawning between central and southern Florida (Figures 4.7, 4.8). Another large pelagic tuna, *Euthynnus alleteratus*, also shows clusters of backtracked spawned larvae in the northwestern GOM for 2009 and 2011 and the cluster of spawning between central and southern Florida in 2011, but in 2010 their spawning is clustered in the northeastern Gulf (Figure 4.9). Lutjanidae, the data-rich family of snappers, had spawning locations off of Louisiana in 2009, 2010, and 2011, as well as on the WFS in 2010 (Figure 4.10). They also showed a group of spawners near central Florida and the FL Keys reef tract in 2011 (Figure 4.10). Scombridae, another data-rich family which includes mackerel, tuna, and bonito, also showed the clusters of spawners in the northwestern GOM in 2009 and 2011 (Figure 4.11). In 2007 and 2009, Scombridae also showed spawners off of northern Florida near the Florida Panhandle, while in 2010 they spawned in the northern GOM similarly to *E. alleteratus*, with one clear different area in the southern WFS (Figure 4.11). In 2011, Scombridae also shows the cluster of spawners from central to southern Florida, while they spawn along the length of the shelf in 2007 (Figure 4.11). Labridae, a reef fish family, shows groups that spawn along the western edges of the WFCOM model domain in 2010, perhaps indicating that they actually spawn in even deeper waters and were constrained by the domain, and other groups that spawn in the northeastern GOM area (Figure 4.12). In 2011, spawning clusters occur in the northwestern GOM and in central and southern Florida across the length of the shelf and into the tip of the Florida Keys, and 2007 shows a similar pattern, but without the western group (Figure 4.12). There are also several groups that spawn just west of Tampa Bay, including Lutjanidae, Scombridae, Scaridae, and both eel families.

Settling Locations

Settling sites were identified by forward integration (Table 4.1, Figures 4.2-4.12). Scaridae settled on the WFS as well as in the northern GOM in all years (Figure 4.2). *Hemanthias* settled on the WFS near central Florida in 2009, and 2010. In 2007 and 2009, there were also settlers in the northwestern GOM (Figure 4.3). The 2007 WFS settlers are more spread out along the shelf than the 2009 and 2010 settlers (Figure 4.3). *T. lathami* also shows settlers all over the shelf edge in 2007 and a group clustered in the northeastern GOM, reaching very close to the Panhandle and Alabama coastline in both 2007 and 2009 (Figure 4.4). In 2009 there is also a group in the northwestern Gulf (Figure 4.4). In 2010, there is one single group off the Panhandle coast, and in 2011, one single group in the northwestern Gulf (Figure 4.4). *D. punctatus* show a cluster of settlers in the northwestern GOM in 2007, 2009, and 2011 (Figure 4.5). In 2007, 2010, and 2011, there are also groups of settlers in the region of the WFS near central Florida and in the FL Keys reef track (Figure 4.5). In 2007, the Keys settlers reach the upper Keys, in 2010, the middle Keys and in 2011, they only reach the tip of the Keys (Figure 4.5). In 2009 and 2011, *K. pelamis* only settles in the northwestern GOM near Louisiana (Figure 4.6). In 2007 they settle in both the northeastern GOM and on the WFS, with 2010 having a group of settling clusters spanning the northeastern GOM and panhandle of Florida and reaching areas close to the Florida coast (Figure 4.6). In 2007, the settlers are clustered on the WFS from central to southern Florida, whereas in 2010 they are clustered near the Keys (Figure 4.6). Eel families Ophichthidae and Ophidiidae show similar patterns in settlement among all four years, settling along the WFS, around the tip of Louisiana in all years except for 2010, and all along the FL Keys reef tract in 2007 and 2011 (Figures 4.7, 4.8). The eel settling groups in the northwestern GOM appear to have reached the edge of the model domain and may have been lost to the ocean if the domain was extended (Figures 7, 8). Two noticeable differences are that in 2009, Ophichthidae on the WFS are closer to the shelf edge and the group near Louisiana is larger, whereas Ophidiidae are spread through the length and width of the WFS, and in 2010, some Ophidiidae reach the FL Keys reefs while Ophichthidae do not (Figures 4.7, 4.8). *E. alleteratus* settles in the northern GOM in all four years, concentrated in the eastern area in 2010 and the western area in 2009 and 2011 (Figure 4.9). In 2007 and 2011, larvae also reach southern areas off the coast of Florida (Figure 4.9). Lutjanids in 2007, 2010, and 2011 show settling off the WFS west of southern FL (Figure 4.10). Settlers in 2011 reach further onto shallower areas of the WFS. Both 2009 and 2011 show settling in the northwestern GOM, and in 2010 show a similar pattern to *E. alleteratus*, where larvae settle near the panhandle (Figures 4.9, 4.10). Scombridae settle in similar areas along the WFS in 2007, 2010 and 2011 (Figure 4.11). Northern settling groups are also present in the Scombridae family (Figure 4.11). In 2007 there are also settlers in the northern GOM and in 2010 in the northeastern GOM area, as well as another group near the tip of the FL Keys (Figure 4.11). Labridae settle along the FL Keys reef tract in 2007, 2010, and 2011 (Figure 4.12). In 2009 they settle along the entire length of the WFS, reaching from right up onto the coast of the FL panhandle all the way to the Keys (Figure 4.12). In 2010 and 2011 there is a cluster west of Tampa Bay. In 2007 and 2011 there is a group of northwestern Gulf settlers and in 2007 there is a group along the central to southern WFS (Figure 4.12).

Atlantis

The distribution of production in Atlantis changes after dispersal is added in to the model (Figure 4.13). Figure 4.13a shows the difference in production between a scenario including dispersal and the parent-location control scenario for reef fish groups. Figure 4.13b shows this production change for pelagic groups. The reef fish groups show the highest increase in production in the polygons directly inward from the polygons at the WFS edge, in the Big Bend area and northeastern GOM, and within the WFS. There is also increased production in the Florida Keys, along the coastal areas of the model, and at the boundary polygons, which could indicate export. There is also one area of high production in the northern GOM along the isobaths off the coast of Louisiana and Texas. For pelagic groups, there is largely the same pattern, but less pronounced, and with additional potential export at the boundary polygons. Groups that needed the highest increases in the steepness parameter of recruitment during the tuning process in Atlantis were Lutjanids, Large Reef Fish, and Large Pelagic Fish, indicating that these groups are more heavily reliant on the inclusion of an accurate dispersal mechanism.

Table 4.1: Spawning and Settling Areas by Taxa and Year

Taxa	**Spawning Area**						**Settling Area**					
	Northern WFS	**Central WFS**	**Southern WFS**	**FL Keys**	**NE Gulf**	**NW Gulf**	**Northern WFS**	**Central WFS**	**Southern WFS**	**FL Keys**	**NE Gulf**	**NW Gulf**
Scaridae	2007, 2009, 2010	2007, 2009, 2010, 2011	2007, 2009, 2010, 2011	2011	2007, 2009, 2010	2009, 2010, 2011	2007, 2009, 2010, 2011	2007, 2009, 2010, 2011	2007, 2010, 2011		2007, 2009, 2010	2007, 2009, 2011
Hemanthias	2010	2007, 2009	2007, 2009		2007, 2009, 2010	2009, 2010	2007, 2010	2007, 2010	2007		2007, 2010	2007, 2009
T. lathami	2007, 2009,	2009			2009	2011	2007, 2009				2009, 2010	2011
D. punctatus	2007, 2011	2007,2011	2007, 2010, 2011	2011	2007, 2010	2009, 2011	2007, 2011	2010, 2011	2011	2007, 2010, 2011		2007, 2009, 2011
K. pelamis	2010	2010	2007, 2010		2007, 2010	2009, 2011	2010	2007, 2010	2007	2010	2010	2009, 2011
Ophicthidae	2007, 2010, 2011	2007, 2010, 2011	2007, 2011		2007, 2009, 2010	2007, 2009, 2010, 2011	2007, 2009, 2010, 2011	2007, 2009, 2010, 2011	2007, 2010, 2011	2007, 2009, 2010, 2011	2007, 2010, 2011	2007, 2009, 2011
Ophidiidae	2007, 2009, 2010, 2011	2007, 2009, 2010, 2011	2007, 2009, 2011	2007, 2011	2007, 2009, 2010, 2011	2009, 2010, 2011	2007, 2009, 2010, 2011	2007, 2009, 2010, 2011	2009, 2010	2007, 2009, 2010, 2011	2007, 2009, 2010, 2011	2007, 2009, 2011

Table 4.1 (continued): Spawning and Settling Areas by Taxa and Year

Taxa	**Spawning Area**						**Settling Area**					
	Northern WFS	**Central WFS**	**Southern WFS**	**FL Keys**	**NE Gulf**	**NW Gulf**	**Northern WFS**	**Central WFS**	**Southern WFS**	**FL Keys**	**NE Gulf**	**NW Gulf**
E. alleteratus	2010, 2011	2010, 2011	2007, 2011	2011	2007, 2010	2009, 2010, 2011	2010, 2011	2011	2007, 2011		2009, 2010, 2011	
Lutjanidae	2010	2010, 2011	2010, 2011	2011	2010	2009, 2010, 2011	2010, 2011	2010, 2011	2007, 2010, 2011		2010	2009, 2011
Scombridae	2007, 2009, 2010	2007, 2010, 2011	2007, 2010, 2011	2011	2007, 2009, 2010	2009, 2010, 2011	2007, 2010, 2011	2007, 2011	2007, 2011	2010	2009, 2010	2007, 2009, 2011
Labridae	2007, 2010	2007, 2010, 2011	2007, 2009, 2010, 2011	2007, 2011	2007, 2009, 2010, 2011	2009, 2010, 2011	2010, 2011	2007, 2009, 2010, 2011	2007, 2010, 2011	2007, 2010, 2011	2009, 2010	2007, 2009, 2011

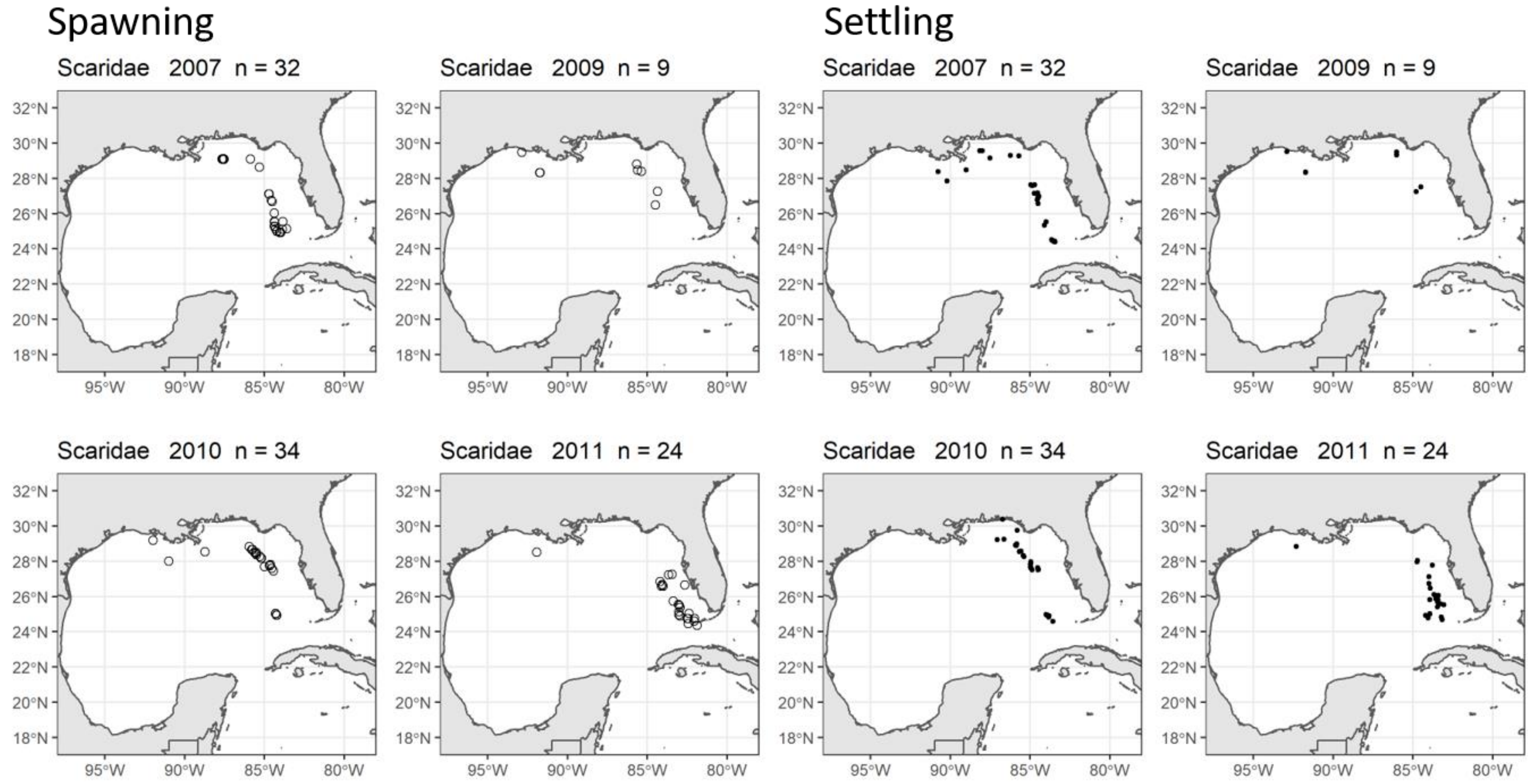
Spawning

Settling

Scaridae 2007 n = 32

Scaridae 2009 n = 9

Scaridae 2007 n = 32

Scaridae 2009 n = 9

Scaridae 2010 n = 34

Scaridae 2011 n = 24

Scaridae 2010 n = 34

Scaridae 2011 n = 24

Figure 4.2: Spawning (left, open circle) and Settling (right, closed circle) sites for Scaridae

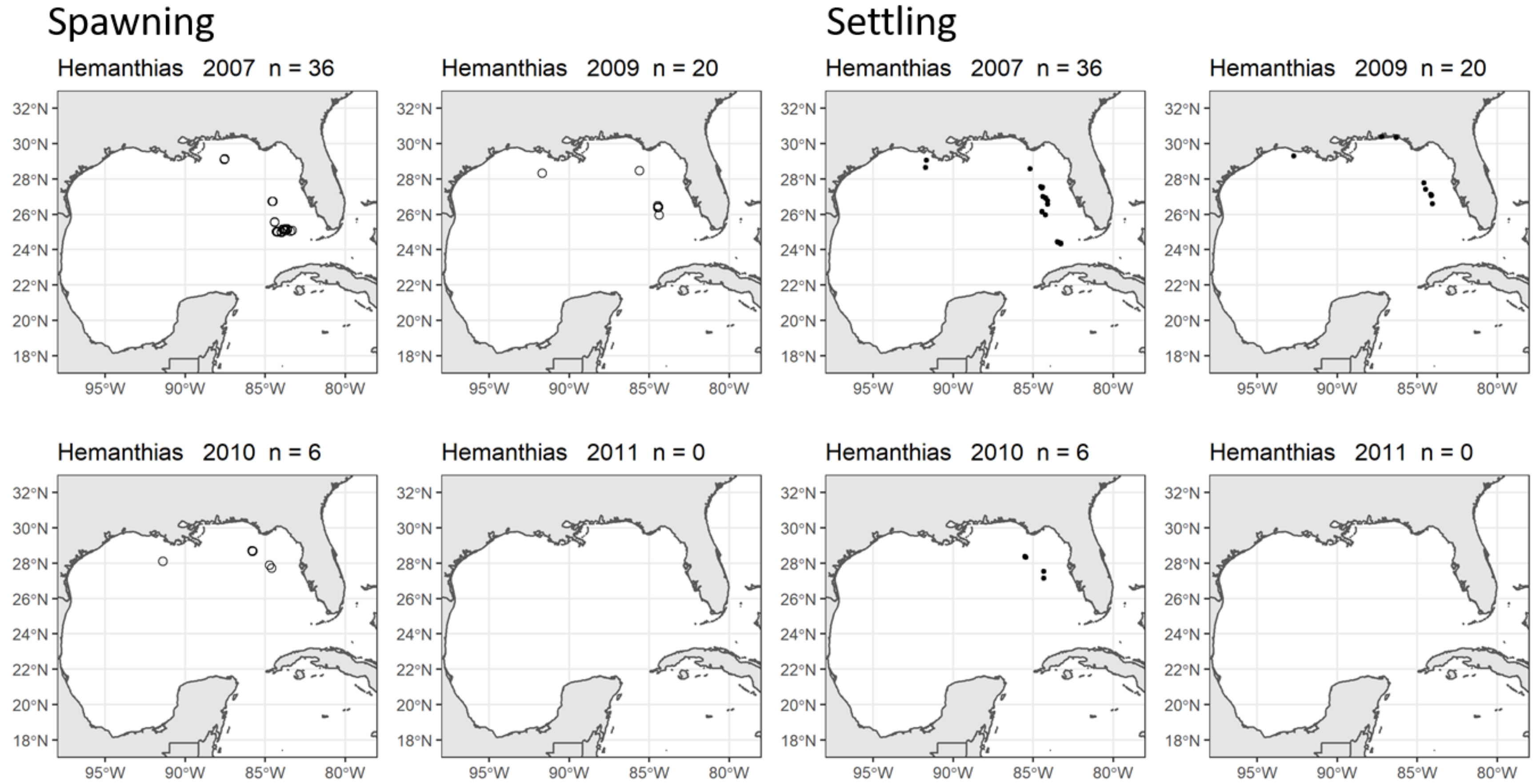

Figure 4.3: Spawning (left, open circle) and Settling (right, closed circle) sites for *Hemanthias*

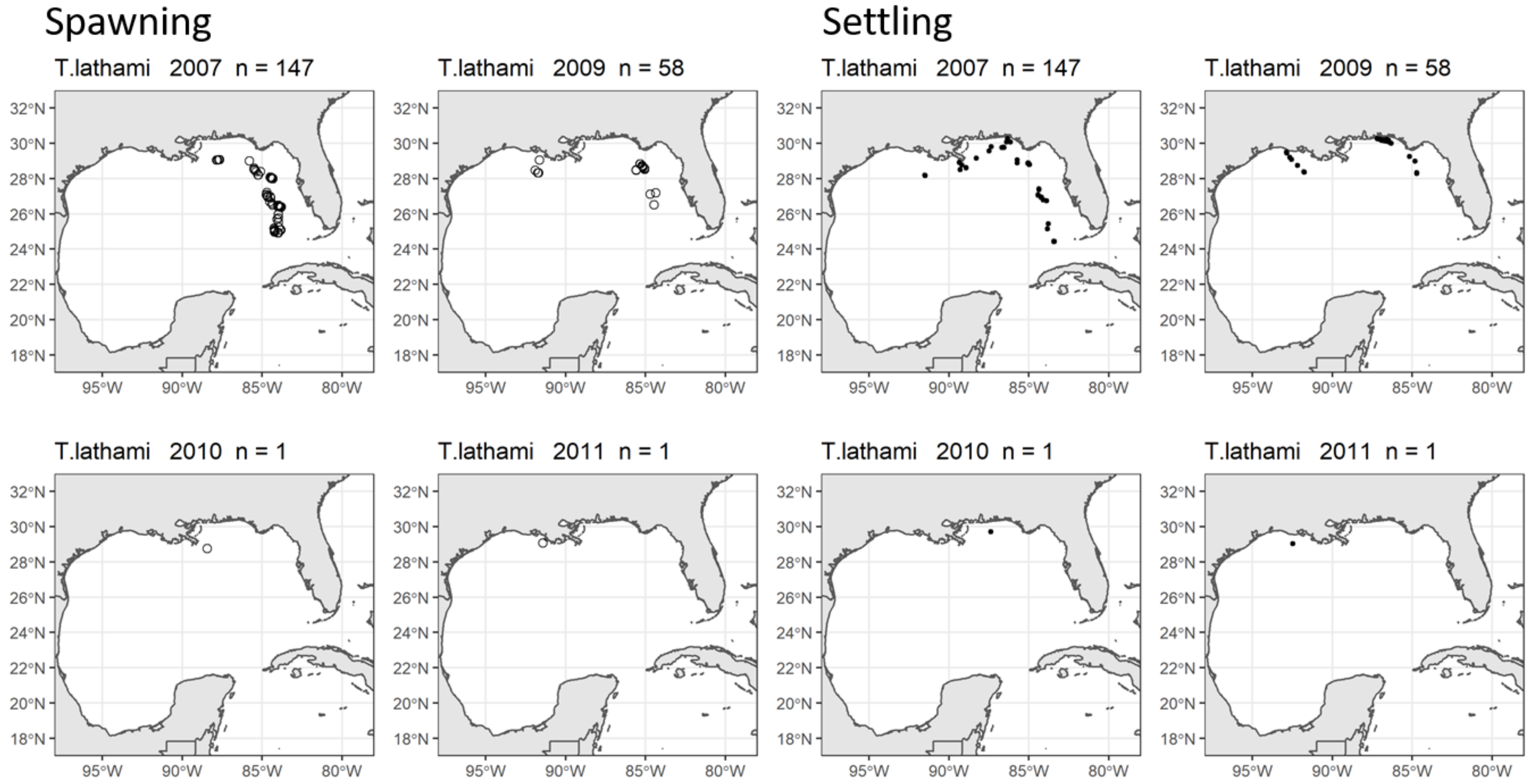

Figure 4.4: Spawning (left, open circle) and Settling (right, closed circle) sites for *T. lathami*

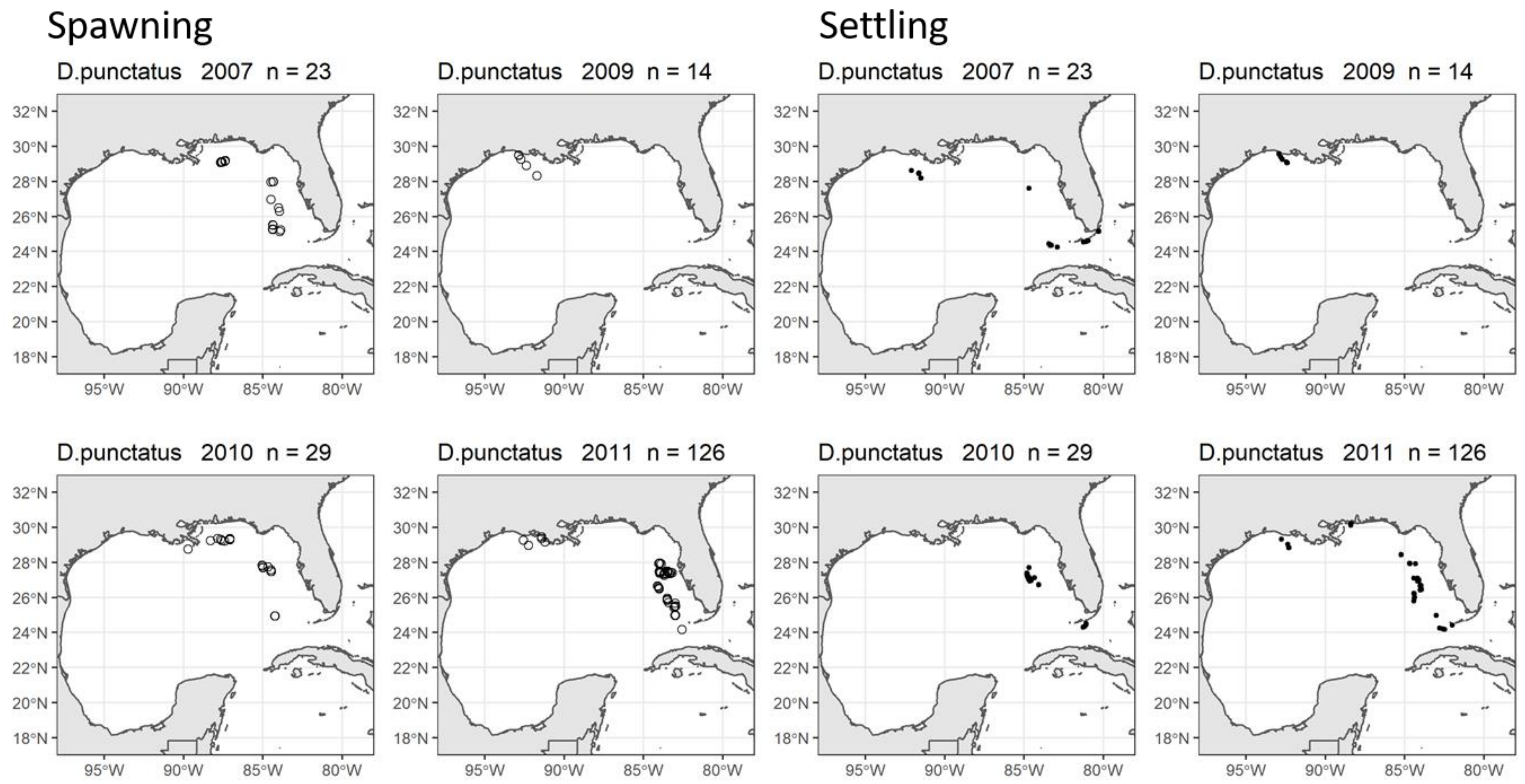

Figure 4.5: Spawning (left, open circle) and Settling (right, closed circle) sites for *D. punctatus*

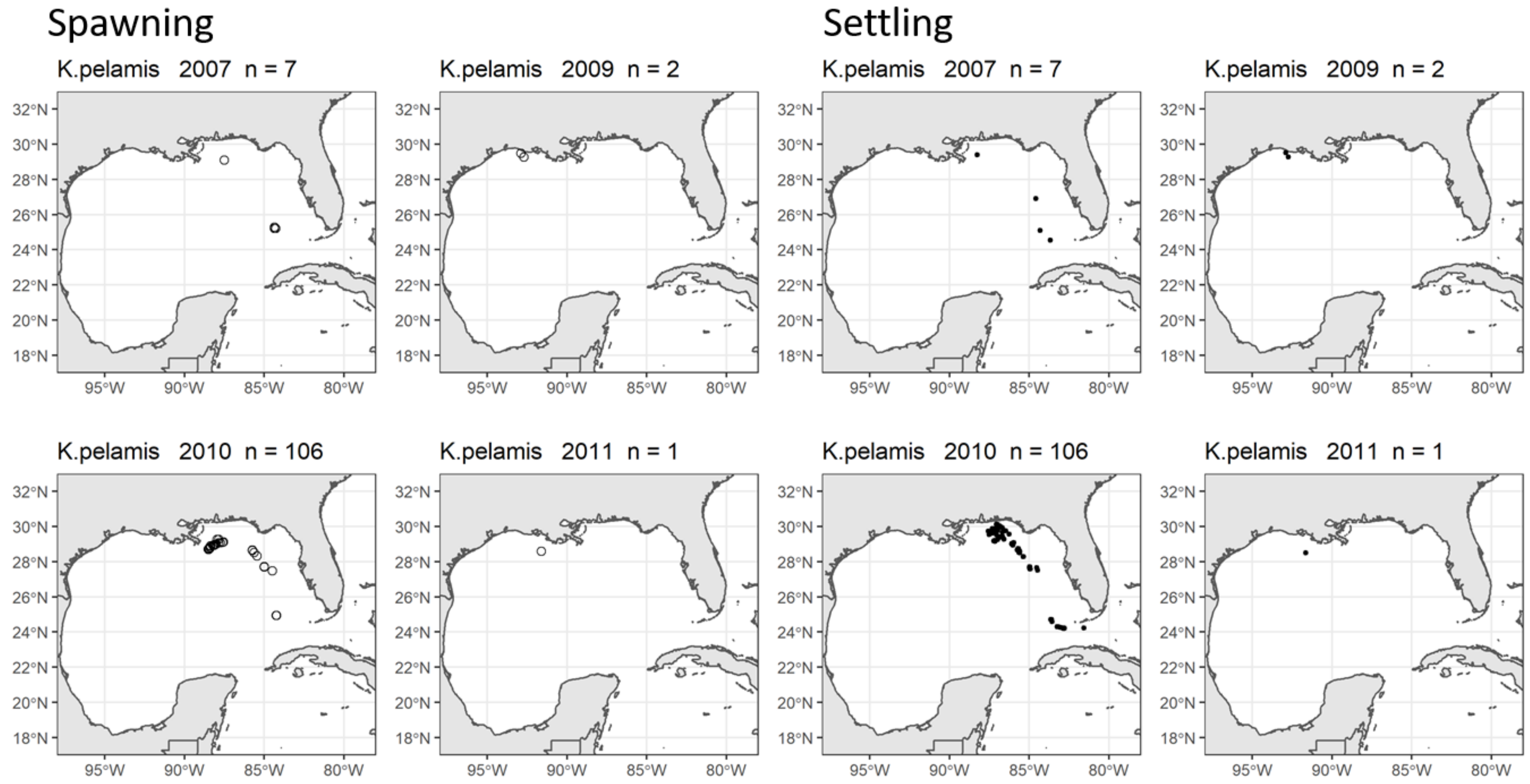

Figure 4.6: Spawning (left, open circle) and Settling (right, closed circle) sites for *K. pelamis*

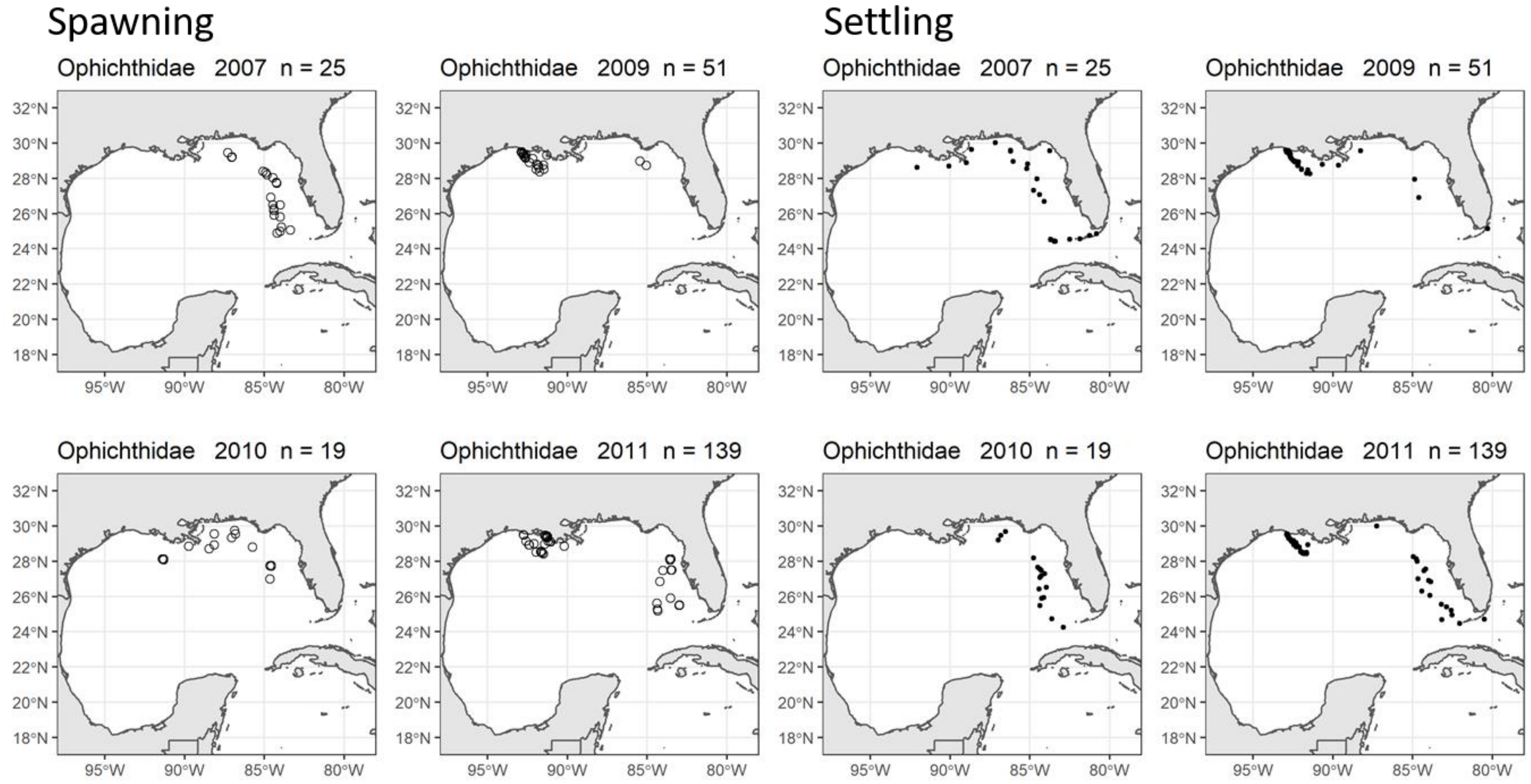

Figure 4.7: Spawning (left, open circle) and Settling (right, closed circle) sites for Ophichthidae

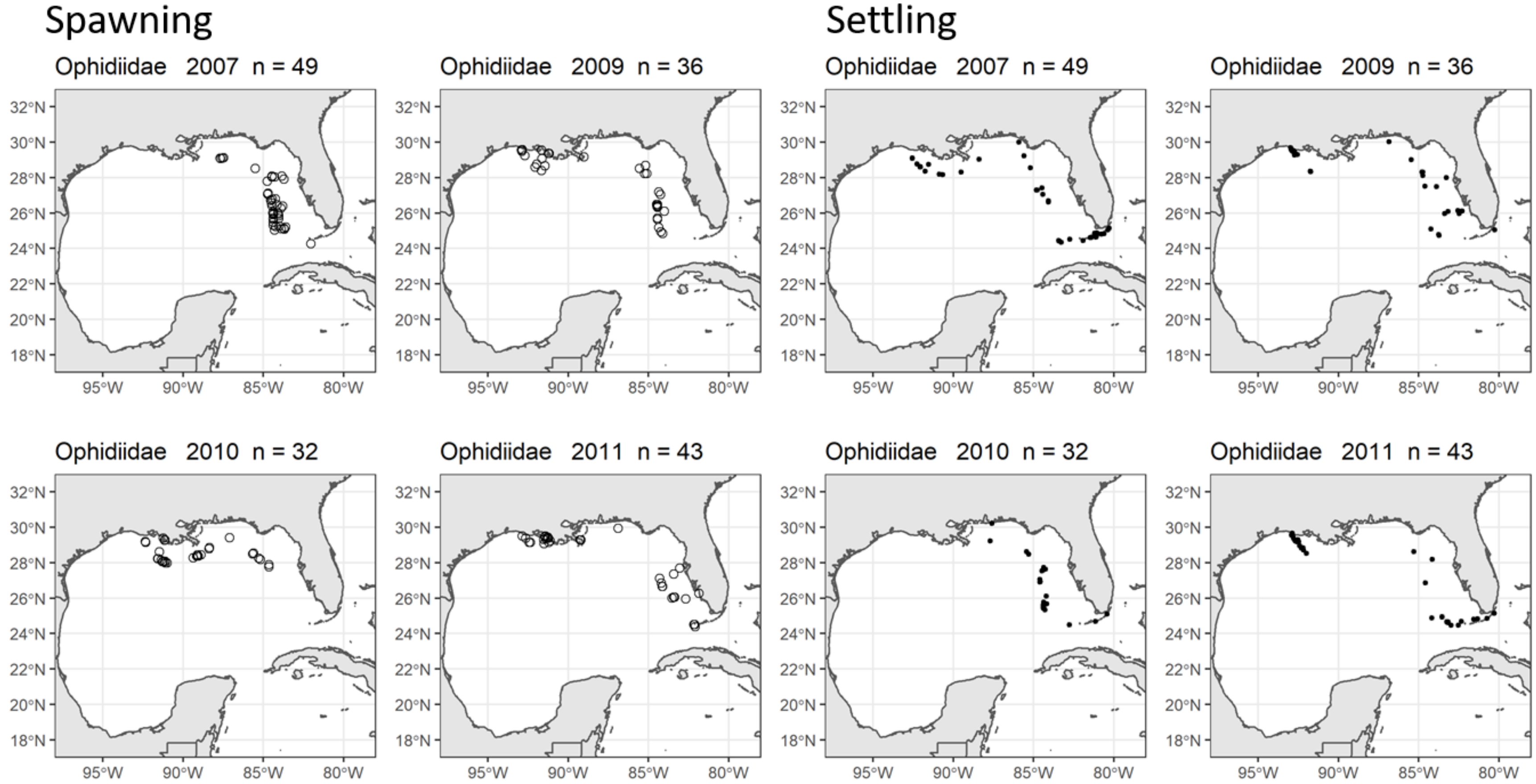

Figure 4.8: Spawning (left, open circle) and Settling (right, closed circle) sites for Ophidiidae

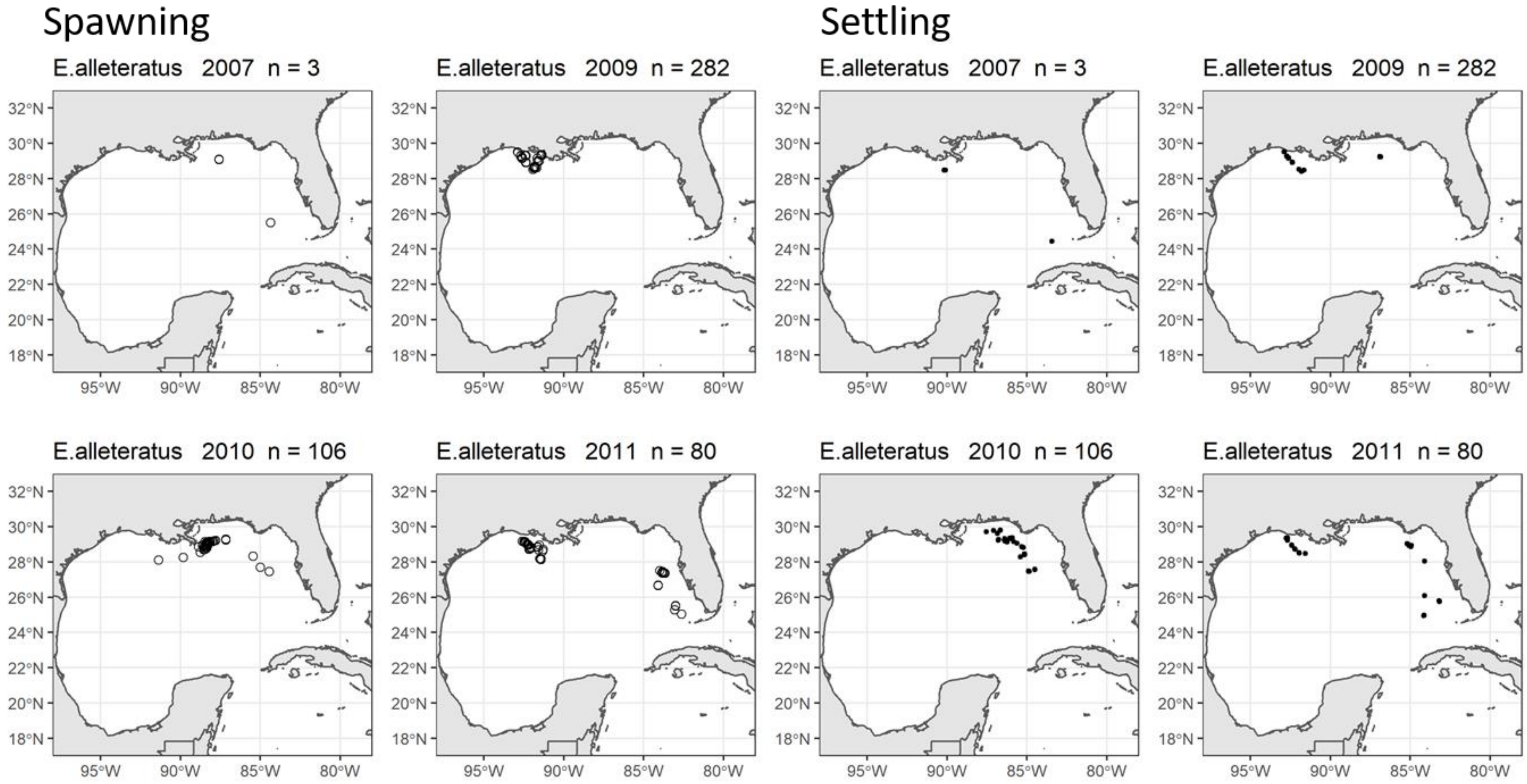

Figure 4.9: Spawning (left, open circle) and Settling (right, closed circle) sites for *E. alleteratus*

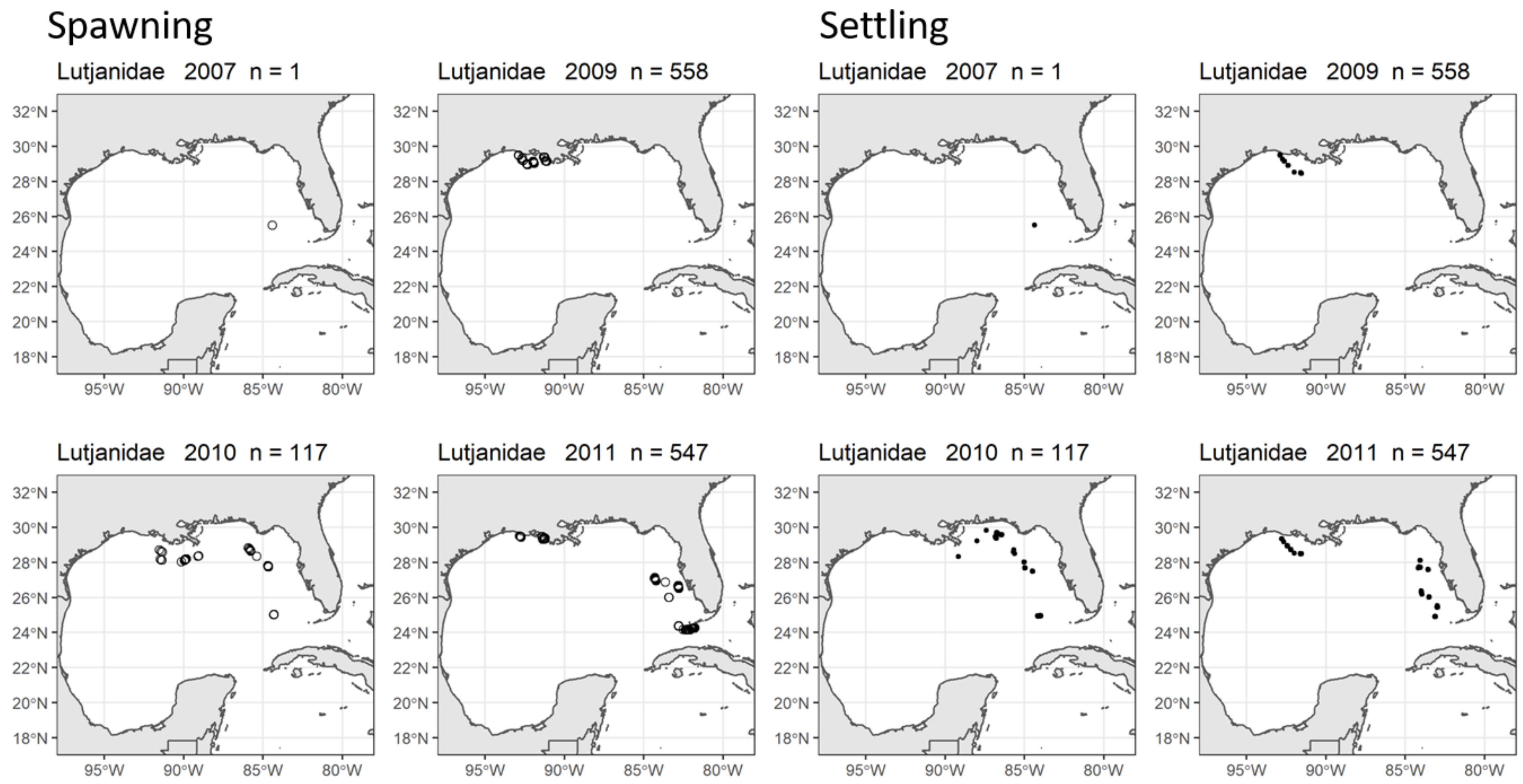

Figure 4.10: Spawning (left, open circle) and Settling (right, closed circle) sites for Lutjanidae

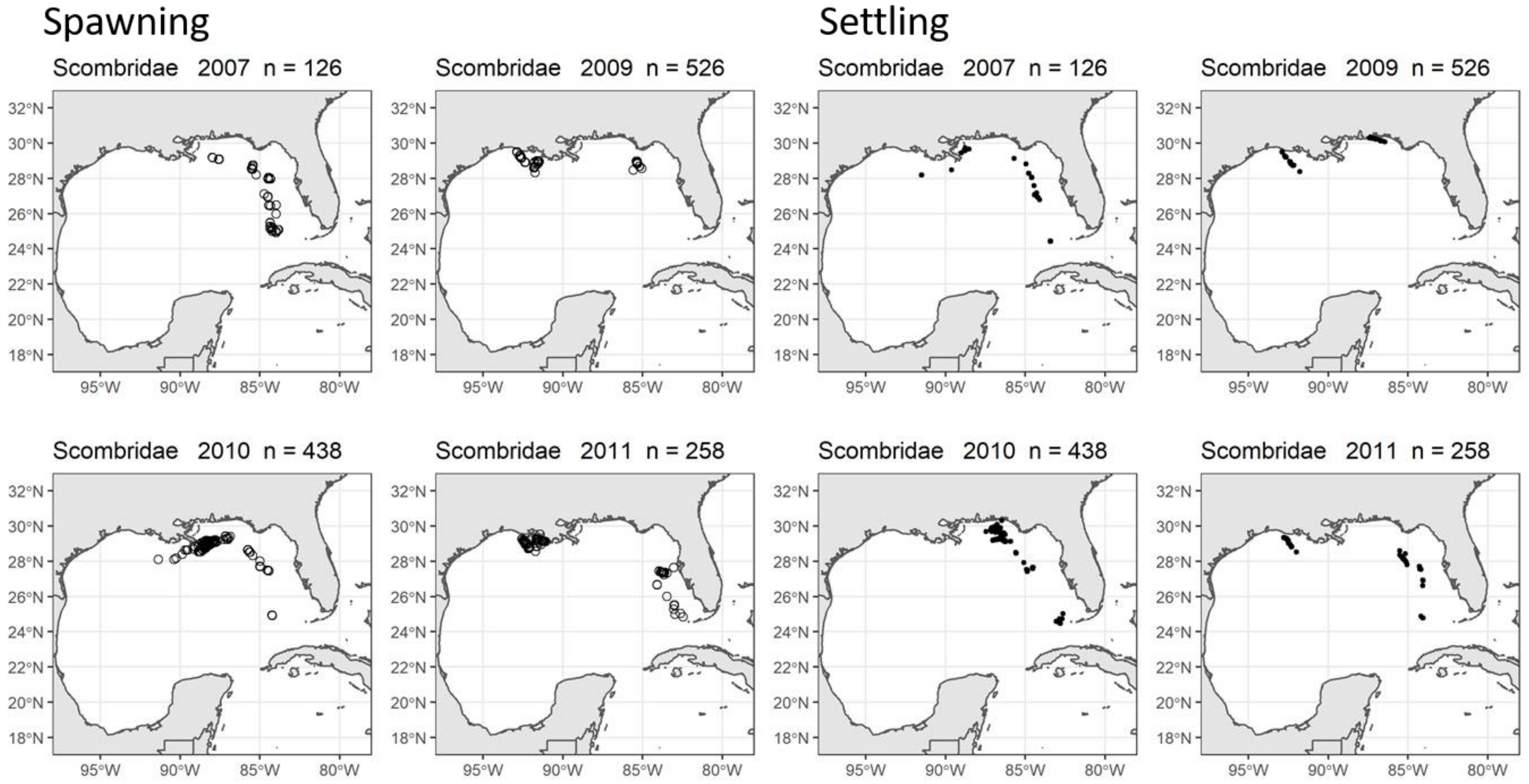

Figure 4.11: Spawning (left, open circle) and Settling (right, closed circle) sites for Scombridae

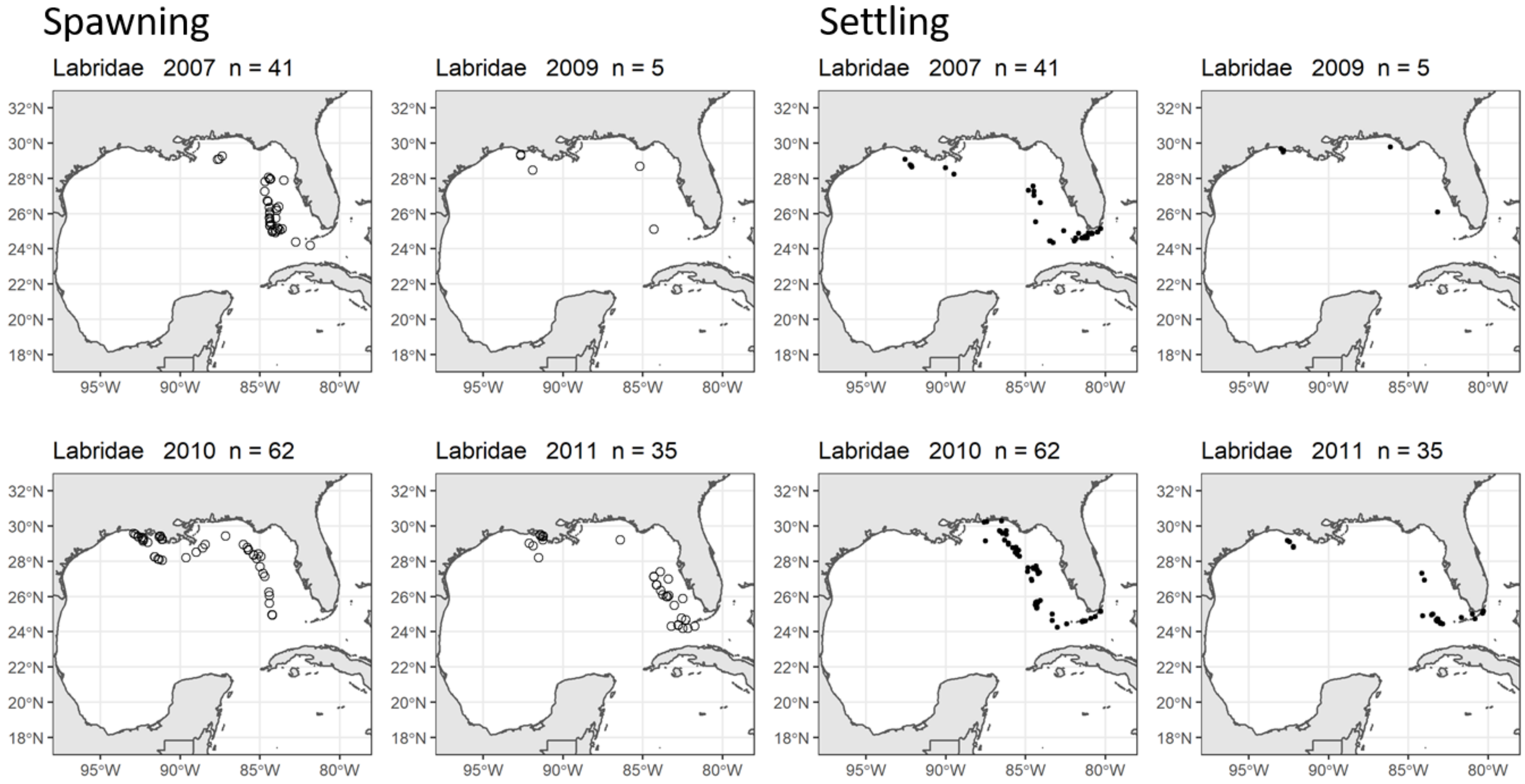

Figure 4.12: Spawning (left, open circle) and Settling (right, closed circle) sites for Labrida

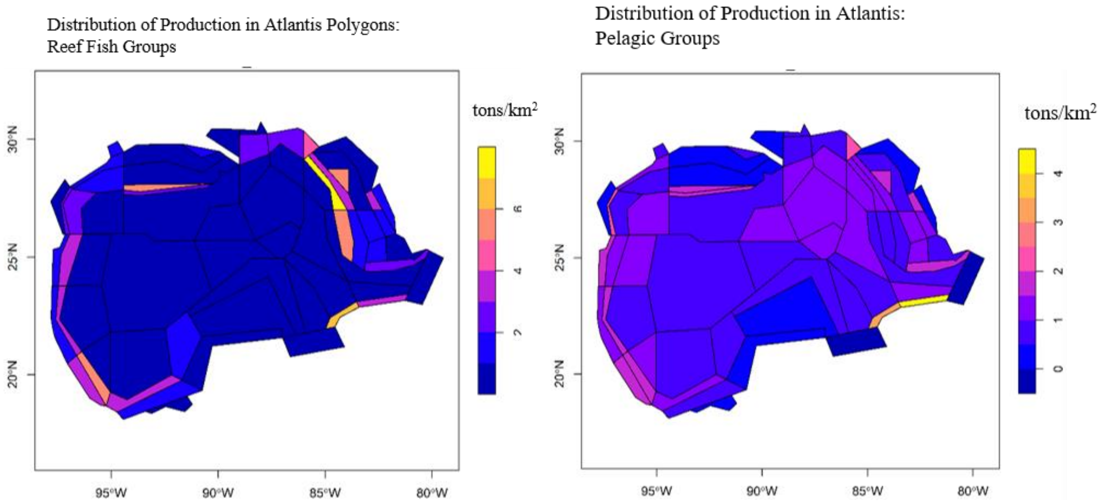
Distribution of Production in Atlantis Polygons: Reef Fish Groups

Distribution of Production in Atlantis: Pelagic Groups

Figure 4.13: Difference in production between dispersal scenario and parent location scenario in Atlantis Reef (left) and Pelagic (Right) groups.

The scale bar represents a difference in production, with production in t·km^{-2}.

Discussion

The spawning and settlement sites in this study are decided by two factors: larval depth occupancy and hydrodynamics. The empirical depth occupancy models in Chapter 3 (Vasbinder et al. in prep) account for a variety of environmental predictors such as wind, temperature, salinity, mid-depth oxygen, and mixed-layer depth, thereby making these factors implicitly accounted for in the depth selection behavior. However, there are other factors that influence settling sites at the end of the pelagic larval period. Habitat suitability, predator dynamics and food availability are not accounted for in the “choice” of settling sites in this study. The most common spawning sites were along the WFS edge, the tip of the FL Keys Reef Tract and an area in the northwestern GOM on the coast of Louisiana. The most common settling sites were the northern GOM area, an area of the WFS spanning from central to southern Florida and reaching from the shelf edge in to the coast, in the northwestern GOM near the Louisiana coast, and along the FL Keys reef tract. These areas each have noticeable hydrodynamic features related to larval retention and export.

The FL Keys reef tract in the southern GOM is a well-studied site of larval retention due to the presence of a hydrodynamic feature known as the “Tortuga Gyres” or “Tortuga Eddies” (Porch 1997, Fratantoni et al. 1998). Cyclonic frontal eddies spin off from the Loop Current boundary, and these frontal eddies then form the Tortuga eddies: quasi-stationary eddies that stay in one place for 50 days until they are approached by another frontal eddy from the Loop Current, at which point they propagate downstream (Fratatoni et al 1998). This process can be slowed by the Loop Current shedding an anticyclonic ring, which halts the downstream movement of the Tortuga eddy and keeps it in one place for up to 140 days (Fratatoni et al. 1998). Almost all of the pelagic larval durations of our families fall into this timeframe, and our families showed settling at the tip or along the FL Keys reef tract, suggesting larval retention that is potentially the result of these Tortuga eddies. This is seen in 2007 and 2011 Ophidiidae, 2007, 2011 Labridae, and 2011 *D. punctatus*. This may also be a potential explanation for FL Keys settling in 2007 and 2011 Ophichthidae, 2007 and 2010 *D. punctatus*, and 2010 *K. pelamis,* which show spawning just west of the FL Keys. A notable exception is the 2010 pattern seen for the Ophidiidae and Labridae families. In most cases in which settling is seen on the FL Keys reef tract, spawning also occurs at the tip of the FL Keys or just west of the FL Keys, but in these two families, 2010 spawning only occurs along the WFS edge and in the northern GOM, indicating that the larvae settling in the FL Keys reef tract must have come from further north. Ophidiidae and Labridae both have an extremely long larval durations in my model, both over 100 days.

This could suggest that although there are no Keys spawned larvae in these two cases for the Tortuga eddies to retain, larvae coming southward from the WFS could have become caught up in an eddy and retained in the Keys for the remainder of their larval period. The WFCOM grid is very fine surrounding the FL Keys reef track and, therefore, the eddies are not sub-grid level occurrences and would be resolved in the model. Another process that could lead to settling in this area is the presence of shoreward Ekman drift cause by prevailing westerly winds that drive a coastal counter current and keep larvae from going seaward (Porch 1997, Lee et al. 1992). Drifter studies in the FL Keys reef tract show that Tortuga released drifters follow four pathways, 1) traveling along the Florida Keys with cyclonic movement south and west, 2) traveling northward to the WFS, 3) traveling in the Florida current and exiting on Florida's east coast, or 4) continuing past the southern tip of Florida and out into the Gulf Stream (Hare and Walsh 2007). The 3rd and 4th pathways involve exiting the GOM, and are outside the range of this model. However, the 1st and 2nd pathways are both potential explanations for the patterns seen in my settlement sites. The 2nd pathway, that of larvae traveling from the Tortugas/Keys area up the WFS, can be seen in 2011 Scaridae, 2011 Euthynnus, 2011 Lutjanids, and 2011 Scombrids.

Another hydrodynamic zone on the southern end of the WFS known as the "forbidden zone" is reflected by our settling sites (Yang et al. 1999). This zone has been observed by drifter and modeling studies as an area where dispersed objects skirt the edge of the shelf due to along-shore wind forcing. This produces an along-shore coastal jet which peels away from the coast. This "forbidden zone" can be seen in the results from Lutjanidae and *D. punctatus,* which settle along the edges of that zone in 2011, as well as in the two eel families in both 2010 and 2011. While objects often skirt this zone, that does not mean that no water or particles can enter it, and indeed some larvae are able to settle in the zone. The very top boundary of this “forbidden zone” is an area near Tampa Bay where larvae can be brought in to shore due to a three-dimensional coastal jet, in which bottom flows are southward and shoreward due to friction in the bottom Ekman layer, while the surface waters experience Ekman transport offshore (Yang et al 1999). Upwelling occurs near Tampa Bay, moving water offshore (Yang et al. 1999). Since settlement occurs along the shelf edge in the region of the WFS to the south of Tampa Bay in many families, this may be an example of the “forbidden zone” phenomenon. This area of the WFS just west of Tampa Bay is also a spawning site for several of the taxa in various years, including Lutjanidae, Scombridae, Scaridae, and both eel families. This could be a good candidate site for spawning due to the high production often associated with upwelling zones.

The northern GOM, including northern parts of the WFS, contains a plethora of reefs and marine protected areas (Locker et al. 2016). We see many of our spawning sites located in these areas. These spawning sites may be occurring near or on these reef sites, including the Pinnacles, Madison Swanson, the Edges, Steamboat Lumps, and the Florida Middle Grounds on the northern WFS. There are reef fish from the families Lutjanidae, Labridae, and Scaridae spawning on these northern GOM reefs. Lutjanids spawn here in 2009, 2010, and 2011, while Labrids and Scarids spawn here in all four years. *T. lathami* from the Jack family spawns on these reefs in 2007, 2009, and 2010. Two large pelagic taxa, *K. pelamis* and the Scombridae family, also show some spawning here in all four years. Another area where there is spawning is an area off of Tampa Bay that contains carbonate structures known as “sticky grounds”, where carbonate mounds occur along the shelf margin (Locker et al. 2016). These “sticky grounds” provide substrate for fish to inhabit (Locker et al. 2016). The presence of this substrate may make the “sticky grounds” an ideal spawning area.

One of the most common areas in both spawning and settlement of larvae was the WFS edge. The WFS is the continental shelf off of the west coast of Florida, and is one of the widest continental shelves on the planet (Li and Weisberg 1999a). From the Panhandle to the Florida Keys, the West Florida Shelf makes up about one fourth of the entire Gulf of Mexico (Li and Weisberg 1999b). On continental shelves, both boundary layer and eddy transport are important processes because the sloping bottom of the shelf imposes constraints on vorticity (Weisberg et al. 2001).

The inner shelf may be a good candidate for spawning, due to the presence of a three-dimensional flow-field that drives an increase in production near shore. Overlapping Ekman and geostrophic flows cause a sea surface deformation inward of the 50m isobath, while another surface layer consists only of Ekman flows (Li and Weisberg 1999a and 1999b). The vertical structure of the flow field shows a coastal jet southeastward where the sea surface is deformed, and then a return northeastward under the surface Ekman layer in more offshore areas (Li and Weisberg 1999a). The development of a bottom Ekman layer occurs as the coastal jet gets faster, and this causes a near bottom across shelf velocity component moving towards shore and leading to upwelling (Li and Weisberg 1999a). The upwelling reaches a maximum where the across shelf flow also reaches a maximum. The northwestward return flow causes downwelling, closing the loop and setting up this three-dimensional flow field (Li and Weisberg 1999b). This three-dimensional flow means that the inner shelf demonstrates mean upwelling in the nearshore areas and mean downwelling in offshore areas (Weisberg et al. 2009). This could make the inner shelf a productive area for spawning, and there is indeed inner shelf spawning occurring in some taxa, such as the family Labridae. The WFS, like all continental shelves, can respond to both local and offshore forcing (Weisberg et al. 2001). The local forcing comes from the input of momentum at the sea surface and buoyancy at both the sea surface and the land, whereas offshore forcing comes from the input of both at the shelf break (Weisberg et al. 2001). While the importance of local and offshore forcing shifts depending on location, local forcing plays a larger role due to the WFS's wide inner shelf (Weisberg et al 2001).

Many groups spawn along the shelf edge, and this could be in part due to the presence of an asymmetrical pattern of upwelling and downwelling that could allow larvae to be advected towards shore. We see Lutjanidae and Ophidiidae settling the furthest inshore on the shelf, and they also show spawning on the shelf edge. Other groups that spawn on the shelf edge also settle in the outer areas of the shelf in various years, including both of our Jack species, *Hemanthias,* which are Serranids, and all of our large pelagic taxa. Some studies of the WFS have found an asymmetry between the upwelling and downwelling responses in stratified models, in which the upwelling response was much stronger than the downwelling response (Weisberg et al. 2001). It is possible that this asymmetry is due to stratification impeding the bottom transport across the shelf due to the density force balancing the along-shelf velocity component's Coriolis force (Weisberg et al. 2001). Essentially, this means that the isopycnals in the upwelling situation enhance the buoyancy force, but detract from it in the downwelling situation, due to direction of the flow being offshore or onshore. This asymmetry has biological implications, meaning that materials are more likely to be transported inshore than away from shore, and chlorophyll evidence in the bottom Ekman layer backs up this hypothesis (Weisberg et al. 2001). This asymmetry could explain why many taxa spawn along the shelf edge, as their larvae have a good chance of being moved towards shore. Stratification of the shelf could also be interacting with the larval depth-at-age choice determined by the statistical model. FVCOM has been used in other studies along the coast of Maine to track the transport of Atlantic cod from spawning to settling sites in an effort to study the impact of spatial and temporal changes in spawning, regional forcing, and vertical mixing on the ability of larvae to reach settling sites (Huret et al. 2007). Larval cod particles were released into the model at a range of vertical positions. Vertical location was found to be an important factor in larval dispersal for stratified areas and was less important in well mixed areas or times of year (Huret et al. 2007).

Finally, the overall mean flow on the WFS is southward along its isobaths (Weisberg et al. 2009). While taxa with shorter larval durations will be largely impacted by short term drivers, taxa with longer larval durations would benefit from this mean flow. Ophichthidae and Ophidiidae, two eel families with long residency times in the pelagic larval stage, demonstrate this potential advantage in 2007 and 2010, where spawning in the northern WFS and settling on the southern WFS occurs.

One mitigating factor in our dispersal simulations is that the WFCOM domain does not include the center or western areas of the GOM. SEAMAP sampling sites were used as the start of the RK4, so any larvae from sites outside the WFCOM domain were seeded into the closest model cell. When calculating the RK4, larvae were allowed to approach the boundaries of the model in both the forward and backward integration of time. Some of the spawning or settling in the northwestern area of the model domain in the sites just west of the Louisiana peninsula could be due to larvae approaching the domain edge, as could some of the larvae in the area outside the shelf approaching the central GOM. If the domain included the entire GOM, these larvae would be exported to the ocean and likely die. Thus, spawning and settlement sites right at the edge of the domain should be treated as potential sites for spawning and settlement and potential sites where the larvae may have entered the western or central GOM if not constrained.

Shifts in the distribution of production in Atlantis with the addition of the dispersal mechanism indicate that larval connectivity is an important factor to consider both when modeling ecosystems and when considering potential management actions. Only the relative change in the production within each polygon is important, because model tuning contributed to the overall production increase through the entire GOM. The effect of dispersal on total recruitment is up for debate because of the need to use ad hoc scaling of the recruitment. Nevertheless, it is still evident that some polygons are experiencing large increases in production under the dispersal experiment relative to other polygons. The increases in production in polygons adjacent to those on the WFS edge and further in to the WFS indicate that the hydrodynamic patterns impacting the dispersal of larvae are being translated into an impact on production, especially for reef fish. We also see some export of production to the Caribbean in our pelagic groups, and increased production in the FL Keys for both groups. The same hydrodynamic factors that drive settlement along the shelf edge, within the WFS, in the northeastern GOM, and in the FL Keys result in an increase in production in those areas. This means that adding dispersal to the model allows us to include the impact of these hydrodynamic processes and to better reflect the WFS in the GOM Atlantis model. With the addition of the larval connectivity matrix to the GOM Atlantis model, we now have a more complete picture of the ecosystem, the ability to include the impacts of early life behavior into future studies, and a compelling case for the inclusion of hydrodynamic data into the process of partitioning recruitment in an ecosystem model.

Acknowledgements

I would like to thank Dr. Robert Weisberg and Dr. Yonggang Liu for providing the WFCOM current trajectories used in this study and for their invaluable advice on this project and Glenn

Zapfe for providing the SEAMAP sampling data. Funding for KV came from the Presidential Doctoral Fellowship from the Office of Graduate Studies at the University of South Florida as well as the William and Elsie Knight Endowed Fellowship at the University Of South Florida College Of Marine Science. This chapter is a part of the degree requirements for the Marine Resource Assessment program at the University Of South Florida College Of Marine Science.

References

Ainsworth, C.H., Schirripa, M.J., Morzaria-Luna, H. (eds.) 2015. An Atlantis ecosystem model for the Gulf of Mexico supporting Integrated Ecosystem Assessment. NOAA Technical Memorandum NMFS-SEFSC-676, 149p

Berger, A., Goethal, D.R., and Lynch, P.D. 2017. Introduction to "Space Oddity: Recent Advances Incorporating Spatial Processes in the Fishery Stock Assessment and Management Interface" Can. J. Fish. Aquat. Sci. 74: 1693–1697 dx.doi.org/10.1139/cjfas-2017-0296

Chassignet, E.P, Hurlburt, H.E., Metzger, E.J., Smedstad, O.M., Cummings, J.,Halliwell, G.R., Bleck, R., Baraille, R., Wallcraft, A.J., Lozano, C., Tolman, H.,Srinivasan, A., Hankin, S., Cornillon, P., Weisberg, R., Barth, A., He, R., Werner, C., Wilkin, J. 2009. U.S. GODAE: global ocean prediction with the HYbrid coordinate ocean model (HYCOM). Oceanography 22: 48–59.

Chen, C.S., Liu, H., Breadsley, R.C. 2003. An unstructured, finite-volume, three-dimensional primitive equation ocean model: application to coastal ocean and estuaries. J. Oceanic Atm. Technol. 20: 159–186.

Costelloa, C., Rassweilerb, A., Siegelc, D., De Leod , G., Michelie, F., Rosenbergf, A.. 2010. The value of spatial information in MPA network design. Proc. Natl. Acad. Sci. 107(43):18294-18299.

Drexler, M. 2018. Evaluating the use of larval connectivity information in fisheries models and management in the Gulf of Mexico. Graduate Theses and Dissertations. https://scholarcommons.usf.edu/etd/7499

Edwards, K.P., Hare, J.A., Werner, F.E., Blanton, B.O. 2006. Lagrangian circulation on the Southeast US Continental Shelf: Implications for larval dispersal and retention. Cont.Shelf Res. 26: 1375–1394.

Fiechter, J. Haus, B. K., Nelson, M., Mooers, C. N. K. 2008. Physical processes impacting passive particle dispersal in the Upper Florida Keys. Cont. Shelf Res. 28: 1261– 1272.

Fratantoni, P.S., Lee, T.N., Podesta, G. P., Muller-Karger, F. 1998. The influence of Loop Current perturbations on the formation and evolution of Tortugas eddies in the southern Straits of Florida. J. Geophys. Res, VOL. 103, NO. Cll, 24:759-24,779

Fulton, E.A., Parslow, J.S., Smith, A.D.M., Johnson, C.R. 2004. Biogeochemical Marine Ecosystem Models. 2. The effect of physiological data on model performance. Ecol. Model. 173: 371-406.

Fulton, E.A., Smith, A.D.M., Smith, D.C. 2007. Alternative management strategies for Southeast Australian commonwealth fisheries: Stage 2: Quantitative management strategy evaluation. Australian Fisheries Management Authority. Fisheries Research and Development Corporation.

Gawarkiewicz, G., Monismith, S., Largier, J. 2007. Observing larval transport processes affecting population connectivity: progress and challenges. Oceanography 20(3):40-53.

Goethel, D.R., Legault, C.M., and Cadrin, S.X. 2015. Testing the performance of a spatially explicit tag-integrated stock assessment model of yellowtail flounder (*Limanda ferruginea*) through simulation analysis. Can. J. Fish. Aquat. Sci. 72(4): 582–601. doi:10.1139/cjfas-2014-0244.

Gruss, A., Rose, K.A., Simons, J., Ainsworth, C.A., Babcock, E., Chagaris, D., de Mutsert, K., Froeschke, J., Himchak, P., Kaplan, I.C., O'Farrell, H., Zetina Rejon, M.J. 2017. Recommendations on the use of ecosystem modeling for Ecosystem-Based Fisheries Management and restoration outcomes in the Gulf of Mexico. Mar. Coast. Fish. 9(1): 281-95. doi: 10.1080/1945120.2017.1330786.

Hare, J.A., Quinlan, J.A., Werner, F.E., Blanton, B.O., Govoni, J.J., Forward, R.B., Settle, L.R., Hoss, D.E., 1999. Larval transport during winter in the SABRE study area: results of a coupled vertical larval behaviour-three-dimensional circulation model. Fish. Oceanogr. 8(2):57-76.

Hare, J.A., Walsh, H.J.. 2007. Planktonic linkages among marine protected areas on the south Florida and southeast Unites States continental shelves. Can. J. Fish .Aquat. Sci. 64:1234 1247.

Huret, M.; Runge, Jeffrey; Chen, C. S.; Cowles, G.; Xu, Q. C., Pringle, J. M. 2007. Dispersal Modeling of Fish Early Life Stages: Sensitivity with Application to Atlantic Cod in the Western Gulf of Maine. Marine Sciences Faculty Scholarship. 36. https://digitalcommons.library.umaine.edu/sms_facpub/36

Joy, K.I. 1999. Numerical Methods for Particle Tracing in Vector Fields [On-line Visualization Notes]. Retrieved from https://web.cs.ucdavis.edu/~ma/ECS177/papers/particle_tracing.pdf.

Karnauskas, M., Walter, J.F., Paris, C.B. 2013. Use of the Connectivity Modeling System to estimate movements of red snapper (*Lutjanus campechanus*) recruits in the northern Gulf of Mexico. SEDAR31-AW10.SEDAR, North Charleston, SC. 20 pp.

Karnauskas, M., Paris, C.B., Zapfe, G., Gruss, A., Walter, J.F., Schirripa, M.J. 2013. Use of the Connectivity Modeling System to estimate movements of Gag Grouper (*Mycteroperca microlepis*) recruits in the northern Gulf of Mexico. SEDAR33 DW18.SEDAR, North Charleston, SC. 12 pp.

Lee, T.N., Rooth, C., Williams, E., McGowan M., Szmant, A.F., and M.E. Clarke. 1992. Influence of Florida Current, gyres and wind-driven circulation on transport of larvae and recruitment in the Florida Keys coral reefs. Cont. Shelf Res., Vol. 12(7): 971-1002.

Lett, C., Verley, P. Mullon, C. Prada, C. Brochier, T. Penven, P. Blanke, B. 2008. A Lagrangian tool for modelling icthyoplankton dynamics. Environ. Model. Softw.23: 1210-12-14.

Li, Z., Weisberg, R.H. 1999a. West Florida shelf response to upwelling favorable wind forcing: Kinematics. J. Geophys. Res. 104(C6):13,507-13,527.

Li, Z., Weisberg, R.H. 1999b. West Florida continental shelf response to upwelling favorable wind forcing: 2. Dynamics. . J. Geophys. Res. 104(C10): 23,427-23,442.

Liu, Y., Weisberg, R.H., Zheng, L. 2020. Impacts of hurricane Irma on the circulation and transport in Florida Bay and the Charlotte Harbor estuary, Estuar. Coast. 43:1194-1216 doi: https://doi.org/10.1007/s12237-019-00647-6.

Locker, S.D., Reed, J.K., Farrington, S., Harter, S., Hine, A.C., and S. Dunn. 2016. Geology and biology of the "Sticky Grounds", shelf-margin carbonate mounds, and mesophotic ecosystem in the eastern Gulf of Mexico. Continental Shelf Research 125: 71–87

Miller, T.J. 2007. Contribution of individual-based coupled physical–biological models to understanding recruitment in marine fish populations. Mar. Ecol. Prog. Ser. 347: 127 -138.

Morzaria-Luna, H.M., Ainsworth, C.H., Tarnecki, J., Gruss, A. 2018. Diet composition uncertainty determines impacts on fisheries following an oil spill. Ecosyst. Serv. 33:187-198.

O'Farrell, H., Gruss, A., Sagarese, S.R., Babcock, E.A., Rose, K.A. 2017. Ecosystem modeling in the Gulf of Mexico: current status and future needs to address Ecosystem-based fisheries management and restoration activities. Rev. Fish. Biol. Fisher. 27:587-614. doi: 10.1007/s11160-017-9482-1

Paris, C.B., Cowen, R.K., Claro, R., Lindeman, K.C. 2005. Larval transport pathways from Cuban snapper (Lutjanidae) spawning aggregations based on biophysical modeling. Mar. Ecol. Prog. Ser. 296:93-106.

Pineda, J., Hare, J. A., Sponaugle, S. 2007. Larval transport and dispersal in the coastalocean and consequences for population connectivity. Oceanography 20(3):22-39.

Porch, C.E. 1997. A numerical study of larval fish retention along the southeast Florida coast. Ecol. Model. 109: 35–59.

Punt, A.E., Haddon, M., and Tuck, G.N. 2015. Which assessment configurations perform best in the face of spatial heterogeneity in fishing mortality, growth, and recruitment? A case study based on pink ling in Australia. Fish. Res. 168: 85–99. doi:10.1016/j.fishres.2015.04.002.

Savina, M., Condie, S.A., and Fulton, E.A. 2013. The Role of Pre-Existing Disturbances in the Effect of Marine Reserves on Coastal Ecosystems: a Modeling approach. PLoS One, doi: 10.1371/journal.pone.0061207.

Siegel, D.A., Kinlan, B.P., Gaylord, Gaines, S.D. 2003. Lagrangian descriptions of marine larval dispersion. Mar. Ecol. Prog. Ser. 260:83–96.

Vaz, A. C., Paris, C.B., Olascoaga, M.J., Kourafalou V.H., Kang, H., Reed, J. K. 2016. The perfect storm: Match-mismatch of bio-physical events drives larval reef fish connectivity between Pulley Ridge mesophotic reef and the Florida Keys. Cont. Shelf Res. 125: 136 -146.

Weisberg, R.H., Li, Z., Muller-Karger, F. 2001. West Florida shelf response to local wind forcing: April 1998. J. Geophys. Res106(C12): 31,239-31,262.

Weisberg, R.H., Barth, A., Alvera-Azca´ rate, A., Zheng, L. 2009. A coordinated coastal ocean observing and modeling system for the West Florida Continental Shelf. Harmful Algae 8: 585-597.

Weisberg, R.H., Zheng, L., Liu, Y., Murawski, S., Hu, C. Paul, J. 2014. Did Deepwater Horizon hydrocarbons transit to the West Florida continental shelf? Deep-Sea Res. II 129: 259-272. http://dx.doi.org/10.1016/j.dsr2.2014.02.002i.

Weisberg, R. H., Zheng, L., Peebles, E. 2014. Gag grouper larvae pathways on the West Florida Shelf. Cont. Shelf Res. 88 :11–23. http://dx.doi.org/10.1016/j.csr.2014.06.003

Werner, F. E., Page, F. H., Lynch, D. R., Loder, J. W., Lough, R. G. Perry, R. I., Greenberg, D. A. and Sinclair, M. M.. 1993. Influences of Mean Advection and Simple Behavior on the Distribution of Cod and Haddock Early Life Stages on Georges Bank. Fish. Oceanogr. 2(2), 43-64.

Woods, L., and W.J. Hargis. 1971. Transport of bivalve larvae in a tidal estuary. In: D.J. Crisp, Ed., Fourth European Marine Biology Symposium. p. 29–44 Cambridge University Press.

Yang, H., Weisberg, R.H., Niiler, P.P, Sturges, W, Johnson.W. 1999. Lagrangian circulation and forbidden zone on the West Florida Shelf. Cont. Shelf Res. 19: 1221}1245

Zheng, L., Weisberg, R. 2012. Modeling the west Florida coastal ocean by downscaling from the deep ocean, across the continental shelf and into the estuaries. Ocean Model.48:10-29. doi: 10.1016/j.ocemod.2012.02.002.

Chapter 5: Conclusions and Discussion

This dissertation addresses three aspects of early life history: growth, ontogenetic vertical migration, and dispersal. These three aspects were chosen for exploration because each builds upon the previous. This work culminates in a larval dispersal model that incorporates larval ontogenetic depth migration for use with the GOM Atlantis model. Understanding growth in early life (Chapter 2 is necessary to calculate larval ages for the ontogeny of vertical migration in Chapter 3, and the depth-at-age predictions in Chapter 3 form the basis for seeding the depths in the dispersal model in Chapter 4. The dissertation culminates with an investigation into the impact of larval dispersal in the GOM through an update to the polygon connectivity matrix in the GOM Atlantis model.

In Chapter 2, published as “Early life history growth in fish reflects consumption-mortality tradeoffs” with Dr. Cameron Ainsworth in the journal Fisheries Research, we explore the differences in growth patterns between groups of fish and conclude that they may be due to differences in risk aversion behavior related to foraging. I constructed and compared length at age models for the early life stages of twelve grouper and snapper species and found that exponentially based models were most often the best representation of growth for these species. We then placed this phenomenon into a wider pattern of growth for demersal fish in a meta-analysis comparing the most common growth models used to represent demersal and pelagic fish. Demersal fish are more likely to be represented by exponent-based growth models, while pelagic fish are more often represented using linear-based growth models. We posit that this is related to risk-abatement in early life based on the trade-off between growth rate and predation risk in foraging arena theory (Walters and Juanes, 1993; Ahrens et al., 2012). Statistical tests indicated that demersal fish reach early life history milestones more slowly than pelagic fish, potentially because refugia shelter them until they exceed predator gape ranges, while pelagic fish need faster growth due to their exposed nature (Vasbinder and Ainsworth 2020).

Chapter 3 is in preparation as a manuscript with Dr. Cameron Ainsworth, Glenn Zapfe, Dr. Robert Weisberg, and Dr. Yonggang Liu as co-authors. In Chapter 3, I built a series of depth-at age models to explore potential patterns in ontogenetic depth occupancy and to identify depths for the seeding of the dispersal model in Chapter 4. Ontogenetic vertical migration has been shown to increase self-recruitment in some reef fish and has been found to significantly impact retention and connectivity of reef larvae alongside eddy perturbations and larval survival (Paris and Cowen 2004, Paris et al. 2007). In my Chapter 3 models, results show differences in depth occupancy between taxa and life stages and I posit that these differences may reflect differing life history strategies between taxa and life stages related to risk taking. Taxa with high depth fidelity produce leptokurtic distributions in water column occupancy indicating a potential choice of specific currents for transport. Uniformly distributed taxa may be instead employing a more risk-averse dispersal strategy. Thus, the patterns in both Chapters 2 and 3 show the potential that things that appear to be intrinsic larval traits, such as growth and ontogenetic vertical migration, may actually be indicative of larger differences in overall life history strategy related to risk taking during early life. The larval period is a particularly vulnerable stage of life for fish so the possibility to mitigate risk may be important.

Chapter 4 applies the findings of Chapter 3 to the construction of a dispersal model for the WFS and associated areas in the GOM using WFCOM and an update of the connectivity matrix for the GOM Atlantis model (Weisberg et al. 2014, Ainsworth et al. 2015). I identify potential spawning and settlement sites for a range of GOM taxa and then scale these results to the functional groups and polygons of the GOM Atlantis model. I find that many of our potential spawning sites on the WFS can be traced to areas where hydrodynamic conditions may be favorable for access to elevated productivity or access to structured substrates. Settlement sites are reflective of several well studied hydrodynamic phenomena on the WFS and FL Keys. The WFS is a hydrodynamically complex region, so the inclusion of both larval behavior and high-resolution hydrodynamic data can elucidate movement patterns in the early life of fish. When these spawning and settlement sites are used in Atlantis through the updated connectivity matrix to partition Age-1 recruits, the addition of dispersal can impact the distribution of fish production in the GOM.

Larval Behavior and Dispersal Modeling

Larval behavior can be difficult to discern using laboratory studies. Larval swimming speeds have been shown to be slower in in situ studies than in laboratory studies (Leis 2010, Leis 2006). In addition, because behaviors can be wildly different between species and habitat, it can be difficult to substitute behavior of one species or area for another (Leis 2010). I address these issues through the use of a set of generalized additive models from Chapter 3 that predict depth at age for a range of taxa in the GOM based on in situ environmental data from the SEAMAP ichthyoplankton survey. The behavioral predictions used in the dispersal model and in Atlantis therefore come from the same geographic area covered by the hydrodynamic and ecosystem model domains, and the families and species for which I predict depth overlap with our Atlantis functional groups. Thus, larval depth occupancy was predicted for the same taxa and area as the ecosystem model it was used in.

While this thesis makes use of larval behavior in terms of vertical water column occupancy, there are other behaviors which may impact dispersal that I was unable to include. For example, the larvae “choose” their depth through the statistical predictive models in Chapter 3, but they are oriented using the direction of the currents in WFCOM. Larvae gain the ability to orient themselves in a specific direction early in ontogeny, and orientation has been suggested as a self-recruitment driver in reef fish (Leis 2010, Staaterman et al. 2012). Larvae may be able to orient based on a variety of cues including reef odor and magnetic field shift cues (Paris et al. 2013, O’Connor and Muheim 2017). Some of this orientation behavior is reliant on environmental cues (Staaterman and Paris 2014). The portion of orientation behavior driven by environmental cues would be at least partially resolved in my GAM models, as they were built using a diversity of environmental variables. Another behavior that could impact larval dispersal is swimming strength. A 2010 review of larval behavior studies showed that among the surveyed studies on larval swimming speeds in the laboratory, larvae of species that did not have pelagic eggs swam fast enough to have an impact on their own dispersal (Leis 2010, Leis 2006). Another study by the same authors found that larvae of both pelagic and demersal-egg species have comparable swimming ability, and this ability increases as the larvae grow (Leis 2007). My model includes the entire larval duration, so it is possible that near the end of their time in the water column, larvae may have more control over where they settle. The inclusion of larval behavior in dispersal modeling is an exciting and emerging field, and this model is one of the few in this region to include depth occupancy choice behavior. Future studies should include expanded categories of larval behavior as *in situ* data become available for a wider range of taxa.

The dataset used to predict depth in this dissertation, the SEAMAP ichthyoplankton survey data, was a good candidate for investigation into ontogenetic migration due to its resolved depth layers associated with sampling. While my work explores the ontogenetic vertical migrations of larvae and their resulting transport, there are still many questions related to larval vertical migrations and dispersal that this dissertation does not address and that we do not have an adequate data set available to explore. For example, larvae also migrate vertically on diel scales, which cannot be resolved by the data from the current sampling surveys in the GOM. In addition, the available sampling data allow for an exploration of transport throughout the entire WFS area, but do not allow pinpointed investigations into differences in larval transport between seasons or between multiple cohorts within a year. Sampling surveys must be designed to gain as much information as possible to address a variety of questions with limited resources.

If resources were not limited, we could design an idealized sampling procedure to address questions surrounding many aspects of early life. The ideal sampling set to resolve some of the questions surrounding diel vertical migration and seasonal current variations would be one with greater temporal resolution. To investigate diel migration, daily and nightly samples taken at set times and intervals would be necessary. In addition, sampling that occurs throughout the year, at regular monthly intervals, could aid in the exploration of the timescales of flow that impact specific fish species. Currently, larvae are released in my Lagrangian dispersal model at the date of sampling. If sampling could be ramped up during anomalous conditions that could change the hydrodynamic fields larvae are exposed to; for example, during storm events. This could further elucidate the impact that these events have on the transport of larvae. Increased sampling during storm seasons could lead to the discovery of alternate pathways for transport and help assess the degree to which anomalous conditions lead to larvae lost in unfavorable areas. Increasing temporal resolution would come at a cost as it would require more frequent sampling. However, some of that cost could be offset through a decrease in spatial resolution of the data. This dissertation provides proposed spawning and settlement sites for many GOM families, so constraining sampling to areas directly related to the transport of target species could decrease the need for high spatial resolution.

This dissertation also provides a potential jumping off point for several other questions regarding larval dispersal and recruitment. In the future, we can determine statistically whether peak recruitment years tend to be characterized by a high degree of overlap in settlement locations (predicted from the larval transport model) and known prime rearing habitat. In addition, future work stemming from this dissertation should investigate the uncertainty surrounding the spawning and settlement sites identified. This could be done by seeding a cloud of points into the Lagrangian model around the identified spawning locations to see how many particles reached suitable settlement habitat. This would allow me to place an error estimate around the number of larvae that could potentially reach a particular habitat. In addition, the GAM could be sampled probabilistically instead of assuming the mode. This would allow the identification of potential depth layers with viable transport pathways other than those that are most common, and could reveal alternate pathways taken by larvae. This would allow for a sensitivity analysis of the depth estimates. This dissertation is focused on what a specific subset of larvae, those caught at SEAMAP sites, do: what depth they travel in, where they go, and where they might come from. This allows us to identify some potential pathways for larvae dispersal in the GOM.

The modeling framework laid out by my dissertation provides the background not just to identify what specific larvae likely do, but also to investigate in the future what they could do given new scenarios or environmental drivers. The models built during the course of my dissertation, especially the custom Lagrangian model that I built based on a highly resolved local hydrodynamic data from the WFCOM model, has the potential to serve as a framework for many further forays into questions concerning larval dispersal and recruitment in the GOM.

Synergy with Future WFS Research Areas and Management Objectives

The identification of spawning and settlement sites has far-reaching management applications. The life history and dispersal of target species can impact the effectiveness of marine reserves. Reserve networks connected by dispersal of larvae or adults have been suggested as a bet-hedging alternative to the risks associated with placing a single reserve in a location that may end up being unbeneficial (Roberts 2000). Atlantis has been used successfully for MPA evaluation off the coast of Australia, in the Gulf of California, and in Guam (Savina et al. 2013, Ainsworth et al. 2012, Weijerman et al 2016). The potential synergy between larval dispersal and MPA siting has also been explored in the GOM (Drexler 2018), and my project expands on that work through a new dispersal model built on high resolution WFS data and the inclusion of depth-occupancy behavior. Habitat essential for spawning or for the early life stages of fish could be candidate habitat for use in future management evaluation scenarios. In addition to MPA siting, these spawning and settlement sites could also be used for identifying potential essential habitat overlaps between fisheries species and endangered taxa such as manatees, turtles and seabirds. Two 2017 papers recommended using ecosystem models to guide habitat restoration efforts and account for the use of habitat by different life stages (Gruss et al. 2017, O’Farell et al. 2017).

Sea grass, for example is known to be an important juvenile habitat for valuable fisheries species (Coleman et al. 1996, Koenig and Coleman 1998). Seagrass is also a food source and habitat for manatees, turtles, and seabirds (Valentine and Duffy 2006, Domning et al. 2001, Valentine et al. 2000). Areas that receive larvae are potentially important habitat to support overlapping fisheries and conservation objectives. Using my identified potential spawning and settling sites in synergy with projects related to the protection of marine mammals and other endangered taxa could help identify areas for conservation and management that would balances the needs of multiple species and sectors. Another GOM management priority is the quantification of red tide impacts on community structure (O'Farrell et al. 2017). Brevotoxins produced by red tide can cause hatching and developmental abnormalities in eggs and larvae, and harmful algal blooms are toxic to juvenile fish (Buskey and Hyatt 2006, Riley et al. 1989, Kimm-Brindson and Ramsdall 2001, Shih et al. 2012). My identified potential spawning and settlement sites could be used as starting points for future investigations into the overlap between red-tide areas and essential habitat for early life stages of fish to assess potential loss of stock due to brevotoxin caused mutation and mortality.

A Case for Place-Based EBFM

The findings in this thesis emphasize the importance of place-based Ecosystem Based Fisheries Management (EBFM). Because EBFM seeks to manage target species within the framework of a range of ecosystem factors, and because EBFM must work within the confines of local management structures, it is already important that EBFM be place-based (Pikitch et al. 2004). I make the case here that in hydrodynamically complex regions, such as the West Florida Shelf, place-based EBFM is especially important so that local circulation drivers are included in ecosystem models. The coupling of hydrodynamic models to ecosystem models by outsourcing the calculations of dispersal to a dispersal model built with local high-resolution hydrodynamic data, as I have done here, is one way to increase the degree of place-based considerations in EBFM. Place-based EBFM has a proven history of increasing the effectiveness of management, and place-based approaches are necessary, because each region has its own social structures and ecological complexities (Barsuto 2005, Cinti et al. 2010, Ainsworth et al. 2012). Atlantis work in the Gulf of California has shown that management policies adapted to the specific goals and needs of the area have the potential to be more effective, especially when the needs of local fisheries and endangered species are taken into account and conflicting interests are explored (Ainsworth et al. 2012).

Place-based management also allows the goals and complexities associated with a specific ecosystem to be scaled to an appropriate spatial and temporal scale (Levin et al. 2009). Ecological complexities related to predator-prey dynamics, the spatial overlap of competing predators, and the need to balance performance measures representing the interests of multiple stakeholders can necessitate place-based ecosystem models (Eero et al. 2012, Fulton et al. 2014). As production and movement on the WFS are driven by a unique, place-specific hydrodynamic environment related to shelf physiography, the WFS is a model candidate for place-based EBFM. One of the major principles of place-based EBFM is that of adaptive management: the ability of management structures to account for changes in complex systems or changes in our understanding of complex systems (Young et al. 2007). Ecosystem models already play a role in place-based EBFM and adaptive management because a variety of scenarios can be played out in the model before actual implementation in that region. The larval connectivity matrix and Atlantis model can play a key role in adaptive management. Including a hydrodynamic modeling component in adaptive management could be a future way forward to give regions the ability to solve specific problems rising from changes in hydrodynamic conditions, and to assess management options related to seasonal and synoptic flow patterns. This dissertation provides the framework to better understand early life stages in the GOM and represents an approach to include the impacts of early life in the way we model fisheries and ecosystems.

References

Ahrens, R.N.M., Walters, C.J., Christensen, V., 2012. Foraging arena theory. Fish Fish. 13, 41 59.

Ainsworth, C.H., Morzaria-Luna, H., Kaplan, I.C., Levin, P.S., Fulton, E.A., Cudney-Bueno, R., Turk-Boyer, P., Torre, J., Danemann, G.D., Pfister, T. 2012. Effective ecosystem-based management must encourage regulatory compliance: A Gulf of California case study. Mar. Policy 36:1275–1283.

Ainsworth, C.H., Schirripa, M.J., Morzaria -Luna, H. (eds.) 2015.An Atlantis Ecosystem Model for the Gulf of Mexico Supporting Integrated Ecosystem Assessment.NOAA Technical Memorandum. NMFS-SEFSC-676, 149 p. doi: 10.7289/V5X63JVH.

Basurto X. 2005. How locally designed access and use controls can prevent the tragedy of the commons in a Mexican small-scale fishing community. Soc. Nat. Res. 18:643–59

Buskey, E.J., Hyatt., C.J. 2006. Use of the FlowCAM for semi-automated recognition and enumeration of red tide cells (*Karenia brevis*) in natural plankton samples. Harmful Algae 5: 685-692.

Cinti A, Shaw W, Torre J. 2010. Insights from the users to improve fisheries performance: fishers’ knowledge and attitudes on fisheries policies in Bahı´a de Kino, Gulf of California, Mexico. Mar. Policy 34:1322–34

Costelloa, C., Rassweilerb, A., Siegelc, D., De Leod, G., Michelie, F., and Rosenbergf, A. 2010. The value of spatial information in MPA network design. Proc. Natl. Acad. Sci. 107(43):18294-18299.

Coleman, F.C., Koenig, C. C., Collins, L. A. 1996. Reproductive styles of Shallow-Water Groupers (Pisces: Serranidae) in the Eastern Gulf of Mexico and the Consequences of Fishing Spawning Aggregations. Environ. Biol. Fish. 47:129-141.

Domning, D.P. 2001. Sirenians, seagrasses, and Cenozoic ecological change in the Caribbean. Palaeogeography, Palaeoclimatology, and Palaeoecology. 166:27-50.

Drexler, M. 2018. Evaluating the use of larval connectivity information in fisheries models and management in the Gulf of Mexico. Graduate Theses and Dissertations. https://scholarcommons.usf.edu/etd/7499

Eero, M. VInther, M. Haslob, H. Huwer, B. Casini, M, Storr-Paulesen, M., Koster, F.W. 2012. Spatial management of marine resources can enhance the recovery of predators and avoid local depletion of forage fish. Conserv. Lett. 5: 486–492

Fulton, E.A., Parslow, J.S., Smith, A.D.M., Johnson, C.R. 2004. Biogeochemical Marine Ecosystem Models. 2. The Effect of Physiological Data on Model Performance. Ecol. Model. 173, 371-406.

Fulton, E.A., Smith, A.D.M., Smith, D.C. 2007. Alternative management strategies for southeast Australian Commonwealth Fisheries: Stage 2: quantitative management strategy evaluation. Australian Fisheries Management Authority. Fisheries Research and Development Corporation.

Fulton EA, Smith ADM, Smith DC, Johnson P. 2014. An integrated approach is needed for Ecosystem Based Fisheries Management: Insights from ecosystem-level management Strategy Evaluation. PLoS ONE 9(1): e84242. doi:10.1371/journal.pone.0084242

Gruss, A., Rose, K.A., Simons, J., Ainsworth, C.A., Babcock, E., Chagaris, D., de Mutsert, K., Froeschke, J., Himchak, P., Kaplan, I.C., O’Farrell, H., Zetina Rejon, M.J. 2017. Recommendations on the use of Ecosystem modeling for Ecosystem-Based Fisheries Management and restoration outcomes in the Gulf of Mexico. Mar. Coast. Fish. 9(1): 281-95. doi: 10.1080/1945120.2017.1330786.

Kimm-Brinson K.L. and Randall, J.S. 2001. The red tide toxin, brevotoxin, induces embryo toxicity and developmental abnormalities. Environ. Health Persp. 109(4):377-381.

Koenig, C.C., Coleman, F.C. 1998. Absolute Abundance and Survival of Juvenile Gags in Sea Grass Beds of the Northeastern Gulf of Mexico. T. Am. Fish. Soc. 127(1) 44-55.

Leis, J.M. 2010. Ontogeny of behaviour in larvae of marine demersal fishes. Ichthyol. Res. 57:325–342

Leis, J.M., Hay, A.C., Lockett, M.M., Chen, J., and Fang, L. 2007. Ontogeny of swimming speed in larvae of pelagic-spawning, tropical, marine fishes. Marine Ecological Progress Series Vol. 349: 255–267, 2007

Levin P.S., Fogarty M.J., Murawski S.A., Fluharty, D. 2009. Integrated ecosystem assessments: Developing the scientific basis for ecosystem-based management of the ocean. PLoS Biol 7(1): e1000014. doi:10.1371/journal.pbio.1000014

National Oceanic and Atmospheric Administration (2006) Evolving an ecosystem approach to science and management through NOAA and its partners. Available: http://www. sab.noaa.gov/Reports/eETT_Final_1006.pdf. Accessed 5 December 2008

O’Farrell, H., Gruss, A., Sagarese, S.R., Babcock, E.A., and Rose, K.A. 2017. Ecosystem modeling in the Gulf of Mexico: current status and future needs to address ecosystem based fisheries management and restoration activities. Reviews in Fish Biology and Fisheries 27:587-614. DOI: 10.1007/s11160-017-9482-1

O'connor, J., Muheim, R. 2017. Pre-settlement coral-reef fish larvae respond to magnetic field changes during the day. J. Exp. Biol. 220, 2874-2877. doi:10.1242/jeb.159491

Paris, C.B., Che'rubin, L. M., Cowen, R. K.. 2007. Surfing, spinning, or diving from reef to reef: effects on population connectivity. Mar. Ecol. Prog. Ser. Vol. 347: 285–300.

Paris, C.B., Cowen, R. K.. 2004. Direct evidence of a biophysical retention mechanism for coral reef fish larvae. Limnol. Oceanogr., 49(6): 1964–1979.

Paris C.B., Atema J., Irisson J-O., Kingsford M., Gerlach G., Guigand, C.M. 2013. Reef Odor: A Wake Up Call for Navigation in Reef Fish Larvae. PLoS ONE 8(8): e72808. doi:10.1371/journal.pone.0072808

Pikitch, E.K., Santora, C., Babcock, E.A., Bakun, A., Bonfil, R., Conover, D.O., Dayton, P., Doukakis, P., Fluharty, D., Heneman, B., Houde, D., Link, J., Livingston, P.A., Mangel, M. McAllister, M.K., Pope, J., Sainsbury, K.J. 2004. Ecosytem Based Fishery Management. Science 305: 346-347.

Riley C.M., Holt S.A., Holt J, Buskey E.J., and Arnold, C.R. 1989. Mortality of larval red drum (*Sciaenops ocellatus*) associated with a Ptychodiscus brevis red tide. Contrib. Mar. Sci. 31:137-146.

Roberts, C. 2000. Selecting marine reserve locations: optimality versus opportunism. Bull. Mar. Sci. 66(3): 581–592, 20

Savina, M., Condie, S.A., Fulton, E.A. 2013. The Role of Pre-Existing Disturbances in the Effect of Marine Reserves on Coastal Ecosystems: a Modeling approach. PLoS One, DOI: 10.1371/journal.pone.0061207.

Shi, F., McNabb, P., Rhodes L., Holland, P., Webb,S. , Adamson, J., Immers , A., Gooneratne, R., Holland, J. 2012. The toxic effects of three dinoflagellate species from the genus Karenia on invertebrate larvae and finfish, New Zeal. J. Mar. Fresh. 46:2, 149-165 doi: 10.1080/00288330.2011.616210

Staaterman, E., Paris, C. B. 2014. Modelling larval fish navigation: the way forward. – ICES J. Mar. Sci.71: 918–924.

Staaterman, E., Paris, C.B., Helgers, J. 2012. Orientation behavior in fish larvae: A missing piece to Hjort's critical period hypothesis. J. Theor. Biol. 304:188–196

United States Government Accounting Office (1994) Ecosystem management: Additional actions needed to adequately test a promising approach. Available: http://archive.gao.gov/

Valentine, J.F., Heck, K.L. 1999. Seagrass herbivory: evidence for the continued grazing of marine grasses. Mar. Ecol. Prog. Ser. 176:291-302.

Valentine, J.F., Duffy, J.E. 2006. The central role of grazing in seagrass ecology. In A.W.D. Larkin, Orth, R.J., Duarte, C. Ed. Seagrasses:Biology, Ecology, and Conservation. 463 501. Springer.

Vasbinder, K., Ainsworth, C. 2020. Early Life History Growth in Fish Reflects Consumption Mortality Tradeoffs. Fish. Res. 227:105538.

Walters, C.J., Juanes, F., 1993. Recruitment limitation as a consequence of natural selection for use of restricted feeding habitats and predation risk taking by juvenile fishes. Can. J. Fish. Aquat. Sci. 50, 2058–2070.

Watson, J. R., Mitarai1, S., Siegel, D. A., Caselle, J. E., Dong, C., McWilliams, J.C. 2010. Realized and Potential Larval Connectivity in the Southern California Bight. Mar. Ecol. Prog. Ser. 401:31-28.

Weijerman M., Fulton E. A., Brainard R. E. 2016. Management strategy evaluation applied to coral reef ecosystems in support of ecosystem based management. PLoS ONE 11(3): e0152577. doi:10.1371/journal.pone.0152 577.

Weisberg, R. H., Zheng, L., Liu, Y. Murawski, S., Hu, C., Paul, J. 2014. Did Deepwater Horizon hydrocarbons transit to the west Florida continental shelf? Deep-Sea Res. II http://dx.doi.org/10.1016/j.dsr2.2014.02.002i.

Young, O., Osherenko, G., Ekstrom, J., Crowder, L., Ogden, J., Wilson, J., Day, J., Douvere, F., Ehler, C., McLeod, K., Halpern, B., Peach, R. 2007. Solving the crisis in ocean governance: Place-Based Management of Marine Ecosystems. Environment 49(4):20-32.

Appendix 1: Online supplementary material associated with Chapter 2: Vasbinder, K and C. Ainsworth. 2020. Early Life History Growth in Fish Reflects Consumption-Mortality Tradeoffs. Fish. Res. 227:105538.

To access this article through the publisher:

https://doi.org/10.1016/j.fishres.2020.105538

This supplementary material related to this article can be found, in the online version, at doi:https://doi.org/10.1016/j.fishres.2020.105538.

This appendix is included in this dissertation under the author permissions guidelines of Elsevier publishers, which includes a release to authors to include their publication in their dissertation.

Supplemental Table 1: Published Larval Growth Models

Species	Family	Model Type	Model	Location of study	Modelers	Location of Published Model
Blue Fin Tuna, *Thunnus thynnus*	Scombridae	Linear	$L = 0.46 * \text{age} + 2.24$	Gulf of Mexico	Malca et al. 2017	Malca et al. 2017
Blue Lanternfish, *Tarleton-beania crenularis*	Myctophidae	Curvi-linear	$L = 1.3451 + 0.4055 * \text{Age} - 0.0028 * Age^2$	Oregon	Bystydzieńska et al. 2010	Bystydzieńska et al. 2010
Camouflage grouper, *Epinephelus polyphekadion*	Serranidae	Expon-ential	Three Versions: $L = 2.0319 * e^{0.01712*age}$ $L = 7.3131 * e^{0.0602*age}$ $L = 2.3223 * e^{0.0469*age}$	Bali province, Indonesia	Jayadi et al. 2017	Jayadi et al. 2017
Southern Bluefin Tuna, *Thunnus maccoyii*	Scombridae	Linear	$L = 0.326 * \text{age} + 2.029$	East Indian Ocean	Jenkins and Davis 1990	Jenkins and Davis 1990
Spanish Mackerel, *Scomb-eromorus maculatus*	Scombridae	Linear	$L = 1.31 * \text{age} - 1.3$	Gulf of Mexico and U.S. South Atlantic Bight.	DeVries et al. 1990	DeVries et al. 1990
King Mackerel, *Scomb-eromorus cavalla*	Scombridae	Linear	$L = 0.82 * \text{age} + 0.37$	Gulf of Mexico and U.S. South Atlantic Bight.	DeVries et al. 1990	DeVries et al. 1990

Black Southern Cod, *Patagonotothen tessellata*	Nototheniidae	Linear, Von Bertalanffy for unfed	age 1 to 5 day: $L = 0.1726 * \text{age} + 5.4901$ age 19-21 day: $L = 0.2779 * \text{age} + 1.2404$ unfed larvae: $L = 7.14 * (1 - \mathrm{e}^{-0.5(\text{age}--2.51)})$	Lapataia Bay, Beagle Channel, Argentina.	Rae et al. 1999	Rae et al. 1999
Sailfish, *Istiophorus platypterus*	Istiophoridae	Exponential	$L = 1.955 * e^{0.1372 * age}$	Straits of Florida	S.A.Luthy et al. 2005	S.A.Luthy et al. 2005
Bay Anchovy, *Anchoa michilli*	Engraulidae	Linear	$L = 0.586 * \text{age} + 2.195$	Unknown	Houde and Schekter 1981	S.A.Luthy et al. 2005
Atlantic Bumper, *Chloroscombrus chrysurus*	Carangidae	Linear	$L = 0.40 * \text{age} - 0.13$	Northern Gulf of Mexico	Leffler and Shaw 1992	S.A.Luthy et al. 2005
Atlantic Herring, *Clupea harengus*	Clupeidae	Gompertz Family	$L = 30.9 * e^{-1.7 * e^{-0.03 * age}}$	Gulf of Maine George's Bank Region	Lough et al 1982	S.A.Luthy et al. 2005
Dolphinfish, *Coryphaena hippurus*	Coryphaenidae	Exponential	$L = 3.19 * e^{0.087 * age}$	Unknown	Benetti 1992	S.A.Luthy et al. 2005
Atlantic Cod, *Gadus morhua*	Gadidae	Exponential	$L = 4.82 * e^{0.025 * age}$	George's Bank	Boltz and Lough 1983	S.A.Luthy et al. 2005
Atlantic Cod, *Gadus morhua*	Gadidae	Modified Exponential	Browns 1984: $L = 1.24 * e^{0.0133 * age}$ Browns 1985 February: $L = 1.04 * e^{0.0217 * age}$ Browns 1985 March: $L = 1.02 * e^{0.0230 * age}$	Gulf of Maine	Campana and Hurley 1989	Campana and Hurley 1989

			Browns 1985 April: $L = 1.13 * e^{0.0161 *age}$ Browns 1985 May: $L = 1.02 * e^{0.0278 *age}$ Browns 1985 June: $L = 1.01 * e^{0.0275 *age}$ Georges 1984, March: $L = 1.04 * e^{0.0186 *age}$ Georges 1985, April: $L = 1.00 * e^{0.0272 *age}$ Georges 1985, May: $L = 1.45 * e^{0.0225 *age}$			
Spot, *Leiostomus xanthurus*	Scianidae	Laird-Gompertz	$Length = 1.609 * e^{2.624*(1-e^{-0.0255*Age})}$	North Carolina	Warlen and Chester 1985	S.A.Luthy et al.
Atlantic Blue Marlin, *Makaira nigricans*	Istiophoridae	Exponential	$L = 2.18 * e^{0.1282 *age}$	Exuma Sound, Bahamas, and the Straits of Florida	Sponaugle et al. 2005	S.A.Luthy et al.
Haddock, *Melanogrammus aeglefinus*	Gadidae	Exponential	$L = 3.54 * e^{0.0346 *age}$	George's Bank	Boltz and Lough 1983	S.A.Luthy et al.
Haddock, *Melanogrammus aeglefinus*	Gadidae	Modified Exponential	Browns 1984, March: $L = 0.828 * e^{0.0234 *age}$ Browns 1985, April: $L = 0.920 * e^{0.0258 *age}$ Browns 1985, May: $L = 0.905 * e^{0.0266 *age}$ Browns 1985, June:	Gulf of Maine	Campana and Hurley 1989	Campana and Hurley 1989

			$L = 0.941 * e^{0.0284\ *age}$			
Bluefish, *Pomatomus saltatrix*	Pomatomidae	Linear	$L = 0.33 * \text{age} + 1.78$	Middle Atlantic Bight	Hare and Cowen 1994	S.A.Luthy et al.
Yellowfin Tuna, *Thunnus albacares*	Scombridae	Linear	$L = 0.47 * \text{age} + 1.67$	Mississippi River plume	Lang et al 1994	S.A.Luthy et al.
Swordfish, *Xiphias gladius*	Xiphiidae	Linear	before and after (including) 13.29 days; $L = 0.26 * \text{age} + 3.2$ $L = 5.86 * \text{age} - 71.22$	Western North Atlantic	Govoni et al 2003	S.A.Luthy et al.
Schoolmaster Snapper, *Lutjanus apodus*	Lutjanidae	Laird-Gompertz	$L = 2.26 * e^{(0.032\ /\alpha)*(1-e^{--0.037*Age})}$	Straits of Florida and Western Atlantic	D'Alesandro et al. 2010	D'Alesandro et al. 2010
Lane Snapper, *L. synagris*	Lutjanidae	Laird-Gompertz	West $L = 2.10 * e^{(0.028\ /\alpha)*(1-e^{--0.053*Age})}$ East $L = 2.10 * e^{(0.040\ /-0.007)*(1-e^{--0.007*Age})}$	Straits of Florida and Western Atlantic	D'Alesandro et al. 2010	D'Alesandro et al. 2010
Mutton Snapper *L. analis*	Lutjanidae	Laird-Gompertz	West: $L = 2.35 * e^{(0.026\ /-0.057)*(1-e^{--0.057*Age})}$ East:	Straits of Florida and Western Atlantic	D'Alesandro et al. 2010	D'Alesandro et al. 2010

			$L = 2.35 * e^{(0.017/-0.079)*(1-e^{--0.079*Age})}$			
Gray Snapper *L. Griseus*	Lutjanidae	Laird-Gompertz	$L = 2.26 * e^{(0.027\ /-0.049)*(1-e^{--0.049*Age})}$	Straits of Florida and Western Atlantic	D'Alesandro et al. 2010	D'Alesandro et al. 2010
Menhaden, *Brevoortia tyrannus*	Clupeidae	Laird-Gompertz	2005–2006: $L = 3.61 * e^{2.2133*(1-e^{-0.0502*Age})}$ 2006-2007: $L = 3.61 * e^{2.1667*\left(1-e^{-0.0580*Age}\right)}$ 2007-2008: $L = 3.61 * e^{2.2765*\left(1-e^{-0.0475\text{x}*Age}\right)}$	Chesapeake Bay	Lozano et al. 2012	Lozano et al. 2012
White Mullet *Mugil curema*	Mugilidae	Exponential	$L = 2.1305 * e^{0.0720\ *age}$	Biscayne Bay, Florida	Houde et al. 1976	Houde et al. 1976
Plaice, *Pleuronexties platessa*	Pleuronectidae	Gompertz	1986: $L = 88.87 * e^{-e^{-0.0188*(t-43.35)}}$ 1987: $L = 109.05 * e^{-e^{-0.0114*(t-78.75)}}$	Red Wharf Bay, Anglesey, North Wales	Al-Hossaini et al. 1989	Al-Hossaini et al. 1989
Anchovy, *Engraulis anchoita*	Engraulidae	Laird-Gompertz	Winter: $L = 8.648 * e^{1.732*(1-e^{-0.020*Age})}$	Southwest Atlantic	Castello and Castello 2003	Castello and Castello 2003

			Spring: $L = 6.512 * e^{1.374*(1-e^{-0.052*Age})}$			
Sardine, *Sardina pilchardus*	Clupeidae	Gompertz Laird-Gompertz	**Adriatic:** Gompertz: $L = 29.58856 * e^{-1.967218*(e^{-0.08410072*Age})}$ Laird: $L = 4.138228 * e^{\left(\frac{0.1654595}{0.08411218}\right)*(1-e^{-0.08411218*Age})}$ **Bay of biscay all data** Gompertz: $L = 18.19694 * e^{-2.934296*(e^{-0.2449932*Age})}$ Laird: $Le = 0.9660789 * e^{\left(\frac{0.7194761}{0.2450811}\right)*(1-e^{-0.2450811Age})}$ **Bay of Biscay 7 day old only** Gompertz: $L = 29.6175 * e^{-3.304057*(e^{-0.1759623*Age})}$ Laird:	Eastern Adriatic and Bay of Biscay	Dulcic 1995	Dulcic 1995

			$L = 1.086755 * e^{\left(\frac{0.582053}{0.1761917}\right)*(1-e^{-0.1761917Age})}$			
Anchovy, *Engraulis encrasicolus*	Engraulidae	Gompertz Laird-Gompertz	Gompertz: $L = 36.87 * e^{-2.609*(e^{-0.077*Age})}$ Laird-: $Le = 2.71 * e^{\left(\frac{0.203}{0.077}\right)*(1-e^{-0.077*Age})}$	Northern Adriatic	Dulcic 1997	Dulcic 1997
Sprat, *Sprattus sprattus phalericus*	Clupeidae	Gompertz Laird-Gompertz	Gompertz: 1995: $L = 25.92 * e^{-1.379*(e^{-0.067*Age})}$ 1996: $L = 25.65 * e^{-1.336*(e^{-0.067\ *Age})}$ Laird: 1995: $L = 6.52 * e^{(0.092/0.067)*(1-e^{-0.067*Age})}$ 1996: $L = 6.74 * e^{(0.089/0.067)*(1-e^{-0.067*Age})}$	Northern Adriatic	Dulcic 1998	Dulcic 1998

Anchovy, *Engraulis encrasicolus*	Engraulidae	Exponential	Gulf of Lions, $L = 4.339 * e^{0.076*age}$ Catalan Sea, $L = 5.106 * e^{0.061*age}$	Gulf of Lions and Catalan Sea	Garcia et al. 1998	Garcia et al. 1998
Anchoveta, *Engraulis ringens*	Engraulidae	Linear, Gompertz, VBGF	Linear: $L = 0.47 * age + 6.4$ Gompertz: $L = 5.4 * e^{1.5 *(1-e^{-0.07*Age})}$ Von Bertalanffy: $L = 27.5(1 - e^{-0.03(age-5.4)})$	Central Chile	Hernandez and Castro 2000	Hernandez and Castro 2000
Flounder *Rhombosela tapirina*	Pleuronectidae	Exponential	$L = 1.939 * e^{0.0415*age}$	Port Phillip Bay, Victoria, Australia	Jenkins 1987	Jenkins 1987
Flounder, *Ammotretris rostratus*	Pleuronectidae	Exponential	$L = 2.207 * e^{0.0434*age}$	Port Phillip Bay, Victoria, Australia	Jenkins 1987	Jenkins 1987
Atlantic Menhaden, *Brevoortia tyrannus*	Clupeidae	Laird Gompertz	$L = 2.980 * e^{2.109*(1-e^{-0.062*Age})}$	Onslow Bay, North Carolina	Maillet and Checkley 1991	Maillet and Checkley 1991

Anchovy, *Engraulis encrasicolus*	Engraulidae	Gomp-ertz	$L = e^{3.4} * e^{2.3931*(1-e^{-0.0781*Age})}$ $L = e^{1.3343} * e^{2.6464*(1-e^{-0.059*Age})}$	Western Mediterranean Sea	Palomera et al. 1988	Palomera et al. 1988
European Smelt, *Osmerus eperlanus*	Osmeridae	Linear	$L = 0.556 * age + i6.191$	Elbow River, Germany	Sepulveda 1994	Sepulveda 1994
English Sole, *Parophrys vetulus*	Pleuronectidae	Gomp-ertz	$L = 2.073 * e^{2.354*(1-e^{-0.045*Age})}$	Oregon	Rosenberg 1982	Rosenberg 1982
Pilchard/Pacific Sardine, *Sardinops sagax*	Clupeidae	Linear and Laird-Gomp-ertz (from Campana and Jones 1992)	$L = 23.936 * e^{-e^{-0.092*(Age-8.14)}}$ Linear: Nov 1998 $L = 0.065 * age + 4.224$ Linear: Jan 1999 $L = 0.796 * age + 0.551$	East Australian Current	Uehara et al. 2005	Uehara et al. 2005
Japanese Sardine, *Sardinops melanostictus*	Clupeidae	Linear	Station 57: $L = 0.605 * \text{age} + 2.851$ Station 83: $L = 0.411 * \text{age} + 3.950$ Station 100: $L = 0.750 * \text{age} + 2.509$	Western Japan	Watanabe and Kuroki 1997	Watanabe and Kuroki 1997
Sardine, *Sardina pilchardus*	Clupeidae	Linear	$L = 0.25 * \text{age} + 3.862$	Bay of Biscay	Garrido et al. 2015	Garrido et al. 2015

Leopard Grouper, *Mycteroperca rosacea*	Serranidae	Linear	24C: $L = 0.4839 * \text{age} + 0.2972$	Lab reared, location of broodstock not listed	Maritinez -Lago and Gracia -Lopez 2009	Maritinez -Lago and Gracia- Lopez 2009
Leopard Grouper, *Mycteroperca rosacea*	Serranidae	Linear	28C: $L = 0.0053 * \text{age} + 1.723$ 26C: $L = 0.0056 * \text{age} + 1.776$ 24C: $L = 0.0047 * \text{age} + 1.869$ 20C: $L = 0.0034 * \text{age} + 2.118$	Isla San Jose, Mexico	Gracia -Lopez et al. 2004	Gracia -Lopez et al. 2004
Atlantic Herring, *Clupea harengus*	Clupeid	Linear	Released at 13 DAF $L = 0.50 * age + 7.22$ Released at 15 DAF $L = 0.56 * age + 7.24$ Newly hatched larvae $L = 0 \cdot 25 \; * age + 8 \cdot 76$	Firth of Clyde	Geffen 2002	Geffen 2002
Southern Herring, *Herklotsichthys castelnaui*	Clupeid	Laird-Gompertz	$L = 5.26 * e^{\left(\frac{0.104}{0.075}\right)*(1-e^{-0.075*Age})}$	Townsville, Northeastern Australia	Thorrold 1988	Thorrold 1988
Greay Snapper *Lutjanus griseus*	Lutjanid	Linear	2000 Florida Bay: $L = 0.8736 * \text{age} + 8.23$ 2000 Biscayne Bay: $L = 0.7953 * \text{age} + 7.214$ 2000 Jupiter: $L = 0.8848 * \text{age} + 6.59$ 2000 Sebastian Inlet: $L = 0.6865 * \text{age} + 9.113$ 2000 Core Sound:	East Coast of United States	Denit & Sponaugle 2004	Denit & Sponaugle 2004

			$L = 0.6172 * \text{age} + 10.949$ 2001 Biscayne Bay: $L = 0.806 * \text{age} + 8.08$ 2001 Jupiter: $L = 0.8023 * \text{age} + 9.242$ 2001 Sebastian Inlet: $L = 0.6757 * \text{age} + 10.071$ 2001 Core Sound: $L = 0.7187 * \text{age} + 10.62$			

Supplemental Plot 1: Clupeids

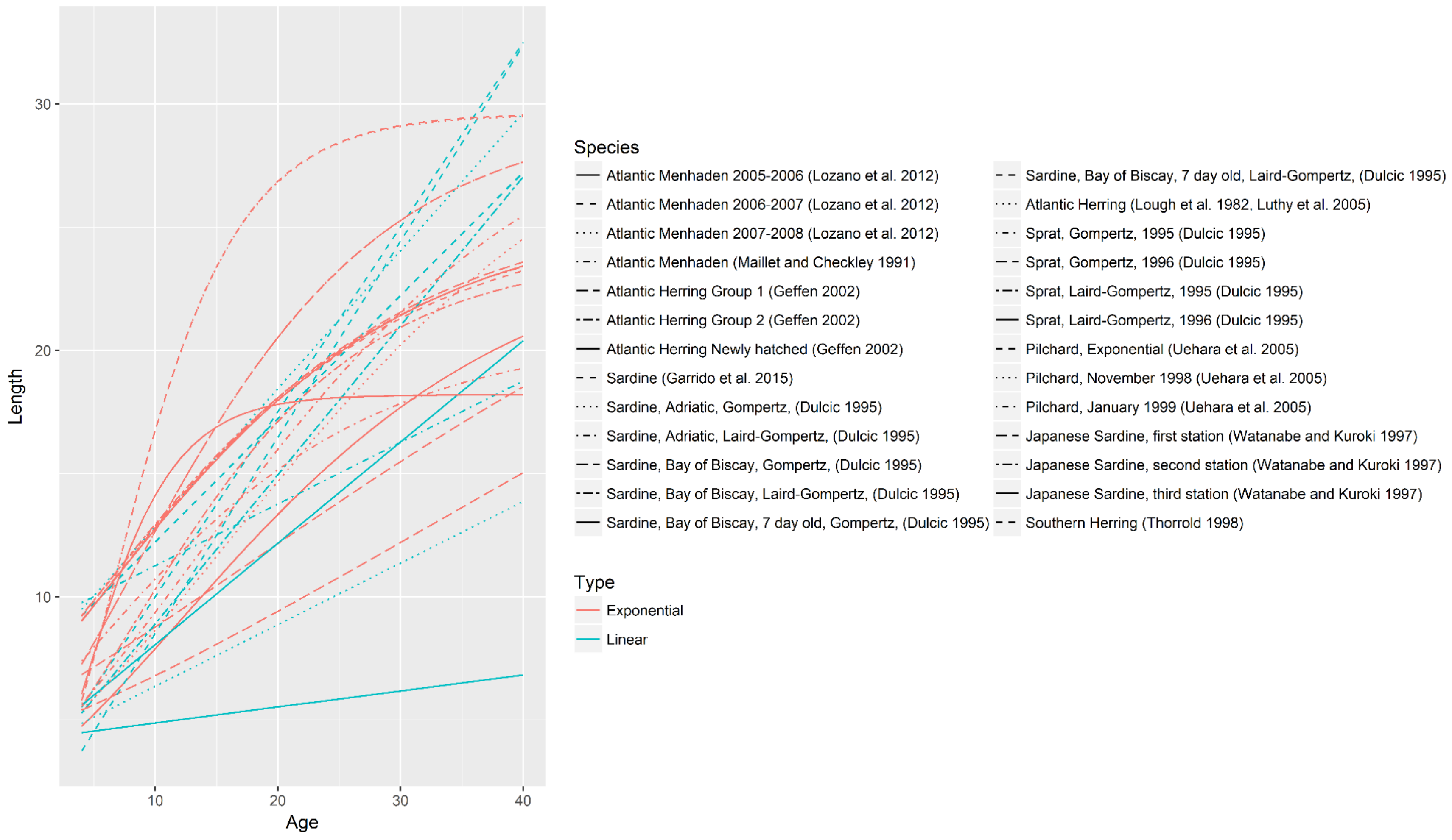

Supplemental Plot 2: Lutjanids

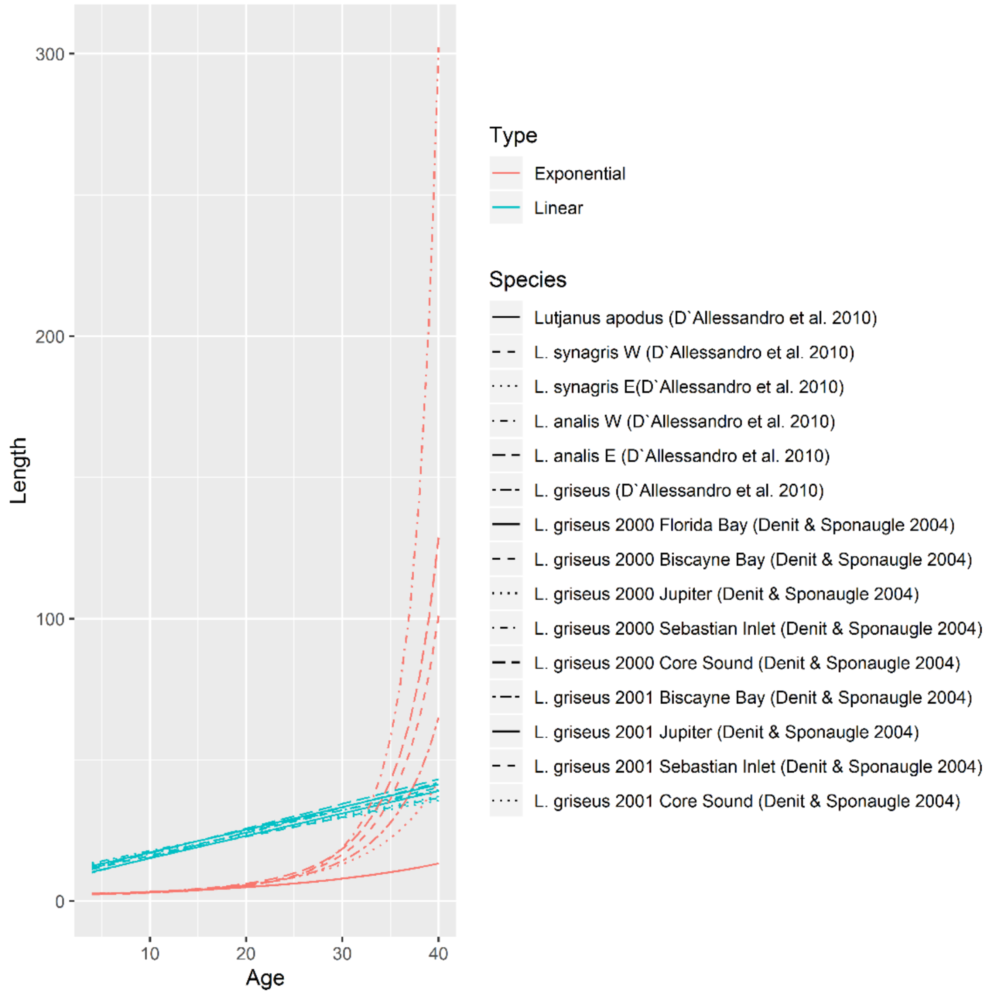

Supplemental Plot 3: Scombrids

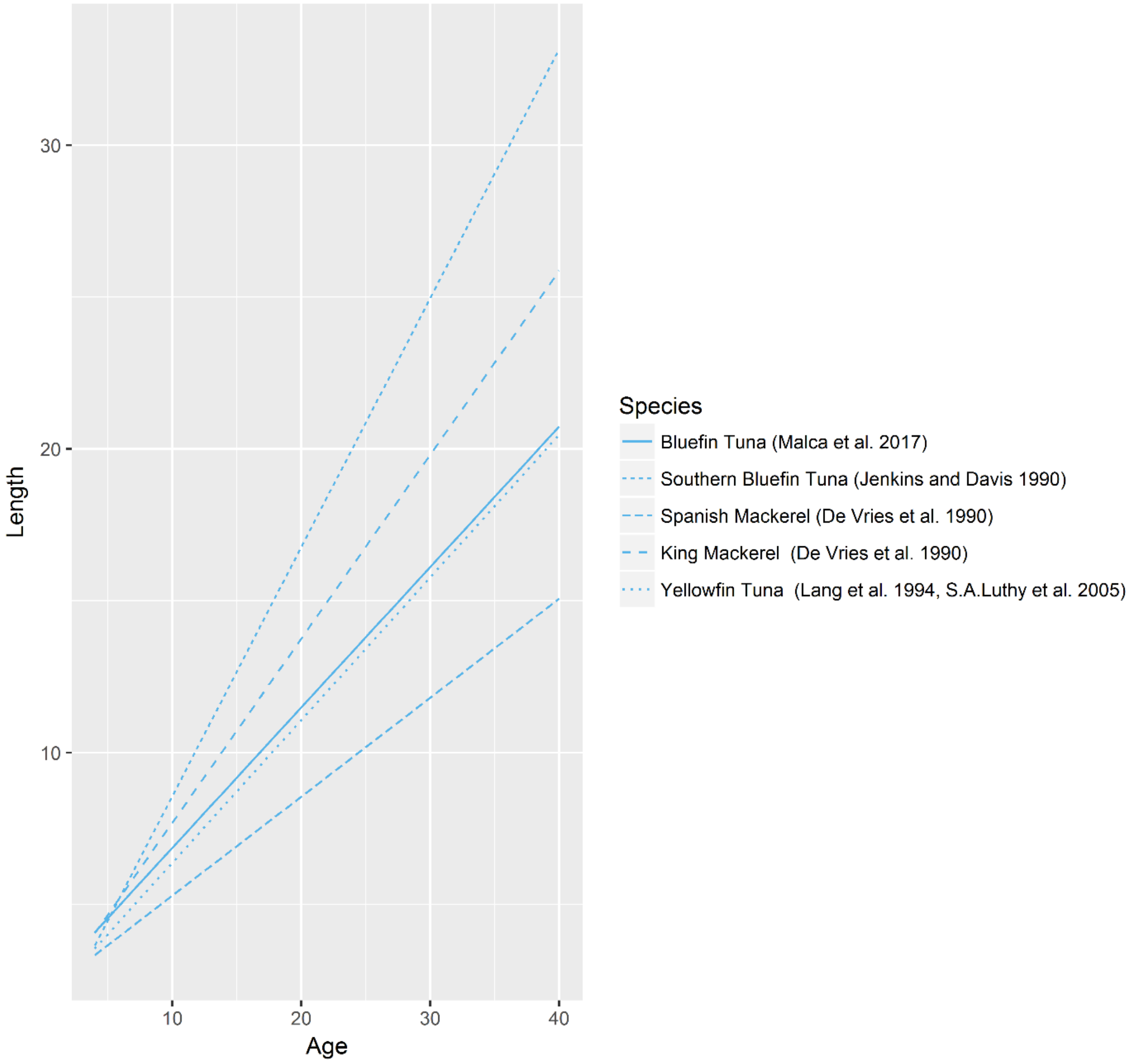

Supplemental Plot 4: Gadids

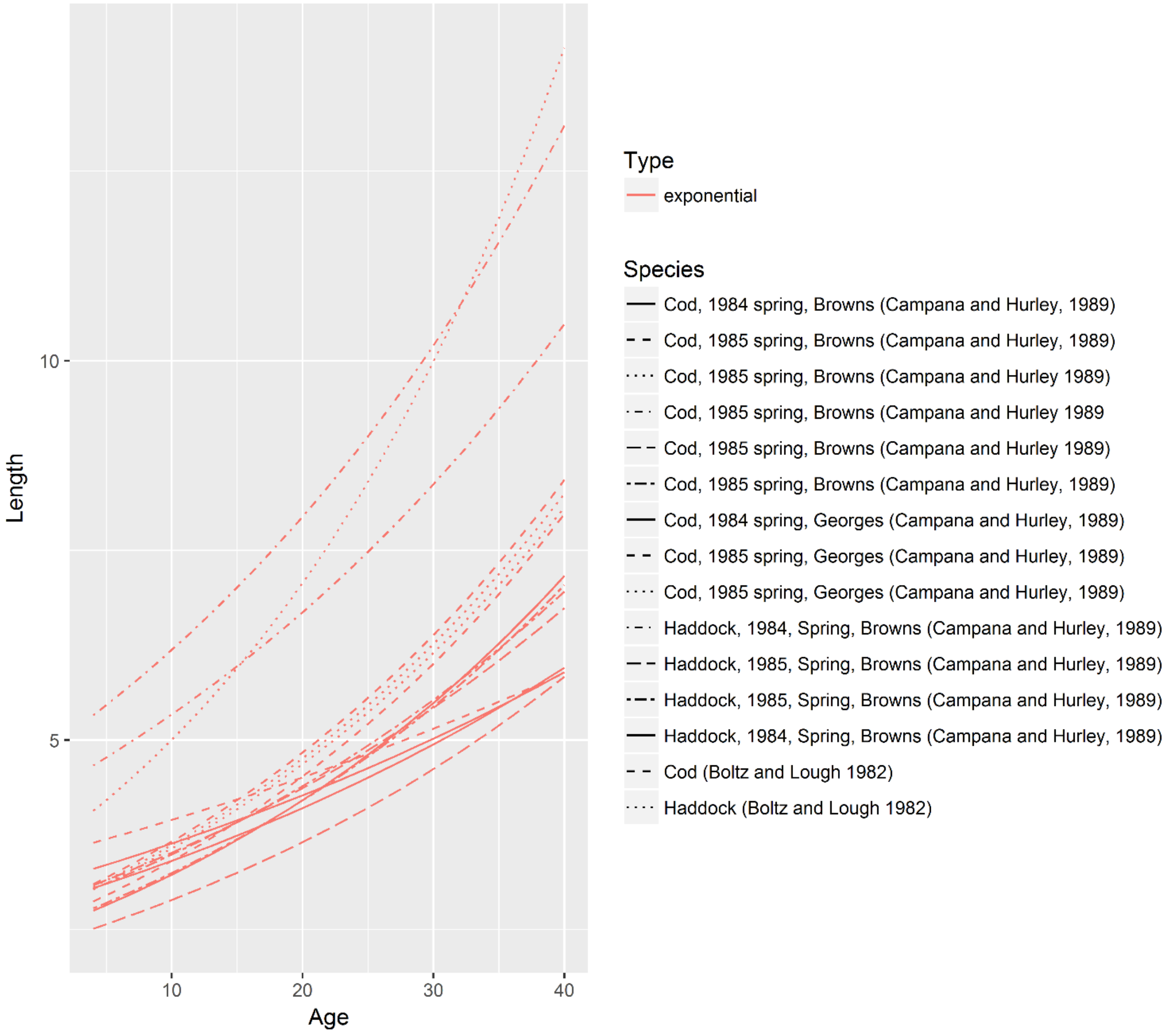

Supplemental Plot 5: Pleuronectids

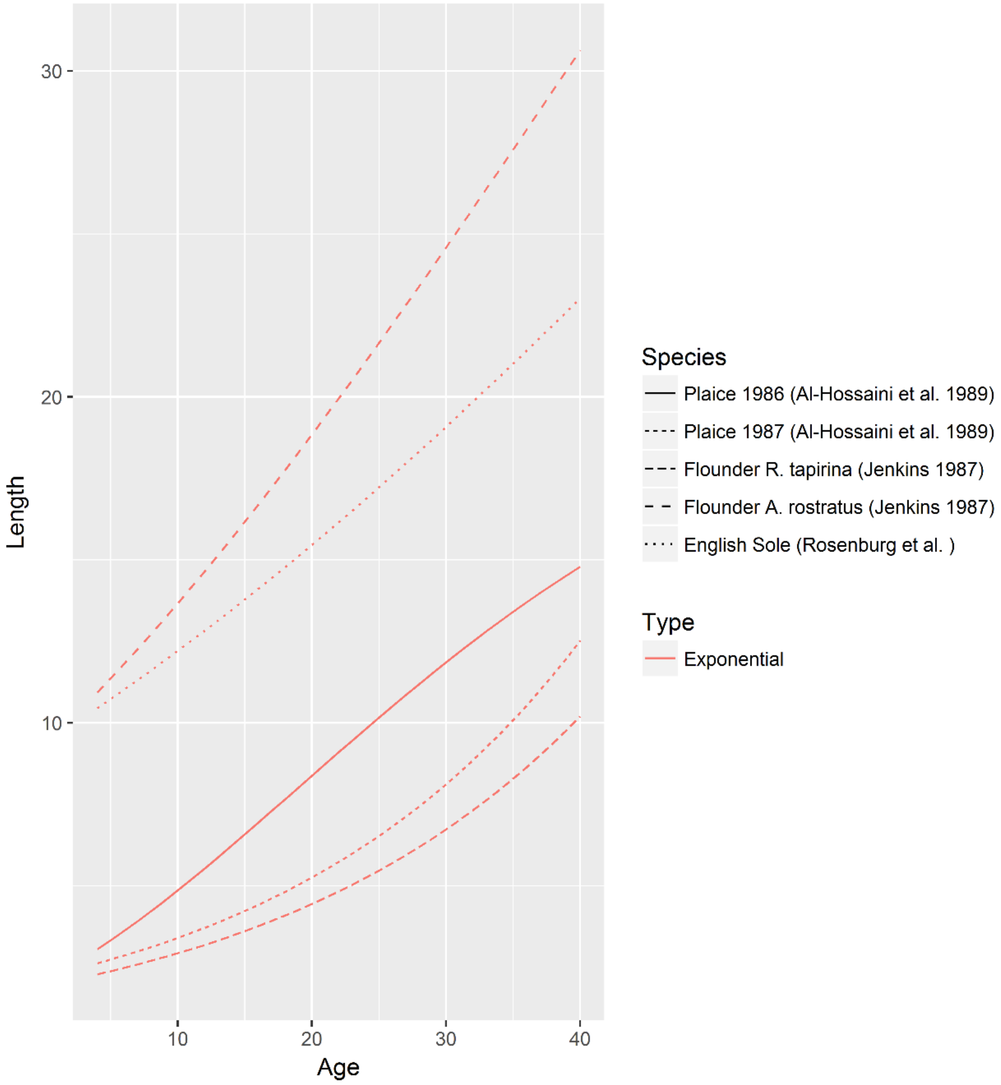

Supplemental Plot 6: Engraulids

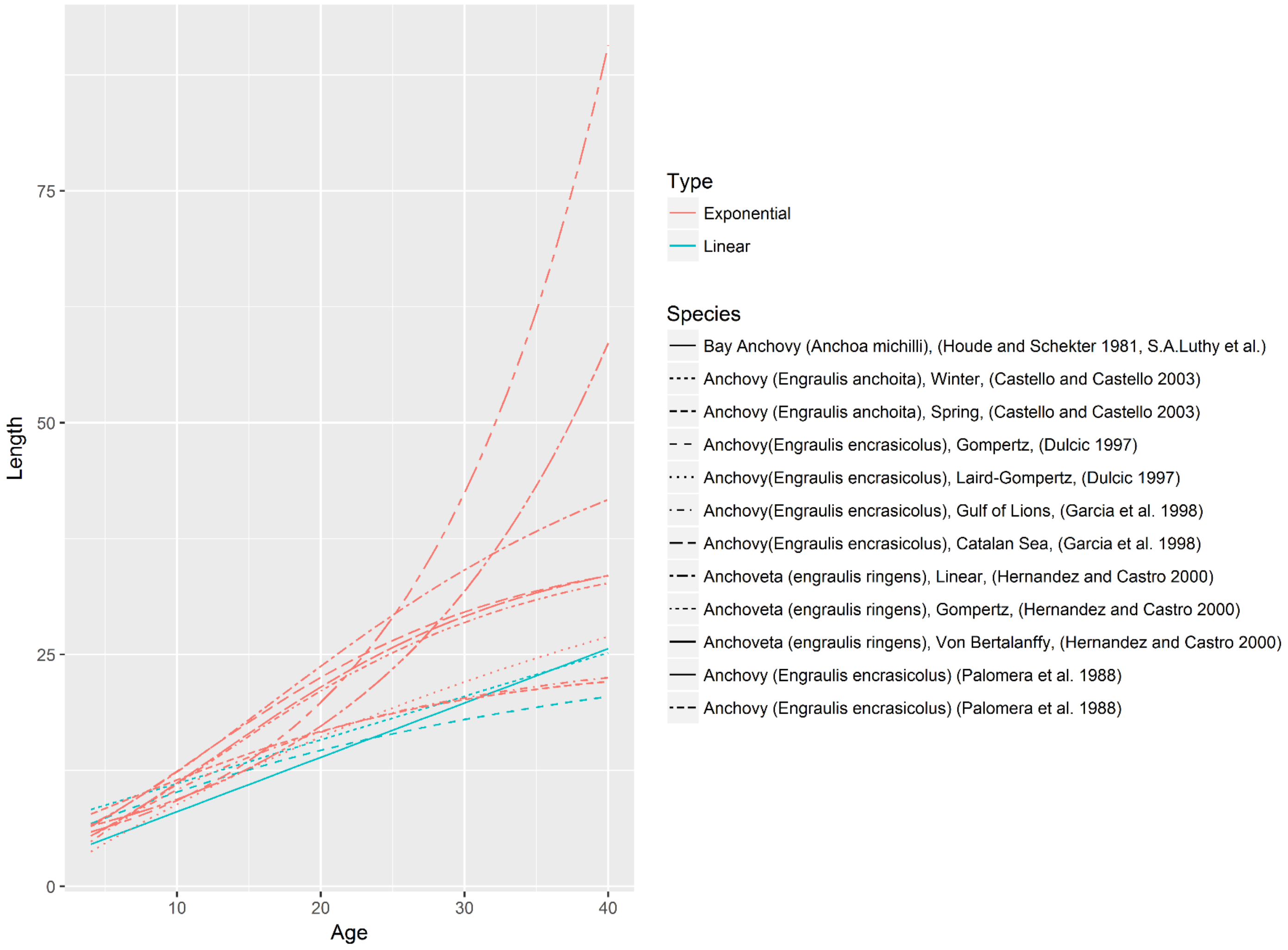

Supplemental Literature Cited:

Al-Hossaini M, Liu Q, Pitcher T J (1989) Otolith microstructure indicating growth and mortality among plaice, *Pleuronectes platessa* L., post-larval sub-cohorts J. Fish Biol. 35 (Supplement A)**:** 81-90.

Benetti D D (1992) Bioenergetics and growth of dolphin, *Coryphaena hippurus*. PhD Thesis. University of Miami, Miami, FL.

Boltz G R, Lough R G (1983) Growth of Larval Atlantic cod, *Gadus morhua,* and haddock, *Melanorammus aeglefinus,* on Georges Bank, Spring 1981. Fish. Bull. (Wash. D. C.) 81:827-836.

Bystydzieńska Z E, Phillips A J, Linkowski T B (2010) Larval Stage Duration, Age and Growth of Blue Lanternfish *Tarletonbeania crenularis* (Jordan and Gilbert, 1880) Derived from Otolith Microstructure." Environ. Biol. Fishes 89: 493–503. doi:10.1007/s10641-010-9681-2.

Campana S E, Hurley P C (1989) An age-and temperature-mediated growth model for cod (*Gadus morhua*) and haddock (*Melanogrammus aeglefinus*) larvae in the Gulf of Maine. Can. J. Fish. Aquat. Sci. 46: 603-613.

Campana S E, Jones C (1992) Analysis of otolith microstructure data. P. 73-100. In: D.K. Stevenson and S.E. Campana (eds). Otolith microstructure examination and analysis. Can. Spec. Publ. Fish. Aquat. Sci. 117.

Castello L, Castello J P (2003) Anchovy stocks (*Engraulis anchoita*) and larval growth in the SW Atlantic. Fish. Res. 89:409-421.

D'Alessandro E K, Sponaugle S, Serafy J E (2010) Larval Ecology of a Suite of Snappers (Family: Lutjanidae) in the Straits of Florida, Western Atlantic Ocean. Mar. Ecol. Prog. Ser. 410: 159–75. doi:10.3354/meps08632.

Denit, K and Sponaugle S. (2004) Growth Variation, Settlement, and Spawning of Gray Snapper across a Latitudinal Gradient. Trans. Am. Fish. Soc. 133:1339-1355.

DeVries D A, Grimes C B, Lang K L, White B D W (1990) Age and Growth of King and Spanish Mackerel Larvae and Juveniles from the Gulf of Mexico and U.S. South Atlantic Bight. Environ. Biol. Fishes 29: 135-43. doi:10.1007/BF00005030.

Dulcic J (1995) Estimation of age and growth of sardine, *Sardina pilchardus* (Walbaum, 1792), larvae by reading daily otolith increments. Fish. Res. 22:265-277

Dulcic J (1997) Growth of anchovy, *Engruulis encrasicolus* (L.) larvae in the Northern Adriatic Sea. Fish. Res. 31: 189-195

Dulcic J (1998) Larval growth of sprat, *Sprattus sprattus phalericus,* larvae in the Northern Adriatic. Fish. Res. 36:117-126

Garci´a A, Corte´s D, Rami´rez T (1998) Daily larval growth and RNA and DNA content of the NW Mediterranean anchovy *Engraulis encrasicolus* and their relations to the environment. Mar. Ecol. Prog. Ser.166:237-245

Garrido S, Ben-Hamadou R, Santos A M P, Ferreira1 S, Teodósio M A, Cotano U, Irigoien X, Peck M A, Saiz E, Ré P (2015) Born small, die young: Intirnsic, size-selective mortality in marine larval fish. Sci. Rep. 5 (17065): 1-10. Doi 10.1038/srep17065.

Geffen A (2002) Length of herring larvae in relation to age and time of hatching. J. Fish Biol. 60(2): 479-485

Govoni J J, Laban E H, Hare J A (2003) The early life history of swordfish (*Xiphias gladius*) in the western North Atlantic. Fish. Bull. (Wash. D. C.)101:778-789

Gracia-Lo´pez V, Kiewek-Martı´nez M, Maldonado-Garcı´a M (2004) Effects of temperature and salinity on artificially reproduced eggs and larvae of the leopard grouper *Mycteroperca rosacea.* Aquaculture 237:485–498

Hare J A, Cowen R K (1994) Ontogeny and otloth microstructure of bluefish *Pomatomus saltatrix* (Pisces, Pomatomidae). Mar. Biol. 118:541-550. Doi: 10.1007/BF00347500.

Hernandez E H, Castro L R (2000) Larval growth of the anchoveta *Engraulis ringens* during the winter spawning season off central Chile. Fish. Bull. (Wash. D. C.)98: 704-710.

Houde E, Berkeley S, Klinovsky J, Schekter R (1976) Culture of Larvae of the White Mullet, *Mugil curema* Valenciennes. Aquaculture 8: 365-370.

Houde E D, Schekter R C (1981) Growth rates, rations and cohort consumption of marine fish larvae in relation to prey concentrations. Rapports et Proces-verbaux des Re´unions, Conseil International pour L'Exploration scientifique de la Mer 178:441-453.

Jayadi, Mallawa A ,Nessa N, Djawad I, Ardiansyah (2016) Growth patterns of Camouflage Grouper (*Epinephelus polyphekadion*, Bleeker, 1849) larvae. Journal of Fisheries and Aquatic Science 12 (1). Science Alert: 12–21. doi:10.3923/jfas.2017.12.21.

Jenkins G P (1987) Age and growth of co-occurring larvae of two flounder species, *Rhombosolea tapirina* and *Ammotretis rostratus.* Mar. Biol. 95:157-166

Jenkins, G P and Davis, T L O (1990) "Age, growth rate, and growth trajectory determined from otolith microstructure of southern bluefin tuna *Thunnus maccoyii* larvae." Mar. Ecol. Prog. Ser. 63: 12.

Lang K L, Grimes C B, Shaw R F (1994) Variations in the age and growth of yellowfin tuna larvae, *Thunnus albacares*, collected in the Mississippi River plume. Environ. Biol. Fishes 39:259-270. Doi:10.1007/BF00005128

Leffler D L, Shaw R F (1992) Age validation, growth, and mortality of larval Atlantic bumper (Carangidae *Chloroscombrus chrysurus*) in the Northern Gulf of Mexico. Fish. Bull. (Wash. D. C.) 90:711-719.

Lough G R, Pennington M, Bolz G R, Rosernberg A A (1982). Age and growth of larval Atlantic herring, *Clupea harengus* L., in the Gulf of Maine-Georges Bank region based on otolith growth increments. Fish. Bull. (Wash. D. C.) 80: 187-199.

Lozano C, Houde E D, Wingate R L, Secor D H (2012) Age, growth and hatch dates of ingressing larvae and surviving juveniles of Atlantic menhaden *Brevoortia tyrannus*. J Fish. Biol. 81: 1665-1685.

Luthy S A, Serafy J E, Cowen R K, Denit K L and Sponaugle, S (2005) Age and growth of larval Atlantic Sailfish, *Istiophorus platypterus*." Mar. Freshw. Res 56:1027–35. doi:10.1071/MF05048.

Maillet G L, Checkley Jr D M (1991) Storm-related variation in the growth rate of otoliths of larval Atlantic menhaden *Brevoortia tyrannus*: a time series analysis of biological and physical variables and implications for larva growth and mortality. Mar. Ecol. Prog. Ser. 79:1-16.

Malca E, Muhling B, Franks J, García A, Tilley J, Gerard T, Ingram W, Lamkin J T (2017) The first larval age and growth curve for bluefin tuna (*Thunnus thynnus*) from the Gulf of Mexico: Comparisons to the Straits of Florida, and the Balearic Sea (Mediterranean). Fish. Res. 190:24-33.

Martinez-Lagos R, Gracia-Lopez V (2009) Morphological development and growth patterns of the leopard grouper *Mycteroperca rosacea* during larval development. Aquac. Res. 41:120-128. doi:10.1111/j.1365-2109.2009.02313.x

Palomera I, Moales-Nin B, Lleonart J (1988) Larval growth of anchovy, *Engraulis encrasicolus*, in the Western Mediterranean Sea. Mar. Biol. 99: 283-291.

Rae G, Roman N S, Spinoglio D E (1999) "Age validation and growth of yolked larvae of *Patagonotothen tessellata* (Richardson, 1845) (Pisces: Nototheniidae) from the rocky littoral of the Beagle Channel, Argentina. Sci. Mar. 63(SUPPL.): 469–76. doi:10.3989/scimar.1999.63s1469.

Rosenberg A (1982) Age and growth of a Pleuronectid, *Parophrys vetulus*, during the pelagic larval period in Oregon coastal waters. Fish. Bull. (Wash. D. C.)80:93-104.

Sepu´lveda A (1994) Daily growth incrememnts in the otoliths of European smelt *Osmerus eperlanus* larvae. Mar. Ecol. Prog. Ser.108:33-42.

Sponaugle S, Denit K L, Luthy S A, Serafy J E, Cowen R K (2005) Growth variation in larval *Makaira nigricans*. J Fish. Biol. 66:822-835. Doi:10.1046/J.1444- 2906.2003.00680.X

Thorrold S R (1988) “Estimating Some Early Life History Parameters in a Tropical Clupeid, *Herklotsichthys castelnaui*, from Daily Growth Increments in Otoliths.” Fish. Bull. (Wash. D. C.) 87: 73–83.

Uehara S, Syahailatua A, Suthers I (2005) recent growth rate of larval pilchards *Sardinops sagax* in relation to their stable isotope composition in an upwelling zone of the East Australian Current. Mar. Freshw. Res. 56:549-560.

Warlen S M, Chester A J (1985) Age, growth and distribution of larval spot, *Leistomus xanthurus*, off North Carolina. Fish. Bull. (Wash. D. C.) 83:587-599.

Watanabe Y, Kuroki T (1997) Asymptotic growth trajectories of larval sardine. (*Sardinops melanostictus*) in the coastal waters off western Japan. Mar. Biol. 127: 369-378.

Appendix 2: Depth at Age plots for the depth occupancy models in Chapter 3

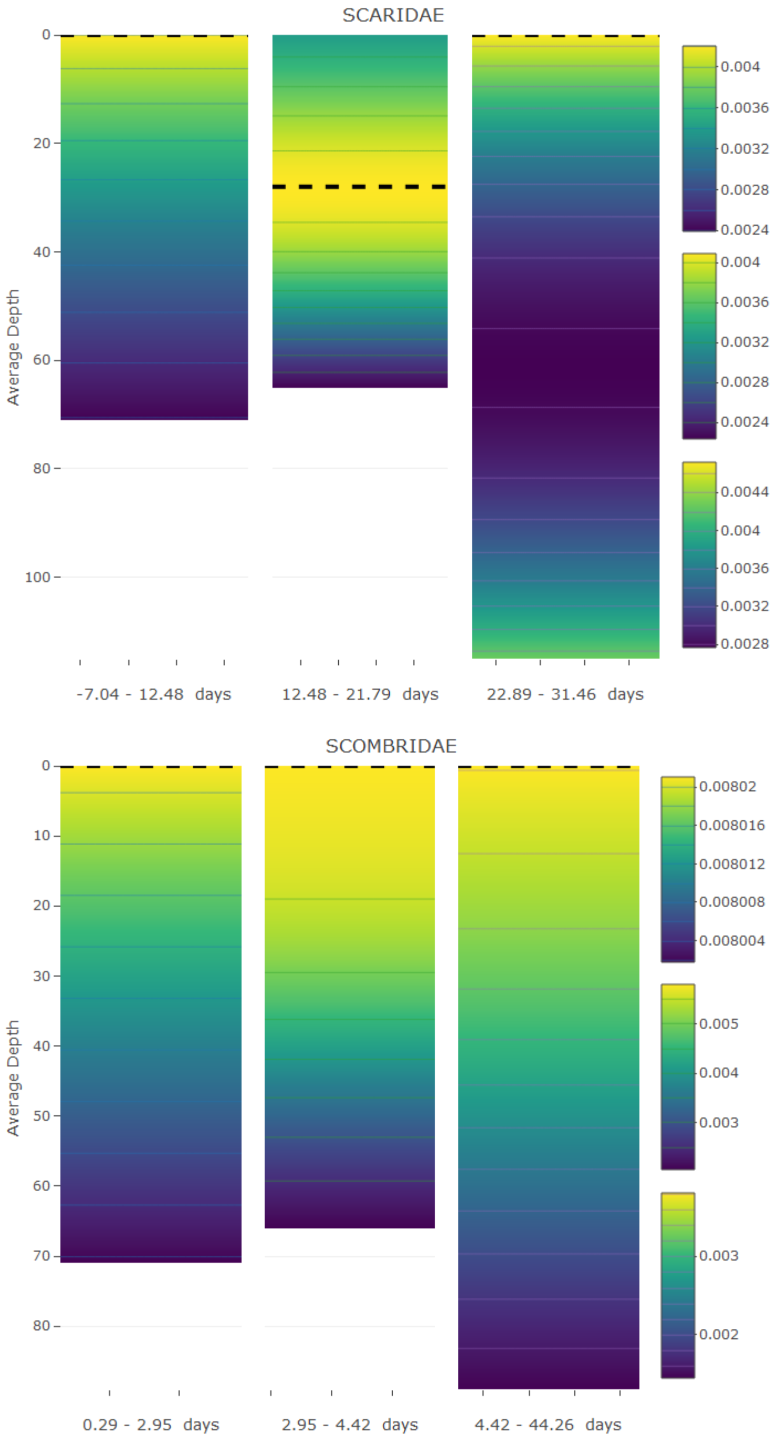

Figure A.1 : Depth at Age plots for all Taxa

Color gradient refers to the concentration of larvae per cubic meter predicted in the water column at each depth from purple (low) to yellow (high). Each age class has its own corresponding gradient, ranging from youngest to oldest on the right side of each plot.

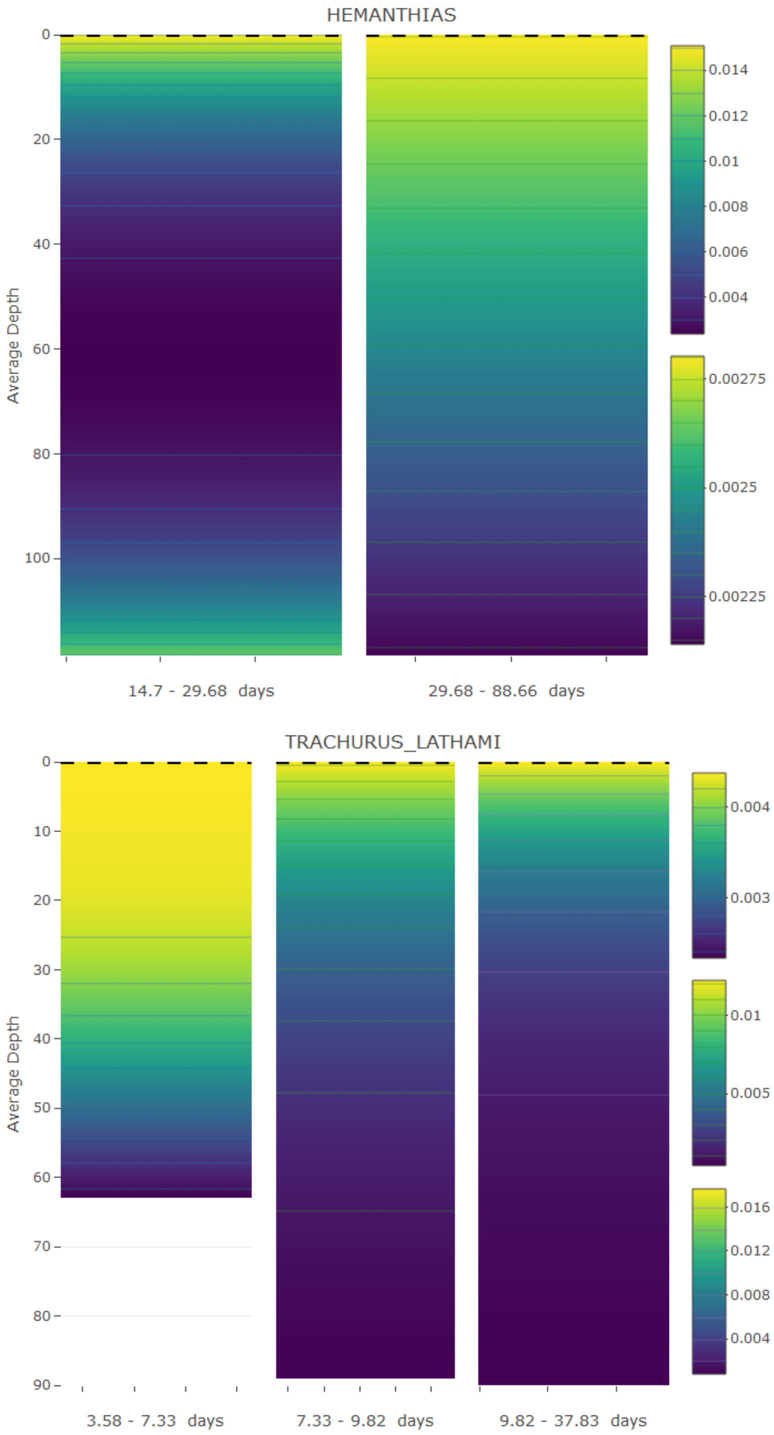

Figure A.1 (continued): Depth at Age plots for all Taxa

Color gradient refers to the concentration of larvae per cubic meter predicted in the water column at each depth from purple (low) to yellow (high). Each age class has its own corresponding gradient, ranging from youngest to oldest on the right side of each plot.

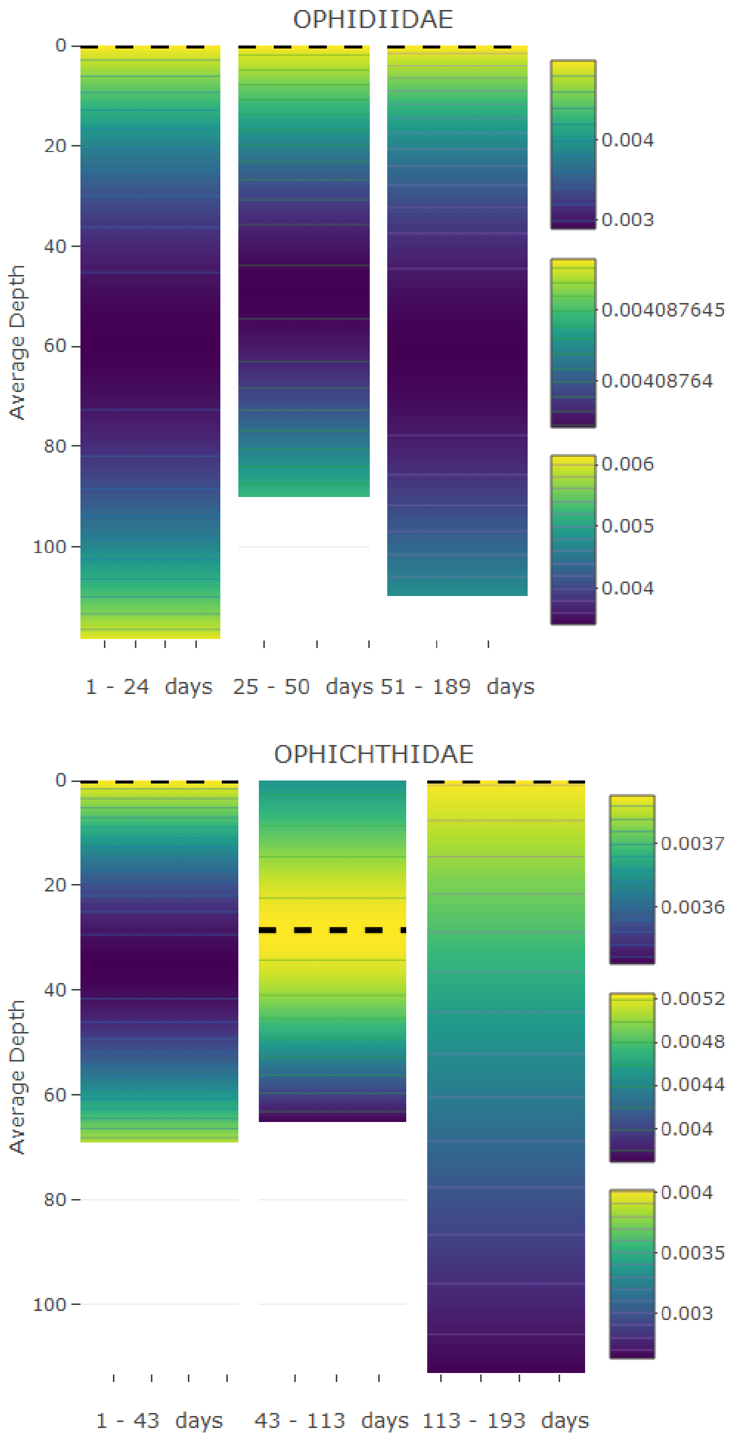

Figure A.1 (continued): Depth at Age plots for all Taxa

Color gradient refers to the concentration of larvae per cubic meter predicted in the water column at each depth from purple (low) to yellow (high). Each age class has its own corresponding gradient, ranging from youngest to oldest on the right side of each plot.

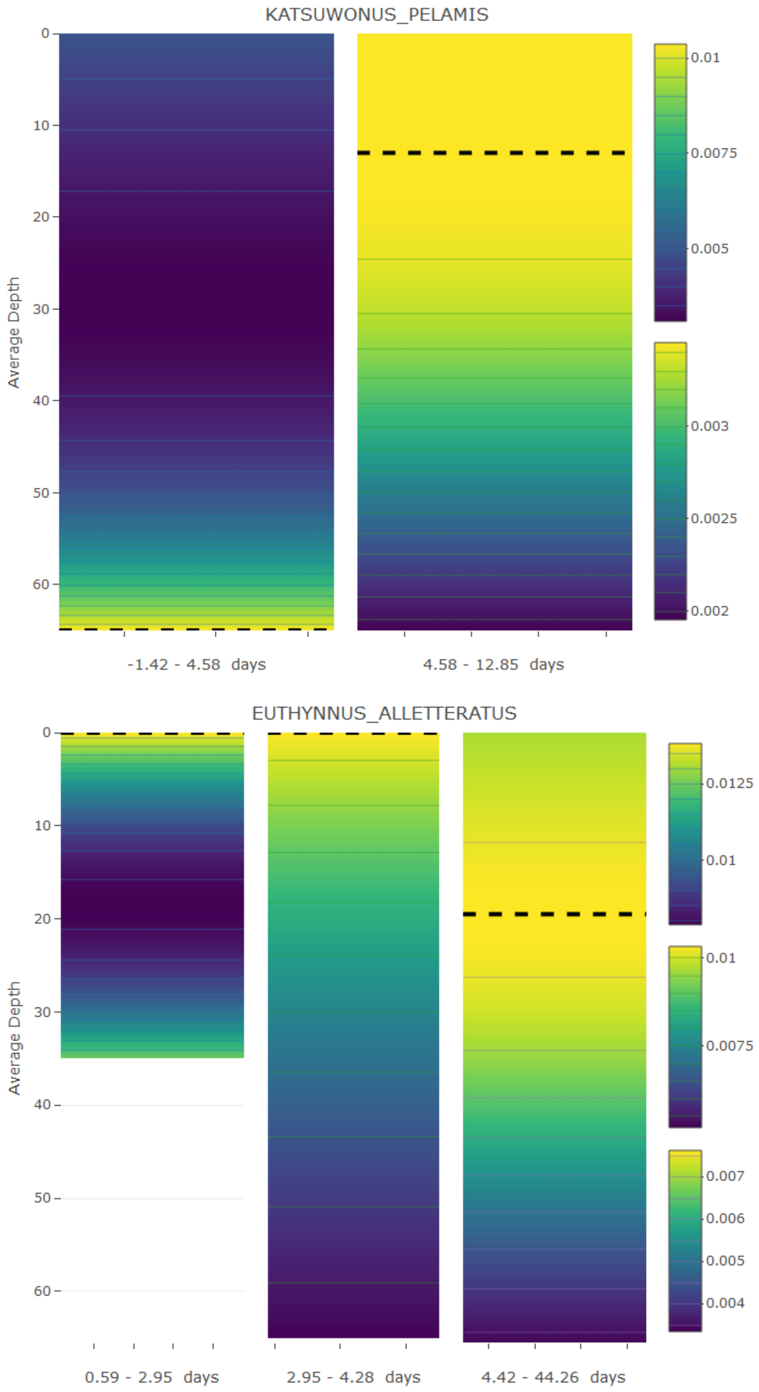

Figure A.1 (continued): Depth at Age plots for all Taxa

Color gradient refers to the concentration of larvae per cubic meter predicted in the water column at each depth from purple (low) to yellow (high). Each age class has its own corresponding gradient, ranging from youngest to oldest on the right side of each plot.

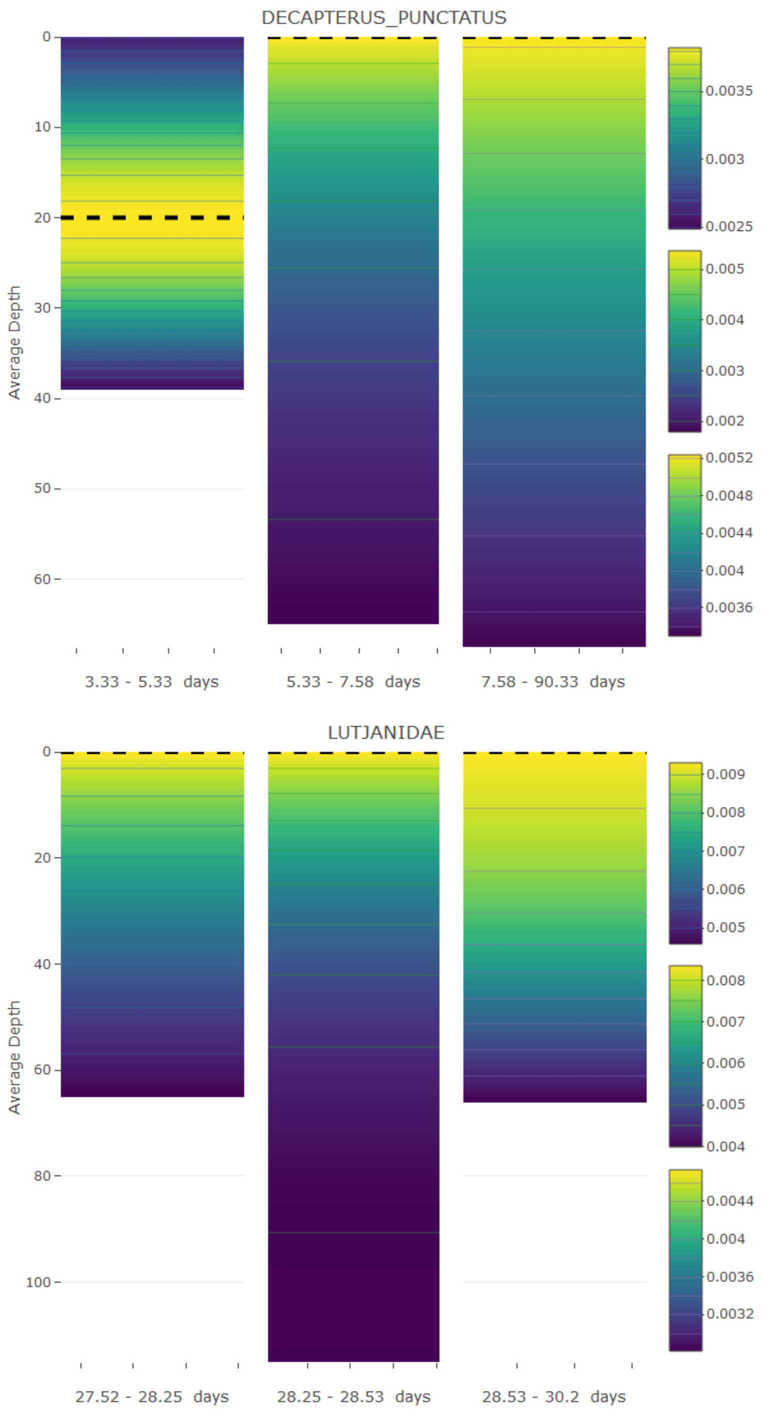

Figure A.1 (continued): Depth at Age plots for all Taxa

Color gradient refers to the concentration of larvae per cubic meter predicted in the water column at each depth from purple (low) to yellow (high). Each age class has its own corresponding gradient, ranging from youngest to oldest on the right side of each plot.

Appendix 3: Early life history growth in fish reflects consumption-mortality tradeoffs

This appendix is the publication of Chapter 2, and was published in the July 2020 issue of Fisheries Research with co-author Cameron Ainsworth, Ph.D. and is included in this dissertation under the author permissions guidelines of Elsevier publishers, which includes a release to authors to include their publication in their dissertation. Its corresponding online supplement is included as Appendix 2 in this dissertation.

Reference:

Vasbinder, K and C. Ainsworth. 2020. Early Life History Growth in Fish Reflects Consumption-Mortality Tradeoffs. Fish. Res. 227:105538.

To access this article through the publisher:

https://doi.org/10.1016/j.fishres.2020.105538

Supplementary material related to this article can be found in the online version at doi:https://doi.org/10.1016/j.fishres.2020.105538.

Fisheries Research 227 (2020) 105538

Contents lists available at ScienceDirect

Fisheries Research

journal homepage: www.elsevier.com/locate/fishres

Early life history growth in fish reflects consumption-mortality tradeoffs

Kelly Vasbinder*, Cameron Ainsworth

University of South Florida College of Marine Science, 140 7th Avenue South, St. Petersburg, FL 33701, United States

ARTICLE INFO

Handled by S. Xavier Cadrin

Keywords:
Early life history
Growth models
Length-at-age
Risk-mediation

ABSTRACT

Growth models used for adult fish are often inadequate to model early larval growth in the first weeks and days of life. However, growth rate during the earliest life stages may be a significant factor in determining survivorship, foraging success, transport, and settlement patterns. We fit growth models for the larvae of twelve grouper and snapper species from the families Lutjanidae and Serranidae, and conducted a survey of published early life growth models to explore growth pattern differences between taxonomic groups. The majority of these papers contained only larval stages but a few included early juvenile stages as well, so from here on we use the term “early life” to refer to larval and early juvenile stages. The majority of the grouper and snapper species are best represented by models with exponential growth patterns, which fits into the results from the literature survey. The surveyed growth literature included 31 papers which provide 94 models spanning 17 different fish families. In a meta-analysis of the growth models from the surveyed literature, exponential growth models were more often used for the early life of demersal fish, whereas linear growth models were more often used for the early life of pelagic fish. These results may indicate that early life growth patterns depend on the risk abatement strategies of each taxa.

1. Introduction

Early life stage survivorship is an important factor affecting population dynamics of exploited marine species. Larval fish must grow through a "window" where vulnerability to predators is high (Cowan et al., 1996; Meekan and Fortier, 1996; Hinrichsen et al., 2002). After larvae reach a threshold length, the risk of predation decreases (Cowan et al., 1996). There are other motivations for understanding growth in larval fish. Hjort’s "critical feeding period" hypothesis posits that the end of yolk reserves is followed by a critical first feeding period in which larval fish must find food or die (Hjort, 1914). Success in that first feeding may be due to hydrodynamic constraints and thus related to larval size (China and Holzman, 2014). Finally, models of larval connectivity also require accurate models of early life stage growth to interpret length-based sampling data and understand migration behavior. Thus, larval growth is a key factor in determining predation mortality, starvation mortality, and spatiotemporal patterns of recruitment, all of which contribute to fisheries production and population viability.

Nevertheless, in many applications it is common to ignore deviations from predicted growth rates during the brief larval period. The ubiquitous von Bertalanffy growth function accurately describes growth across a wide range of taxa because growth rates are determined by predictable physiological relationships. Failure of the von Bertalanffy model to represent larval growth can be traced to the theoretical description of growth by von Bertalanffy (1938, 1951). He suggested that the growth in fish could be viewed as the difference between organic synthesis and destruction (Eq. (1)).

$$\frac{dw}{dt} = HS - kw \tag{1}$$

The growth of a fish is represented as a change in weight per unit time (dw/dt). Von Bertalanffy proposed H and k as anabolic and catabolic coefficients and he suggested that synthesis and destruction were limited by the surface area for resorption of nutritive material (S) and by the weight of the organism (m), respectively. In answer to a criticism by Beverton and Holt (1957) concerning the anabolic term, Pauly (1981) suggested that respiration rate is limiting to growth, and that S should be viewed as a function of gill area instead of gut area. Thus, under isometric growth, surface area increases with the square of body length while weight increases with the cube. Scope for growth is therefore limited by a 2/3 power relationship that results in an asymptotic weight (Eq. (2)).

$$\frac{dw}{dt} = Hw^{2/3} - kw \tag{2}$$

This offers a nearly universal growth model for fish, particularly

---

* Corresponding author.
E-mail address: kmvasbinder@mail.usf.edu (K. Vasbinder).

https://doi.org/10.1016/j.fishres.2020.105538
Received 7 November 2019; Received in revised form 12 February 2020; Accepted 14 February 2020

when an additional allometric parameter is included. However, it also predicts the fastest growth rate at small body sizes, which is often not the case for larval fish. The poor fit of the von Bertalanffy growth model at larval ages is evidenced by an *ad hoc* additive factor t_0(the theoretical age at length zero), which is found in this familiar equation (Eq. (3)).

$$W_t = W_\infty(1 - \exp(-K(t - t_0)))^3 \tag{3}$$

A small negative value for t_0 is required to account for the fact that the von Bertalanffy growth model underestimates the rate of larval growth. W_∞ is an asymptotic weight and K is the growth constant. Larvae have been shown to have an exponentially increasing rate of growth, although this varies by species and larval condition (Jenkins, 1990). Pauly (1981) maintains it is because larval fish can respirate through their skin and are therefore not bound to the 2/3 power relationship that limits the scope for growth at older ages. This continues until scale development thickens the skin. Thus, models with an initial exponential growth period that transition to asymptotic growth may better represent growth patterns throughout ontogeny.

Early exponential growth of this form is offered in some alternative growth models. Zweifel and Lasker (1976) showed that both fish egg development and larval growth could be adequately described by Gompertz-style curves (Gompertz, 1825). They suggested that both the Laird-Gompertz and Logistic models are better options for fish growth than the von Bertalanffy growth model (Laird 1969, Zweifel and Lasker 1976). These models both contain an initial exponential growth phase followed by an inflection point.

We propose that the exponential family of models may be more appropriate for representing the early life stages of some fish taxa because early growth may reflect feeding rate. Feeding rate could be affected by predation risk mediation. We suggest that the differences in larval and early juvenile growth between demersal/reef associated and pelagic fish may be related to strategies employed in predation risk mediation. Even though risk abatement strategies come into play at juvenile ages, the strong statistical differences in growth patterns between demersal and pelagic taxa at larval ages suggests that larval growth is indicative of the strategy to be employed later during the juvenile stage. Predation risk mediation behaviors establish the tradeoff between growth rate and predation mortality early in life, as younger fish move from safe or invulnerable areas to vulnerable areas to feed. Foraging arena theory articulates this idea (Walters and Juanes, 1993; Ahrens et al., 2012). Vulnerable prey exist in the foraging arena and are at risk for predation, while invulnerable prey are in a refuge. The exchange rate between the vulnerable and invulnerable pools impacts the predation rate (Ahrens et al., 2012). Risk averse populations have higher survival but lower fecundity and consumption rates, while risk prone populations have lower survival but higher fecundity and consumption rates, with some optimal balance between the two extremes (Walters and Juanes, 1993). Thus, maximum fitness occurs at a feeding time which balances the long-term survival gains with the risk of predation (Walters and Juanes, 1993). Young fish achieve this balance by limiting their time outside of the refugia (Walters and Juanes, 1993). As they get older, they become less vulnerable to predation and can spend more time feeding, potentially following an exponentially increasing rate of growth. Young fish that have access to refugia may therefore have the option to grow more slowly during the earlier and more vulnerable life stages, whereas young fish without access to refugia may need to grow more quickly to ensure that they are out of the gape range of predators.

A second possibility that would explain differences between groups showing exponential and linear growth relates to the seasonality of spawning. Seasonality impacts environmental factors driving larval development, such as temperature and productivity (Hernandez and Castro, 2000). Larval growth rates may be highly sensitive to variable environmental conditions. Some variants to the von Bertalanffy growth model account for this by incorporating sinusoidal terms at seasonal or daily periodicities (Somers, 1988; Campana and Hurley, 1989; Campana and Jones, 1992). A cohort that is born in the spring would show a growth pattern beginning on the upswing of a sinusoidal curve, whereas a cohort that is born in the fall would be on the downswing of a sinusoidal curve. We explore whether differences in growth patterns between taxa could be due to the seasonality of their spawning.

This study aims to determine the length at age relationship during early life history for twelve species of grouper and snapper. We chose these species based on the availability of length at age data in literature, and fit the data with the Von Bertalanffy, logistic, exponential, Laird-Gompertz, and linear growth models in order to determine which model best represented grouper and snapper growth during early life. These models have been used in the past to model early life history growth in different species (e.g. Houde and Schekter 1981, Jenkins and Davis, 1990; Benetti, 1992; Rae et al., 1999; Lozano et al., 2012; Luthy et al., 2005; Jayadi et al., 2016).

In addition to evaluating the best models to represent grouper and snapper larval growth, we conducted a meta-analysis examining previously published larval growth models from a wider variety of taxa in order to place the grouper and snapper growth models into a broader context. The meta-analysis examines whether differences in early life history growth patterns exist between taxa, and whether these differences relate to risk abatement feeding strategies. The null hypothesis for the meta-analysis is that early-linear and early-exponential growth models are independent of the fish family. We will make the case that changes in larval growth rate are indicative of risk abatement strategies during early life history.

2. Methods

2.1. Species-level analysis

We chose twelve grouper and snapper species based on the availability of early life growth data in literature and the temperatures at which those studies were conducted. The twelve species, study locations, spawning seasons, and publications in which they appear can be found in Table 1. Five of the species chosen were from the Gulf of Mexico and Caribbean, while the other seven are from studies that were conducted between 23 – 31 °C. This is within the temperature range found in the Gulf of Mexico. Larval staging studies provide length at age data. Fish were reared under conditions similar to their natural environment. Typically, age is known and larvae are measured to obtain length data at designated time or stage intervals (e.g. Powell &Tucker, 1992; Drass et al., 2000; Song et al., 2013). Thus, all species chosen for the species level analysis contained length at age data for similar temperature ranges. Models were then fit to the length at age data.

2.2. Model fitting and selection

Larval fish are typically measured using standard length (Moser, 1996; Kahn et al., 2004). Standard length is measured from the snout to the base of the tail, which is the hypural bone or caudal peduncle (Kahn et al., 2004). Body length is the same as standard or notochord length for larval fish (Drass et al., 2000). Notochord length is the measurement from the snout to posterior end of the notochord (Drass et al., 2000). After we extracted length at age data from the literature, we fit five types of growth models to each set of data: a linear model, an exponential model, a logistic model, the von Bertalanffy growth model, and a Laird-Gompertz growth model. The generic forms of each of these growth models are in Table 2. These five growth models for each species can be split into two groups, the exponential family and the linear family. The exponential family is comprised of the logistic, Laird-Gompertz, and exponential models, which have an increasing rate of growth at small body sizes. The linear family includes the linear and von Bertalanffy growth model.

We fit the models with least squares regression using the R statistical software (R Core Team, 2015; Maechler et al., 2017). Non-least

Table 1
Species used, temperature or location of study, and citation for study.

Species	Region/Temperature	Sample Size	Location Published	Spawning Season
Red Snapper *Lutjanus campechanus*	Texas and Alabama	n = 96	Drass et al. (2000) Fish. Bull. (Wash. D. C.) 98(3): 507–527.	Late spring through fall with peaks in the warmer months (Ed. Richards, 2006)
Nassau Grouper *Epinephelus striatus*	Grand Cayman	n = 32	Powell and Tucker, 1992. Bull. Mar. Sci. 50(1): 171–185.	December to February at full moon (Ed. Richards, 2006)
Yellowtail Snapper *Ocyurus chrysurus*	Florida Keys, FL, Corpus Christi, TX (27–28 C)	n = 21	Riley et al., 1995. Fish. Bull. (Wash. D. C.) 93: 179–185	Throughout the year with local peaks (Ed. Richards, 2006)
Red Grouper *Epinephelus morio*	Gulf of Mexico (22–24 C)	n = 28	Colin et al., 1996. ICLARM Conf. Proc. 48: 399–414.	April through May in the Gulf of Mexico (Ed. Richards, 2006)
Gray Snapper *Lutjanus griseus*	Florida Keys (26–28 C)	n = 15	Richards and Saksena, 1980. Bull. Of Mar. Sci. 30(2):515-522.	Summer through fall with a peak in August in some areas (Ed. Richards, 2006)
Sevenband Grouper *Epinephelus septemfasciatus*	Korea (25C)	n = 7	Song et al., 2013. Dev.Reprod. 17(4): 369–377.	Unknown
Dusky Grouper *Epinephelus marginatus*	Southeastern Adriatic (23C)	n = 6	Glamuzina et al., 1998. Sci. Mar. 62 (4): 373–378	Spawning aggregations begin in May through July with spawning from late June to late September with peaks in July and August (Bertucci et al., 2015)
Blacktip Grouper *Epinephelus fasciatus*	Japan (22.5–27 C).	n = 13	Kawabe and Kohno, 2009. Fish. Sci. 75:1239–1251.	Unknown
Brown Spotted Grouper *Epinephelus tauvina*	Kuwait (22.6–30.4 C)	n = 9	Hussain and Higuchi, 1990. Aquaculture 19: 339–350	October through February and April through July (Froese and Pauly, 2019)
Malabar Grouper *Epinephelus malabaricus*	Taiwan (26.1–26.88 C)	n = 11	Leu et al., 2008. J. Mar. Biol. Ass. U.K. 85: 1249–1254	September through February with a peak in November (Gaspare and Bryceson, 2013)
Longtooth Grouper *Epinephelus bruneus*	Jeju Island, Korea (24.5–25.5 C)	n = 16	Song et al., 2005. Aquacult. Soc. 36(2):209–216	Unknown
Mangrove Snapper *Lutjanus argentimaculatus*	Panay Island, Central Philippines (28–31 C) Note:(28–31 C) is for spawners, larvae were kept in ambient flow through tank in which all fish died by end of study	n = 9	Emata et al., 1994. Aquaculture 121:381–387	Year round spawning (Froese and Pauly, 2019)

Table 2
General Forms of Common Growth Models.

Growth Model	General Form
von Bertalanffy	$Length = L_\infty(1 - e^{-K(age - t_0)})$
Linear	$Length = m * age + intercept$
Logistic*	$Length = Asym/(1 + e^{\frac{t_{mid} - age}{Scal}})$
Exponential**	$Length = Lo * e^{C * age}$
Laird-Gompertz***	$Length = Lo * e^{G*(1 - e^{-\alpha * age})}$

* Asym is the asymptote, t_{mid} is the age that corresponds to the inflection point of the curve, and Scal is a scale parameter.

** L_o is the length at first feeding and C is the specific growth rate.

*** Zweifel and Lasker, 1976, as cited in Palomera et al., 1988. L_o is the length at time 0 (first feeding), alpha is the instantaneous rate of decrease in growth rate, and G is a ratio of instantaneous growth rate to alpha.

squares regression with a Gauss-Newton fitting algorithm was used for all five model types for species with sample sizes of 15 or greater, with the exception of Longtooth Grouper. (R Core Team, 2015, Elzhov et al., 2016). For the other species, we used a Levenberg-Marquardt algorithm to fit all models other than linear (Elzhov et al., 2016). Both types of algorithms yield identical results for large data sets.

Choosing a model from competing options requires a model selection criterion that assesses model parsimony. AICc is a corrected version of the Akaike Information Criterion, AIC, and has been shown to have a smaller bias than AIC. In some cases, it provides better model selection when the sample size is not large (Hurvich and Tsai, 1991). We calculated the AICc for each model using the AICcmodavg package (Mazerolle, 2016). Some species had multiple models with low AICc scores, so the models were ranked. In order to rank models, we calculated delta scores from the AICc according to the method outlined in Burnham and Anderson (2004). In this method (Eq. 5), the winning AIC score is subtracted from each of the other scores to produce a delta value for each model (Burnham and Anderson, 2004). Delta values less than 2 represent substantially supported models that are not considered different from the most parsimonious model. A model with a delta score between 4 and 7 is less supported, and a model with a delta score greater than 10 is considered to have no support (Burnham & Anderson 2004). In order to use this method, we substituted AICc scores for AIC scores, so delta values were produced by subtracting the minimum AICc score from each of the other AICc scores. In Eq. (4), AICi is the Akaike Information Criterion evaluated for model i, and AICmin is the minimum AIC value of all of the models. This means that the model for which AIC is lowest will have a delta value of zero (Burnham and Anderson, 2004).

$$\Delta AICc_i = AICc_i - AICc_{min} \tag{4}$$

2.3. Meta-analysis

In order to place the grouper and snapper growth patterns into context with respect to other taxa, we conducted a survey of larval growth literature to examine the variability among published growth models for a variety of families (Supplemental Table 1). The majority of these studies are studies in which larvae are caught during a sampling trip and measured, then aged later using an otolith age-interval relationship (e.g., Lozano et al., 2012). To demonstrate these previously published models, we generated random test age data for 100 fish by generating 100 random ages between 1 and 40 days and plotted the models by family (Supplement Figs. 1 through 6). We chose this age range to agree with the range of ages used earlier in the examination of grouper and snapper growth patterns. Ninety-four models for a range of species were included, some of which came from the same papers but refer to different cohorts, year classes, or locations. Length at age was plotted to visualize growth patterns within families.

In order to assess whether there was a difference in larval growth patterns between larval fish of demersal and pelagic taxa, we performed a chi-squared analysis. We gathered length at flexion and length at the transformation data from larval to juvenile stages for as many species as

Table 3

Model Parameters and associated p-values*** indicates highly significant p-value at < 0.001,** indicates significance at 0.001,“.” indicates significance at 0.05. “ ~ ” indicates lowest AICc.

Red Snapper	Coefficients	P-values
Linear	$\boldsymbol{Length} = 0.453 * \boldsymbol{age} + 0.186$	Slope: < 2e-16 *** Intercept: 0.602
Exponential	$\boldsymbol{Length} = 1.75 * \boldsymbol{e}^{(0.0736 * \boldsymbol{age})}$	Lo: < 2e-16 *** C: < 2e-16 ***
Logistic ~	$\boldsymbol{Length} = 40.1/(1 + \boldsymbol{e}^{\left(\frac{33.1 - \boldsymbol{age}}{9.96}\right)})$	Asym: 0.00181 ** t_{mid}: 2.97e-07 *** Scal: 3.95e-13 ***
von Bertalanffy	$\boldsymbol{Length} = 2.57 * 10^{+03} * (1 - \boldsymbol{e}^{(-1.51 * 10^{-04} * (\boldsymbol{age} - -3.06 * 10^{-01}))})$	Linf: 0.993 K: 0.993 t0: 0.829
Laird-Gompertz	$\boldsymbol{Length} = 1.52 * \boldsymbol{e}^{8.39 * (1 - \boldsymbol{e}^{(-0.0111 * \boldsymbol{age})})}$	G: 0.136 Alpha: 0.246 Lo: 6.86e-10 ***
Nassau Grouper	**Coefficients**	**P-values**
Linear	$\boldsymbol{Length} = 0.291 * \boldsymbol{age} + 0.800$	Slope: < 2e-16 *** Intercept: 0.00593 **
Exponential	$\boldsymbol{Length} = 2.77 * \boldsymbol{e}^{(0.0401 * \boldsymbol{age})}$	Lo: < 2e-16 *** C: < 2e-16 ***
Logistic	$\boldsymbol{Length} = 24.5/(1 + \boldsymbol{e}^{\left(\frac{37.4 - \boldsymbol{age}}{16.5}\right)})$	Asym: 0.003358 ** t_{mid}: 0.000809 *** Scal: 1.08e-06 ***
von Bertalanffy	$\boldsymbol{Length} = 4.72 * 10^{+03} * \left(1 - \boldsymbol{e}^{(-5.97 * 10^{-05} * (\boldsymbol{age} - -3.58 * 10^{-01}))}\right)$	Linf: 0.997 K: 0.997 t0: 0.920
Laird-Gompertz ~	$\boldsymbol{Length} = 2.134 * \boldsymbol{e}^{3.31 * (1 - \boldsymbol{e}^{(-0.0200 * \boldsymbol{age})})}$	G: 0.000121 *** Alpha: 0.0275 * Lo: 5.51e-08 ***
Yellowtail Snapper	**Coefficients**	**P-values**
Linear	$\boldsymbol{Length} = 0.201 * \boldsymbol{age} + 2.33$	Slope: 1.79e-08 *** Intercept: 5.69e-07 ***
Exponential ~	$\boldsymbol{Length} = 2.71 * \boldsymbol{e}^{(0.0408 * \boldsymbol{age})}$	Lo: 4.79e-12 *** C: 6.65e-11 ***
Logistic	$\boldsymbol{Length} = 105/(1 + \boldsymbol{e}^{\left(\frac{82.6 - \boldsymbol{age}}{22.1}\right)})$	Asym: 0.916 t_{mid}: 0.745 Scal: 0.0721.
von Bertalanffy	$\boldsymbol{Length} = 4.97 * 10^{+03} * \left(1 - \boldsymbol{e}^{(-5.36 * 10^{-05} * (\boldsymbol{age} - -3.46 * 10^{-01}))}\right)$	Linf: 0.999 K: 0.999 t0: 0.932
Laird-Gompertz	$\boldsymbol{Length} = 2.72 * \boldsymbol{e}^{8.33 * (1 - \boldsymbol{e}^{(-0.00483 * \boldsymbol{age})})}$	G: 0.835 Alpha: 0.848 Lo: 3.32e-07 ***
Red Grouper	**Coefficients**	**P-values**
Linear	$\boldsymbol{Length} = 0.342 * \boldsymbol{age} + 0.829$	Slope: 9.77e-14 *** Intercept: 0.016 *
Exponential ~	$\boldsymbol{Length} = 1.65 * \boldsymbol{e}^{(0.0794 * \boldsymbol{age})}$	Lo: 1.94e-13 *** C: < 2e-16 ***
Logistic	$\boldsymbol{Length} = 103/(1 + \boldsymbol{e}^{\left(\frac{67.4 - \boldsymbol{age}}{17.4}\right)})$	Asym: 0.967 t_{mid}: 0.894 Scal: 0.379
von Bertalanffy	$\boldsymbol{Length} = 3.63 * 10^{+03} * \left(1 - \boldsymbol{e}^{(-8.57 * 10^{-05} * (\boldsymbol{age} - -3.11 * 10^{-01}))}\right)$	Linf: 0.999 K: 0.999 t0: 0.912
Laird-Gompertz	$\boldsymbol{Length} = 2.05 * \boldsymbol{e}^{10.3 * (1 - \boldsymbol{e}^{(-0.00653 * \boldsymbol{age})})}$	G: 0.838 Alpha: 0.852 Lo: 1.01e-05 ***
Gray Snapper	**Coefficients**	**P-values**
Linear ~	$\boldsymbol{Length} = 0.401 * \boldsymbol{age} + 0.795$	Slope: 8.32e-12 *** Intercept: 0.0186 *
Exponential	$\boldsymbol{Length} = 2.75 * \boldsymbol{e}^{(0.0505 * \boldsymbol{age})}$	Lo: 1.1e-07 *** C: 2.1e-09 ***

(*continued on next page*)

Table 3 (*continued*)

Gray Snapper	Coefficients	P-values
Logistic	$\boldsymbol{Length} = 19. 8/(1 + \boldsymbol{e}^{\left(\frac{22.9-\boldsymbol{age}}{10.4}\right)})$	Asym: 5.08e-06 *** t_{mid}: 1.02e-05 *** Scal: 1.77e-06 ***
von Bertalanffy	$\boldsymbol{Length} = 2. 61 *10^{+03} *\left(1 - \boldsymbol{e}^{(-1.65 *10^{-04} * (\boldsymbol{age} - -3.18 *10^{-01}))}\right)$	Linf: 0.990 K: 0.990 t0: 0.844
Laird-Gompertz	$\boldsymbol{Length} = 1. 71 * \boldsymbol{e}^{2.82 * (1 - \boldsymbol{e}^{(-0.0425 * \boldsymbol{age})})}$	G: 1.09e-08 *** Alpha: 0.00149 ** Lo: 3.78e-05 ***

Sevenband Grouper	Coefficients	P-values
Linear	$\boldsymbol{Length} = 0. 0649 * \boldsymbol{age} + 2. 06$	Slope:7.09e-06 *** Intercept:0.00853 **
Exponential ~	$\boldsymbol{Length} = 2. 09 * \boldsymbol{e}^{(0.0262*\boldsymbol{age})}$	Lo: 2.84e-06 *** C: 0.00695 **
Logistic	$\boldsymbol{Length} = 38. 2/(1 + \boldsymbol{e}^{\left(\frac{101-\boldsymbol{age}}{25.7}\right)})$	Asym: 0.993 t_{mid}: 0.985 Scal: 0.905
von Bertalanffy	$\boldsymbol{Length} = 8. 22 *10^{+02} *(1 - \boldsymbol{e}^{(-7.92 *10^{-05} * (\boldsymbol{age} - -3.17*10^{-01}))})$	Linf: 1.000 K: 1.000 t0: 0.856
Laird-Gompertz	$\boldsymbol{Length} = 2. 08 * \boldsymbol{e}^{6.18 * (1 - \boldsymbol{e}^{(-0.00436 * \boldsymbol{age})})}$	G: 0.98464 Alpha: 0.98511 Lo: 0.00186 **

Dusky Grouper	Coefficients	P-values
Linear ~	$\boldsymbol{Length} = 0. 200 * \boldsymbol{age} + 1. 85$	Slope: 0.027840 * Intercept: 0.000336 ***
Exponential	$\boldsymbol{Length} = 1. 89 * \boldsymbol{e}^{(0.0823 *\boldsymbol{age})}$	Lo: 0.00031 *** C: 0.04144 *
Logistic	$\boldsymbol{Length} = 22. 5/(1 + \boldsymbol{e}^{\left(\frac{26.0-\boldsymbol{age}}{10.9}\right)})$	Asym: 0.987 t_{mid}: 0.978 Scal: 0.891
von Bertalanffy	$\boldsymbol{Length} = 4. 59 *10^{+02} *\left(1 - \boldsymbol{e}^{(-4.37 *10^{-04} * (\boldsymbol{age} - -9.24))}\right)$	Linf: 0.999 K: 0.999 t0: 0.811
Laird-Gompertz	$\boldsymbol{Length} = 1. 53 * \boldsymbol{e}^{0.513* (1 - \boldsymbol{e}^{(-1.53 * \boldsymbol{age})})}$	G: 0.00104 ** Alpha: 0.00955 ** Lo: 0.00013 ***

Blacktip Grouper	Coefficients	P-values
Linear	$\boldsymbol{Length} = 0. 605 * \boldsymbol{age} - 1. 58$	Slope: 2.45e-07 *** Intercept: 0.306
Exponential	$\boldsymbol{Length} = 3. 21 * \boldsymbol{e}^{(0.0433*\boldsymbol{age})}$	Lo: 7.42e-05 *** C: 2.59e-08 ***
Logistic ~	$\boldsymbol{Length} = 50. 0/(1 + \boldsymbol{e}^{\left(\frac{42.9-\boldsymbol{age}}{12.0}\right)})$	Asym: 2.13e-11 *** t_{mid}: 8.43e-13 *** Scal: 4.12e-11 ***
von Bertalanffy	$\boldsymbol{Length} = 1. 66 *10^{+04} *\left(1 - \boldsymbol{e}^{(-3.66 *10^{-05} * (\boldsymbol{age} - -2.62))}\right)$	Linf: 0.997 K: 0.997 t0: 0.336
Laird-Gompertz	$\boldsymbol{Length} = 0. 923 * \boldsymbol{e}^{4.62* (1 - \boldsymbol{e}^{(-0.0286 * \boldsymbol{age})})}$	G: 7.11e-11 *** Linf: 2.24e-05 *** Lo: 0.00419 **

Brown Spotted Grouper	Coefficients	P-values
Linear	$\boldsymbol{Length} = 0. 577 * \boldsymbol{age} - 0. 430$	Slope: 2.07e-05 *** Intercept: 0.745
Exponential	$\boldsymbol{Length} = 3. 03 * \boldsymbol{e}^{(0.0474 *\boldsymbol{age})}$	Lo: 0.00102 ** C: 8.72e-06 ***
Logistic ~	$\boldsymbol{Length} = 39. 5/(1 + \boldsymbol{e}^{\left(\frac{34.9-\boldsymbol{age}}{11.0}\right)})$	Asym: 6.60e-05 *** t_{mid}: 2.86e-05 *** Scal: 0.00015 ***
von Bertalanffy	$\boldsymbol{Length} = 2. 50 *10^{+04} *\left(1 - \boldsymbol{e}^{(-2.31 *10^{-05} * (\boldsymbol{age} - -0.746))}\right)$	Linf: 0.999 K: 0.999 t0: 0.800
Laird-Gompertz	$\boldsymbol{Length} = 1. 47 * \boldsymbol{e}^{4.03* (1 - \boldsymbol{e}^{(-0.0286 * \boldsymbol{age})})}$	G: 1.28e-05 *** Alpha: 0.0146 * Lo: 0.0259 *

Malabar Grouper	Coefficients	P-values
Linear	$\boldsymbol{Length} = 0.670 * \boldsymbol{age} - 1.24$	Slope: 7.11e-06 *** Intercept: 0.44
Exponential ~	$\boldsymbol{Length} = 2.47 * \boldsymbol{e}^{(0.0629 * \boldsymbol{age})}$	Lo: 7.29e-05 *** C: 9.14e-08 ***
Logistic	$\boldsymbol{Length} = 57.8/(1 + \boldsymbol{e}^{\left(\frac{39.6 - \boldsymbol{age}}{11.6}\right)})$	Asym: 0.053701. t_{mid}: 0.003654 ** Scal: 0.000538 ***
von Bertalanffy	$\boldsymbol{Length} = 1.49 * 10^{+04} * \left(1 - \boldsymbol{e}^{(-4.51 * 10^{-05} * (\boldsymbol{age} - -1.86))}\right)$	Linf: 0.998 K: 0.998 t0: 0.512
Laird-Gompertz	$\boldsymbol{Length} = 1.72 * \boldsymbol{e}^{5.80 * (1 - \boldsymbol{e}^{(-0.0169 * \boldsymbol{age})})}$	G: 0.0468 * Alpha: 0.2148 Lo: 0.0204 *

Longtooth Grouper	Coefficients	P-values
Linear	$\boldsymbol{Length} = 0.666 * \boldsymbol{age} - 2.88$	Slope: 1.12e-08 *** Intercept: 0.0815.
Exponential	$\boldsymbol{Length} = 2.65 * \boldsymbol{e}^{(0.0512 * \boldsymbol{age})}$	Lo: 2.33e-09 *** C: 1.59e-14 ***
Logistic	$\boldsymbol{Length} = 96.1/(1 + \boldsymbol{e}^{\left(\frac{58.8 - \boldsymbol{age}}{15.3}\right)})$	Asym: 0.000387 *** t_{mid}: 9.78e-08 *** Scal: 6.63e-10 ***
von Bertalanffy	$\boldsymbol{Length} = 1.56 * 10^{+04} * \left(1 - \boldsymbol{e}^{(-4.26 * 10^{-05} * (\boldsymbol{age} - -4.35))}\right)$	Linf: 0.9974 K: 0.9974 t0: 0.0977.
Laird-Gompertz ~	$Length = 1.78 * \boldsymbol{e}^{6.66 * (1 - e^{(-0.0118 * \boldsymbol{age})})}$	G: 2.39e-05 *** Alpha: 0.00238 ** Lo: 6.24e-06 ***

Mangrove Snapper	Coefficients	P-values
Linear	$Length = 0.277 * \boldsymbol{age} + 1.40$	Slope: 0.000189 *** Intercept: 0.0472 *
Exponential ~	$Length = 2.07 * \boldsymbol{e}^{(0.0573 * \boldsymbol{age})}$	Lo: 0.000639 *** C: 0.000151 ***
Logistic	$Length = 33.0/(1 + \boldsymbol{e}^{\left(\frac{39.6 - \boldsymbol{age}}{14.3}\right)})$	Asym: 0.677 t_{mid}: 0.475 Scal: 0.110
von Bertalanffy	$Length = 4.48 * 10^{+03} * \left(1 - \boldsymbol{e}^{(-6.19 * 10^{-05} * (\boldsymbol{age} - -5.04))}\right)$	Linf: 0.999 K: 0.999 T0: 0.355
Laird-Gompertz	$Length = 1.88 * \boldsymbol{e}^{5.15 * (1 - e^{(-0.0141 * \boldsymbol{age})})}$	G: 0.582 Alpha: 0.670 Lo: 0.0166 *

possible in the meta-analysis. The majority of these flexion and transformation lengths, as well as spawning information when possible, were found in Richards (2006), with remaining species filled in from larval fish guides, and technical memos on early life stages (Auditore et al., 1994; Moser, 1996; Fahay et al., 1999; Ed. Richards, 2006; Ré and Meneses, 2008; Froese and Pauly, 2019). We sorted each individual model into a demersal or pelagic group, and performed one tailed t-tests comparing flexion lengths and transformation lengths between the two groups. We gathered spawning dates and seasons for as many species in the meta-analysis as possible and we assigned the taxa a binary score for each season based on the spawning time of that fish: 1 for presence of spawning and 0 for absence of spawning. We calculated the total number of spawning presences in each season for demersal and pelagic groups, and then compared them using a chi-squared test. We also found spawning seasons for the grouper and snapper species in this paper (Hussain and Abdullah, 1977; Jeyaseelan, 1998; Ed. Richards, 2006; Gaspare and Bryceson, 2013; Bertucci et al., 2015; Froese and Pauly, 2019).

3. Results

3.1. Grouper and snapper species-level analysis

In this analysis of grouper and snapper, the group of models with an exponential basis describes growth in early life better than the models with a linear basis. Model parameters and their associated p-values for all models and all species can be seen in Table 3 and the plots of all five models for every species can be found in Fig. 1. Upon comparing AICc scores (Table 4), several patterns emerged in relation to both the winning scores and the order in which the delta values ranked under the winning scores. Ten of the twelve grouper and snapper species had a model with an exponential basis as their most parsimonious model, and in eight of those cases, multiple models with an exponential basis were shown to be at least somewhat supported. In contrast, only two species, Dusky Grouper and Gray Snapper, had the linear model as the most supported model, and in both of these cases, the second-best supported model was still relatively well supported and was from the exponential family of models. The model with the lowest AICc score for the most species was the exponential model. The von Bertalanffy ranked last or second to last in every species, and had delta scores indicative of completely unsupported models in all but two cases.

The demersal species Yellowtail Snapper, Sevenband Grouper, Mangrove Snapper, and Malabar Grouper were all best represented by the exponential model (Table 4, Fig. 1). For Sevenband Grouper, the linear model was also supported with a delta AICc score less than 1. Four more demersal species, Nassau Grouper, Longtooth Grouper, Red Snapper, and Brown Spotted Grouper, were best represented by either the Laird-Gompertz or logistic model, with another model from the exponential family coming in second. Nassau Grouper and Longtooth Grouper showed two supported models, as they were best represented

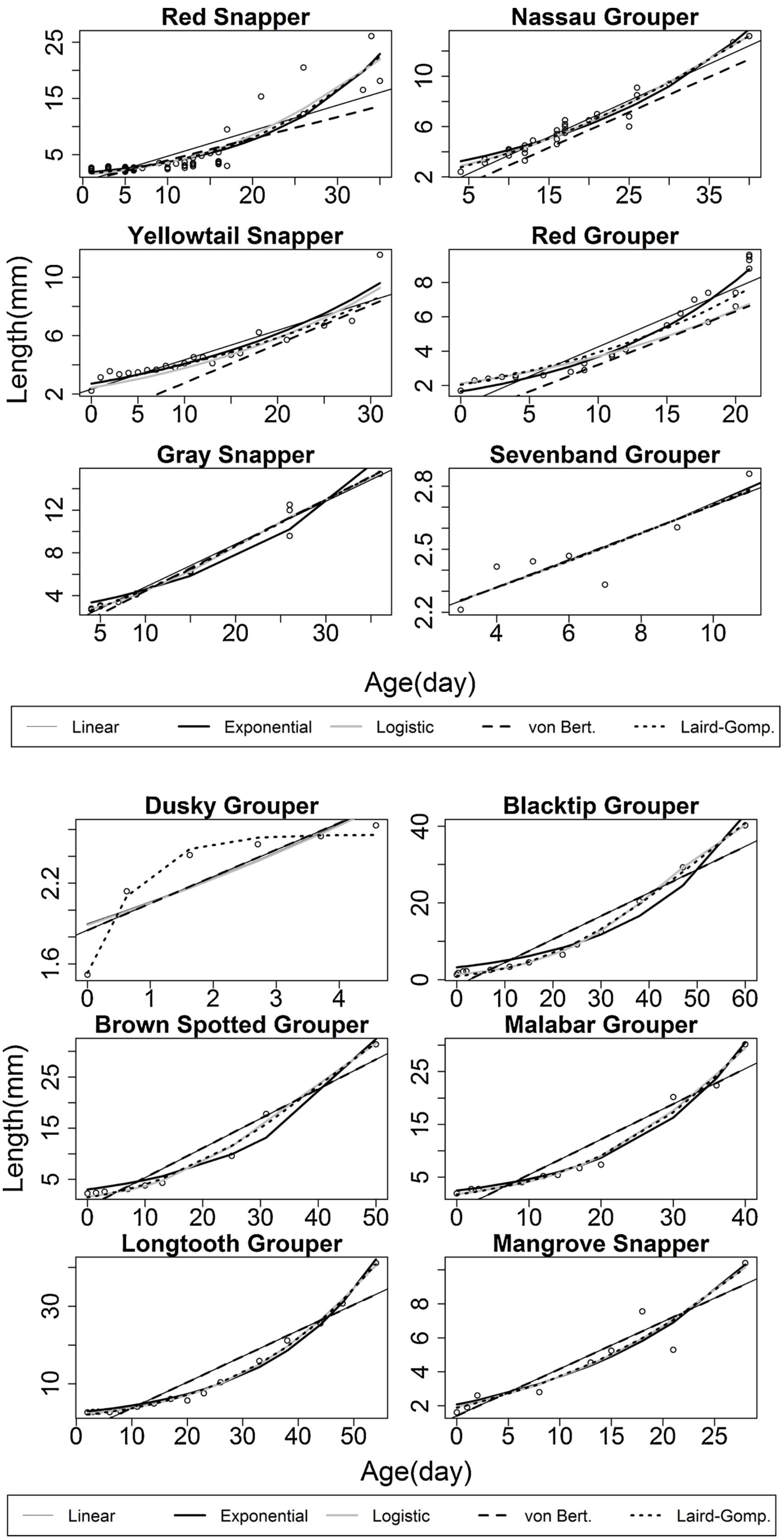

Fig. 1. Fitted growth models plotted with length at age data.

by the Laird-Gompertz model but also had the logistic model with a delta AICc score under 1 (Table 4, Fig. 1). Of the remaining four species, two species were clearly represented by a single exponential-family model with no secondarily supported models. Blacktip Grouper showed a low AICc score for only the logistic model, while Red Grouper showed a low AICc score for only the exponential model (Table 4). Only two

Table 4
AICc scores and Delta Scores.

Red Snapper	AICc Scores	Delta AICc	Nassau Grouper	AICc Scores	Delta AICc
Logistic	368.7	0	Laird-Gompertz	63.1	0
Exponential	371.9	3.2	Logistic	63.9	0.7
Laird-Gompertz	372.6	3.8	Exponential	65.7	2.6
Linear	433.0	64.3	Linear	66.8	3.7
von Bertalanffy	446.4	77.7	von Bertalanffy	104.6	41.4
Yellowtail Snapper	**AICc Scores**	**Delta AICc**	**Red Grouper**	**AICc Scores**	**Delta AICc**
Exponential	49.1	0	Exponential	51.4	0
Logistic	56.6	7.5	Laird-Gompertz	75.5	24.1
Laird-Gompertz	56.7	7.7	Linear	76.7	25.4
Linear	58.7	9.7	Logistic	95.9	44.6
von Bertalanffy	94.3	45.2	von Bertalanffy	107.9	56.5
Gray Snapper	**AICc Scores**	**Delta AICc**	**Sevenband Grouper**	**AICc Scores**	**Delta AICc**
Linear	37.4	0	Exponential	−0.1	0
Logistic	37.7	0.3	Linear	0.2	0.3
Laird-Gompertz	38.3	0.8	Logistic	13.9	14.0
von Bertalanffy	46.1	8.7	Laird-Gompertz	13.9	14.1
Exponential	49.2	11.8	von Bertalanffy	14.2	14.3
Dusky Grouper	**AICc Scores**	**Delta AICc**	**Blacktip Grouper**	**AICc Scores**	**Delta AICc**
Linear	15.2	0	Logistic	26.7	0
Exponential	16.1	0.8	Laird-Gompertz	44.7	18.0
Laird-Gompertz	27.2	12.0	Exponential	66.9	40.1
von Bertalanffy	45.2	30.0	Linear	77.0	50.3
Logistic	45.9	30.7	von Bertalanffy	81.4	54.7
Brown-Spotted Grouper	**AICc Scores**	**Delta AICc**	**Malabar**	**AICc Scores**	**Delta AICc**
Logistic	41.2	0	Exponential	47.2	0
Laird-Gompertz	44.6	3.4	Logistic	49.5	2.3
Exponential	46.8	5.6	Laird-Gompertz	50.1	3.0
Linear	52.0	10.8	Linear	63.7	16.6
von Bertalanffy	59.2	18.0	von Bertalanffy	69.0	21.8
Longtooth Grouper	**AICc Scores**	**Delta AICc**	**Mangrove Snapper**	**AICc Scores**	**Delta AICc**
Laird-Gompertz	46.2	0	Exponential	33.3	0
Logistic	46.7	0.5	Linear	35.4	2.1
Exponential	54.4	8.2	Laird-Gompertz	40.3	6.9
Linear	93.2	47.0	Logistic	40.3	7.0
von Bertalanffy	96.8	50.6	von Bertalanffy	42.6	9.3

species, Dusky Grouper and Gray Snapper, had the linear model as the winner, with Dusky Grouper having a well-supported exponential runner up and Gray Snapper having well-supported logistic and Laird-Gompertz runners up (Table 4, Fig. 1). Although the linear model is the most parsimonious for Dusky Grouper, it is clear from the plot that the growth pattern looks most similar to the von Bertalanffy. Dusky Grouper is the only species to exhibit a growth plateau in the time period covered by the data.

3.2. Grouper and snapper: seasonality and spawning

The two species which had the linear model as the most parsimonious, Dusky Grouper and Gray Snapper, also have similar spawning seasons. They both begin spawning in the summer and continue spawning through fall, while the other grouper and snapper species we were able to find spawning information on showed different spawning patterns (Table 1). There are four patterns evident: 1) spawn starting in spring, 2) spawn year-round, 3) spawn from fall through winter, and 4) spawn from fall to winter and again from spring to summer (Hussain and Abdullah, 1977; Jeyaseelan, 1998; Ed. Richards, 2006; Gaspare and Bryceson, 2013; Bertucci et al., 2015; Froese and Pauly, 2019).

3.3. Meta-analysis

The surveyed growth literature included 31 papers which provide 94 models spanning 17 different fish families from around the globe. The majority of the ninety-four models used for the meta-analysis can be sorted into six families; and upon examination of the plotted models, marked differences between taxa emerged (Supplemental Plots 1–6). Demersal taxa included Serranidae, Nototheniidae, Gadidae, Scianidae, Lutjanidae, Mugilidae, and Pleuronectidae. Pelagic taxa included Scombridae, Myctophidae, Istiophoridae, Carangidae, Coryphaenidae, Pomatomidae, and Xiphiidae. Forage taxa included Engraulidae, Clupeidae, Osmeridae. The models found for two demersal families, Gadidae and Pleuronectidae all had an exponential basis, as did additional models found for Lutjanids (Supplemental Figs. 2, 4, and 5). The Gadidae family contains Cod and Haddock, and the Pleuronectidae family contains flatfish such as Flounder and Sole. All models found for

Table 5
Chi-squared Comparison of Linear and Exponential Models among Pelagic and Demersal Groups.

Observed:				Expected:			
Observed Values	Exponential	Linear	Total	Expected Values	Exponential	linear	Total
Demersal	31	16	47	Demersal	27.084	19.915	47
Pelagic	3	9	12	Pelagic	6.915	5.085	12
Total	34	25	59	Total	34	25	59
				Chi-Squared Value		6.567	
				p-value		0.0104	

the Scombrid family, which contains tuna, were linear (Supplemental Fig. 3). Other large pelagic taxa showed both linear and exponential patterns, but linear was more common. The chi-squared value calculated to compare the 59 models from demersal and pelagic families was well below the threshold needed to reject the null hypothesis that linear and exponential models were split between pelagic and demersal taxa proportionally (Table 5). When models including juvenile snapper in addition to larval snapper were added, the difference between demersal and pelagic families was still significant (Denit and Sponaugle, 2004). Thus, of the ninety-four previously published models examined here, the models of early life growth in demersal taxa tended to have an exponential growth pattern, while models of early life growth in pelagic taxa tended to have a linear basis. Interestingly, previously published larval growth models of forage fish from the Engraulid and Clupeid family fell between these two groups, with a mixture of linear based and exponential based models in both families (Supplemental Plots 1 and 6). The one tailed t-tests comparing flexion lengths and transformation lengths in demersal and pelagic fish showed that demersal fish had significantly longer flexion lengths ($p = 0.037$) than pelagic fish, and that demersal fish had longer transformation lengths ($p = 0.074$) as well. There were no significant differences in seasonality of spawning patterns between the demersal and pelagic groups in the meta-analysis using the chi-squared analysis.

4. Discussion

Groupers and snappers were best modeled with equations having an exponential basis and we found a significant difference between the early life growth patterns of pelagic fish and demersal fish. These findings suggest that demersal and reef associated fish like grouper, snapper, cod, haddock, and flatfish follow an exponential growth curve early in life while pelagic fish like tuna more often follow a linear growth pattern. This supports our suggestion that differences in larval and early juvenile growth between taxa may relate to predation risk mediation tactics. As described in Foraging Arena Theory (Walters and Juanes, 1993; Ahrens et al., 2012), predator-prey interactions are restricted in space and time, and prey are partitioned into vulnerable and invulnerable pools. Young fish may spend large amounts of time in refugia for protection from predation, but this limits the area in which they can feed (Walters and Juanes, 1993; Ahrens et al., 2012). There is therefore an inherent trade-off between growth rate and predation risk (Walters and Juanes, 1993; Ahrens et al., 2012). Exchange between these two pools impacts the overall predation rate and the form of the density dependent predation functional response (Walters and Juanes, 1993; Walters and Christensen, 2007; Ahrens et al., 2012). Increasing the exchange rate between pools allows for more feeding and faster growth but also increases risk of predation. Refugia can be thought of as microhabitats, and these may be present in differing degrees in the pelagic and demersal environments. Refugia may be available to both pelagic and demersal fish, but early life stages of demersal and reef associated species may have more refuge available in the form of physical structure and hiding places, whereas pelagic fish may have to rely on microhabitats such as the centers of schools. We suggest that demersal and reef associated species may rely on structural refugia to help mediate predation risk and gradually take on more risk and increase consumption as they increase in size, resulting in early exponential growth. In contrast, young pelagic fish that rear without available structural refugia need to grow large quickly to get out of the gape range of predators, or develop swimming skills quickly to increase mobility. The results of the flexion and transformation t-tests are consistent with this idea. They indicate that demersal fish may take longer to achieve these early life history milestones than pelagic fish. The refugia may allow them the luxury of remaining at small sizes for longer amounts of time, as they have the ability to utilize these hiding places until they grow out of the gape range of their predators. This could suggest that the life history strategies to either favor slow growth in protected habitat or fast growth in exposed habitat may manifest in the larval stage. Forage fish had a mixture of growth models in the linear and exponential families, which could indicate that the degree of refuge present is greater than that offered to other pelagic fish in the form of schooling, but lower than that available to demersal and reef fish that can utilize structural refuge. We found a strong distinction between the growth rates of pelagic and demersal fish, even at larval ages, which suggests that growth rate may show a low degree of plasticity throughout the early life history and is indicative of risk mediation strategy among juvenile fish. Even if larvae are not using these mediating strategies in the same way that older juveniles or adults would, the pattern supported in our results would still suggest that differences in larval growth patterns are tied to risk mediation behavior and may be indicative of physiology implications later in life. Unpublished predictive models indicate that larvae of different taxa inhabit different areas in the water column (Vasbinder, unpublished data). Larvae have been demonstrated to have the ability to make choices surrounding their movement behaviors, so we do not believe that the idea that larval stages can exhibit risk mediation behavior is out of the question (Codling et al., 2004).

The second possibility that we considered may be impacting growth rate was the seasonality of spawning time, which changes the season in which the young fish are growing and feeding. While there was not a clear case for this hypothesis in the meta-analysis, comparing spawning dates for grouper and snapper species did support this possibility as Dusky Grouper and Gray Snapper, which showed strong support for the linear family of growth models, have similar spawning seasons in the summer and fall (Ed. Richards, 2006; Bertucci et al., 2015). It is possible that the statistical correlation between spawning date and the probability of exponential growth was not seen in the meta-analysis due to the wide breadth of climatic regimes included. Since the environmental factors at play in each of the ninety-four models included in the literature survey are different, these factors could impact the results of the survey. There are some other subtleties in the change in growth rates over age, such as discontinuous growth, that were not considered in the present study. Step changes between ontogenetic states can be represented by discontinuous growth functions. In fish and invertebrates whose growth rates are limited by oxygen availability, changes in habitat, feeding ecology, or physiology reveal strategies to decrease basal metabolic oxygen needs and increase scope for growth (Pauly, 2010).

The impact of temperature on growth cannot be neglected in this conversation on comparative growth modeling. Temperature is one of the most important drivers of larval development before first feeding. It impacts several of the parameters commonly used in growth models including instantaneous growth rate, initial length or length at t = 0, predicted length at metamorphosis, time to metamorphosis, and time of first feeding (Dulcic, 1997; Pepin, 1991; Benoit et al., 2000; Castello and Castello, 2003). Temperature impacts on larval growth have been demonstrated in many species (Dulcic, 1998; Folkvord, 2005; Gracia-Lo´pez et al., 2004; Fielder et al., 2005). In one study, differences in growth in sardine larvae from different locations were suggested to be the result of temperature (Dulcic, 1995). All data for the grouper and snapper species modeled in this paper came from temperature ranges similar to the Gulf of Mexico. The literature surveyed in the meta-analysis includes a group of climatologically diverse regions, from the North Pacific and North Atlantic, to the Indian Ocean and the Gulf of Mexico. In an extensive review of marine fishes, Pepin (1991) concluded that increasing temperature led to increases in daily development rates and daily mortality rates, but led to decreases in stage specific mortality at very young stages. Higher temperatures also resulted in faster hatching, faster transition out of the yolk-sac stage, higher mean growth rates and increased growth rates of post larvae (Pepin, 1991; Benoit et al., 2000). Thus, we should anticipate temperature differences between regions to impact the rate at which young fish grow and reach major developmental landmarks, but the shape of the growth curve may remain the same. Temperature can also change within a spawning season, which may lead to differences in growth rates among consecutively spawned cohorts (Hernandez and Castro, 2000). If temperature increases throughout a season, young fish that grow in a linear growth pattern may begin to grow faster in response to temperature changes, leading to the appearance of an exponential growth pattern instead.

Surveying a wide range of published studies on early life growth and using those results to draw conclusions about larvae in the field raises another question: to what extent can laboratory reared larval growth studies inform our understanding of larval growth in the sea? This question has been addressed by Pepin (1991), who decided to use only use field studies when gathering development rates for a meta-analysis. Some authors use length at t_0 interchangeably with length at first feeding, and differences in this parameter between laboratory reared and field caught anchovy larvae have been observed (Dulcic, 1997). Some growth studies have found that larvae grow faster in the field than in the lab, while others found no difference between wild caught fish and reared fish in their growth studies (Benoit et al., 2000; Jenkins, 1987). In this paper, growth models from both wild caught and laboratory reared fish are included, which could be a potential source of error. Variability between models could also be impacted by the way in which length was measured as some studies in the clupeid family used standard length while others used total length (eg, Geffen, 2002, Luthy et al., 2005, Lozano et al., 2012). There is potential for error due to allometric growth, as the difference between standard length and total length increases as fish length increases (Beckman, 1948). Another source of error could be the simplifying assumptions we made regarding the mortality regimes experienced by young fish in different stages. Fish undergo qualitative shifts as they grow, and we did not consider discrete changes in mortality regimes as fish participate in ontogenetic movement or behavioral or physiological changes. These are likely species or population specific, but because we were doing a broad survey, we did not fit or plot growth models for different stages. Ricker (1979) proposed the use of a sigmoidal curve called a “Sachs Cycle” (Ricker, 1979), and suggested that ontogenetic growth is more accurately modeled in stages separated by “crises”, such as metamorphosis. A variety of other co-variates such as yolk-sac duration or pigmentation onset may have an effect as well. Although all co-variates cannot be eliminated, the highest source of error in this meta-analysis is that fitting techniques are not standardized between authors. Thus, while co-variates such as temperature, stage specific mortality, and measurement techniques cannot be controlled, controlling co-variates to this level of precision would be unwarranted by the level of precision in the data that comes from comparing models fit by different authors. Even with imperfect data sources, valuable observations of patterns between taxa can still be recognized and demonstrated statistically.

This paper also explores whether the same models can be used for young fish and adult fish. The von Bertalanffy growth model is typically the growth model chosen to represent adult fish growth, and has even been found to describe fish growth in fresh water taxa better than polynomial functions with three and four parameters for fish aged one year and older (Chen et al., 1992). The von Bertalanffy growth model ranked lowest or second lowest in all twelve grouper and snapper species, indicating that models commonly used to predict age or length in adult fish may not be appropriate for use with early life history data. At young ages, growth is not constrained by gill surface area in the same way that it is in adults (Pauly, 1981). Young fish are not limited to an ever-diminishing scope for growth as is suggested by the von Bertalanffy growth model, so the linear or exponential growth models may be more appropriate. In addition, models that include exponential growth and an inflection point may be appropriate for early life stages because they allow the growth to slow as the fish approaches metamorphosis (e.g. logistic, Laird-Gompertz, generalized von Bertalanffy growth function), at least for demersal species that are able to regulate predation risk via a consumption-mortality trade off behavior (Pauly 1981). As fish get older, other growth models become more appropriate than those used in early life. For example, our meta-analysis showed that Scombrid fish in early life grow linearly. One of those linear models is for Bluefin Tuna (Malca et al., 2017). Juvenile Bluefin Tuna display a saturating growth rate at large sizes, eventually showing von Bertalanffy growth from one year onward (Cort, 2002; Megalofonou et al., 2002). Thus, the appropriate growth model for Bluefin Tuna changes throughout ontogeny (Cort, 2002; Megalofonou et al., 2002; Malca et al., 2017). These findings support the idea that early life history growth is best represented using different growth models than adult growth.

Author contributions

I affirm that my co-authors and I carried out this research and have agreed to be listed. All authors have approved the submitted version of the manuscript.

Kelly Vasbinder: Conceptualization, Methodology, Software, Formal analysis, Data Curation, Writing - Original Draft, Writing - Review & Editing, Visualization, Funding acquisition.

Cameron Ainsworth: Conceptualization, Methodology, Writing - Original Draft, Writing - Review & Editing, Resources, Funding acquisition, Supervision.

Declaration of Competing Interest

The authors declare that they have no known competing financial interests or personal relationships that could have appeared to influence the work reported in this paper.

Acknowledgements

KV’s portion of the project was funded by the Presidential Doctoral Fellowship awarded by the University of South Florida. CA's time was funded by a National Oceanic and Atmospheric Administration grant for the Marine Resource Assessment Program at the University of South Florida (95-NA10OAR4320143). Thanks to Estrella Malca for sharing and communicating her data to the authors to help in this project.

Appendix A. Supplementary data

Supplementary material related to this article can be found, in the online version, at doi:https://doi.org/10.1016/j.fishres.2020.105538.

References

Ahrens, R.N.M., Walters, C.J., Christensen, V., 2012. Foraging arena theory. Fish Fish. 13, 41–59.

Auditore, P.J., Lough, R.G., Broughton, E.A., 1994. A review of the comparative development of atlantic cod (*Gadus morhua* L.) and Haddock (*Melanogrammusaeglefinus* L.) based on an illustrated series of larvae and juveniles from georges bank. NAFO Sci. Counc. Stud. 20, 7–18.

Beckman, W.C., 1948. The length-weight relationship factors for conversions between standard and total lengths and coefficients of condition for seven Michigan fishes. Trans. Am. Fish. Soc. 75, 237–256.

Benetti, D.D., 1992. Bioenergetics and growth of dolphin, *Coryphaena hippurus*. PhD Thesis. University of Miami, Miami, FL.

Benoit, H.P., Pepin, P., Brown, J.A., 2000. Patterns of metamorphic age and length in marine fishes, from individuals to taxa. Can. J. Fish. Aquat. Sci. 57, 856–869.

Bertucci, F., Lejeune, P., Payrot, J., Parmentier, E., 2015. Sound production by dusky grouper *Epinephelus marginatus* at spawning aggregation sites. J. Fish Biol. 87, 400–421.

Beverton, R.J.H., Holt, S.J., 1957. On the dynamics of exploited fish populations. Fish. Invest. 19, 1–533.

Burnham, K.P., Anderson, D.R., 2004. Multimodel inference: understanding AIC and BIC in model selection. Sociol. Methods Res. 33, 261–304. https://doi.org/10.1177/0049124104268644.

Campana, S.E., Hurley, P.C., 1989. An age-and temperature-mediated growth model for cod (*Gadus morhua*) and haddock (*Melanogrammus aeglefinus*) larvae in the Gulf of Maine. Can. J. Fish. Aquat. Sci. 46, 603–613.

Campana, S.E., Jones, C., 1992. Analysis of otolith microstructure data. P. 73-100 In: Stevenson, D.K., Campana, S.E. (Eds.), Otolith Microstructure Examination and Analysis. Can. Spec. Publ. Fish. Aquat. Sci., pp. 117.

Castello, L., Castello, J.P., 2003. Anchovy stocks (*Engraulis anchoita*) and larval growth in the SW Atlantic. Fish. Res. 89, 409–421.

Chen, Y., Jackson, D.A., Harvey, H.H., 1992. A comparison of von Bertalanffy and polynomial functions in modelling fish growth data. Can. J. Fish. Aquat. Sci. 49, 1228–1235.

China, V., Holzman, R., 2014. Hydrodynamic starvation in first-feeding larval fishes. PNAS 111, 8083–8088. https://doi.org/10.1073/pnas.1323205111. published ahead of print May 19, 2014.

Codling, E.A., Hill, N.A., Pitchford, J.W., Simpson, S.D., 2004. Random walk models for the movement and recruitment of reef fish larvae. Mar. Ecol. Prog. Ser. 279, 215–224.

Colin, P.L., Koenig, C., Laroche, W.A., 1996. Development from egg to juvenile of the Red Grouper (*Epinephelus morio*) (Pisces: Serranidae) in the laboratory [Desarollo de huevo a juvenildelmeroamericano (*Epinephelus morio*) (Pisces: Serranidae) en-laboratorio]. p. 399-414 In: In: Arreguin-Sanchez, F., Munro, J.L., Balgos, M.C., Pauly, D. (Eds.), Biology, Fisheries and Culture of Tropical Groupers and Snappers. ICLARM Conf. Proc. 48. pp. 449.

Cort, J.L., 2002. Age and growth of Bluefin Tuna (*Thunnus thynnus thynnus*) of the Northeast Atlantic. In: Bridges, C.R., Garcia-Gomez, A., Gordin, H. (Eds.), Domestication of *Thunnus thynnus*: Proceeding of the First International Symposium Held at the University of Cartagena. Spain. pp. 36–41.

Cowan Jr, J.H., Houde, E.D., Rose, K.A., 1996. Size-dependent vulnerability of marine fish larvae to predation: an individual-based numerical experiment. ICES J. Mar. Sci. 53, 23–37. https://doi.org/10.1006/jmsc.1996.0003.

Denit, K., Sponaugle, S., 2004. Growth variation, settlement, and spawning of gray snapper across a latitudinal gradient. Trans. Am. Fish. Soc. 133, 1339–1355.

Drass, D.M., Bootes, K.L., Lyczkowski-Shultz, J., ComynsB, H., Holt, G.J., Riley, C.M., Phelps, R.P., 2000. Larval development of red snapper, *Lutjanus campechanus*, and comparisons with co-occurring snapper species. Fish. Bull. (Wash. D. C.) 98, 507–527.

Dulcic, J., 1995. Estimation of age and growth of sardine, *Sardina pilchardus* (Walbaum, 1792), larvae by reading daily otolith increments. Fish. Res. 22, 265–277.

Dulcic, J., 1997. Growth of anchovy, *Engruulis encrasicolus* (L.) larvae in the Northern Adriatic Sea. Fish. Res. 31, 189–195.

Dulcic, J., 1998. Larval growth of sprat, *Sprattuss prattus phalericus*, larvae in the Northern Adriatic. Fish. Res. 36, 117–126.

Ed. Richards, W.J., 2006. Early Stages of Atlantic Fish: an Identification Guide for the Western Central North Atlantic. CRC Press, Taylor and Francis Group LLC, Boca Raton, FL.

Elzhov, T.V., Mullen, K.M., Spiess, A.-N., Bolker, B., 2016. minpack.lm: R Interface to the Levenberg-Marquardt Nonlinear Least-Squares Algorithm Found in MINPACK, Plus Support for Bounds. R package version.

Emata, A.C., Eullaran, B., Bagarinao, T.U., 1994. Induced spawning and early life description of the mangrove red snapper *Lutjanus argentimaculatus*. Aquaculture 121, 381–387.

Fahay, M.P., Berrien, P.L., Johnson, D.L., Morse, W.W., 1999. Essential Fish Habitat Source Document: Atlantic Cod, *Gadus morhua*, Life History and Habitat Characteristics. NOAA Technical Memorandum NMFS-NE-124. National Marine Fisheries Serv. James J. Howard Marine Sciences Lab, Highlands, NJ, pp. 41.

Fielder, D.S., Bardsley, W.J., Allan, G.L., Pankhurst, P.M., 2005. The effects of salinity and temperature on growth and survival of Australian snapper, *Pagrus auratus* larvae. Aquaculture 250, 201–214.

Folkvord, A., 2005. Comparison of size-at-age of larval Atlantic cod (*Gadus morhua*) from different populations based on size- and temperature-dependent growth models Can. J. Fish. Aquat. Sci. 62, 1037–1052.

Froese, R., Pauly, D., 2019. FishBase. World Wide Web Electronic Publication. (Accessed June 2019). www.fishbase.org.

Gaspare, L., Bryceson, I., 2013. Reproductive biology and fishery-related characteristics of the Malabar Grouper (*Epinephelus malabaricus*) caught in the coastal waters of Mafia Island, Tanzania. Hindawi Publishing Corporation. J. Mar. Biol. 2013, 11. https://doi.org/10.1155/2013/786589.

Geffen, A., 2002. Length of herring larvae in relation to age and time of hatching. J. Fish Biol. 60, 479–485.

Glamuzina, B., Skaramuca, B., Glavic, N., Kozul, V., Dulcic, J., Kraljevic, M., 1998. Egg and early larval development of laboratory reared dusky grouper *Epinephelus marginatus* (Lowe 1834) (Picies Serranidae). Sci. Mar. 62, 373–378.

Gompertz, B., 1825. On the nature of the function expressive of the law of human mortality, and on a new mode of determining the value of life contingencies. Philos. Trans. R Soc. Lond. 115, 513–585.

Gracia-Lo´pez, V., Kiewek-Martı´nez, M., Maldonado-Garcı´a, M., 2004. Effects of temperature and salinity on artificially reproduced eggs and larvae of the leopard grouper *Mycteroperca rosacea*. Aquaculture 237, 485–498.

Hernandez, E.H., Castro, L.R., 2000. Larval growth of the anchoveta *Engraulis ringens* during the winter spawning season off central Chile. Fish. Bull. (Wash. D. C.) 98, 704–710.

Houde, E.D., Schekter, R.C., 1981. Growth rates, rations and cohort consumption of marine fish larvae in relation to prey concentrations. Rapports et Proces-verbaux des Re´unions. Conseil International pour L'Exploration scientifique de la Mer 178, 441–453.

Hinrichsen, H.H., Möllmann, C., Voss, R., Köster, F.W., Kornilovs, G., 2002. Biophysical modeling of larval Baltic cod (*Gadus morhua*) growth and survival. Can. J. Fish.Aquat. Sci. 59, 1858–1873. https://doi.org/10.1139/F02-149.

Hjort, J., 1914. Fluctuations in the Great Fisheries of Northern Europe Viewed in the Light of Biological Research. ICES.

Hurvich, C.M., Tsai, C., 1991. Bias of the corrected AIC criterion for underfitted regression and time series models. Biometrika 78, 499–509. https://doi.org/10.1093/biomet/78.3.499.

Hussain, N.A., Abdullah, M.A.S., 1977. The length-weight relationship, spawning season and food habits of six commercial fishes in Kuwaiti waters. Indian J. Fish. 24, 181–194.

Hussain, N.A., Higuchi, M., 1990. Larval rearing and development of the brown spotted grouper, *Epinephelustauuina*. Forskai) Aquaculture 19, 339–350.

Jayadi, Mallawa, A., Nessa, N., Djawad, I., Ardiansyah, 2016. Growth patterns of Camouflage Grouper (*Epinephelus polyphekadion*, Bleeker, 1849) larvae. J. Fish. Aquat. Sci. 12 (1), 12–21. https://doi.org/10.3923/jfas.2017.12.21. Science Alert:.

Jenkins, G.P., 1987. Age and growth of co-occurring larvae of two flounder species, *Rhombosolea tapirina* and *Ammotretis rostratus*. Mar. Biol. 95, 157–166.

Jenkins, G.P., 1990. What can growth trajectory tell us about the nutritional state of fish larvae? Australian Government Publishing Service, Canberra. Proc. Bureau Rural Resour. 15, 44–48.

Jenkins, G.P., Davis, T.L.O., 1990. "Age, growth rate, and growth trajectory determined from otolith microstructure of southern Bluefin tuna *Thunnus maccoyii* larvae". Mar. Ecol. Prog. Ser. 63, 12.

Jeyaseelan, M.J.P., 1998. Manual of Fish Eggs and Larvae from Asian Mangrove Waters. United Nations Educational, Scientific and Cultural Organization, Paris, pp. 193.

Kahn, R.G., Pearson, D.E., Dick, E.J., 2004. Comparison of standard length, fork length, and total length for measuring west coast marine fishes. Mar. Fish. Rev. 66, 31–33.

Kawabe, K., Kohno, H., 2009. Morphological development of larval and juvenile Blacktip grouper, *Epinephelus fasciatus*. Fish. Sci. 75, 1239–1251.

Laird, A.K., 1969. The dynamics of growth. Res. Dev. 28–31.

Leu, M.Y., Liou, C.H., Fang, L.S., 2008. Embryonic and larval development of the Malabar grouper, *Epinephelus malabaricus* (Pisces: Serranidae). J. Mar. Biol. Assoc. U.K. 85, 1249–1254.

Lozano, C., Houde, E.D., Wingate, R.L., Secor, D.H., 2012. Age, growth and hatch dates of ingressing larvae and surviving juveniles of Atlantic menhaden *Brevoortiatyrannus*. J. Fish Biol. 81 (5), 1665–1685.

Luthy, S.A., Serafy, J.E., Cowen, R.K., Denit, K.L., Sponaugle, S., 2005. Age and growth of larvalAtlantic Sailfish, *Istiophorus platypterus*". Mar. Freshw. Res. 56, 1027–1035. https://doi.org/10.1071/MF05048.

Maechler, M., Rousseeuw, P., Struyf, A., Hubert, M., Hornik, K., 2017. Cluster: Cluster Analysis Basics and Extensions. R Package Version 2.0.6.

Malca, E., Muhling, B., Franks, J., García, A., Tilley, J., Gerard, T., Ingram, W., Lamkin, J.T., 2017. The first larval age and growth curve for Bluefin tuna (*Thunnus thynnus*) from the Gulf of Mexico: comparisons to the Straits of Florida, and the Balearic Sea (Mediterranean). Fish. Res. 190, 24–33.

Mazerolle, M.J., 2016. AICcmodavg: Model Selection and Multimodel Inference Based on (Q)AIC(c). R Package Version 2.1-0. https://cran.r-project.org/package=AICcmodavg.

Meekan, M.G., Fortier, L., 1996. Selection for fast growth during the larval life of Atlantic cod *Gadus morhua* on the Scotian Shelf. Mar. Ecol. Prog. Ser. 137, 25–37.

Megalofonou, P., Platis, K., De Metrio, G., Santamaria, N., 2002. Age estimation of juvenile Bluefin tuna, *Thunnus thynnus*, from the Mediterranean sea. In: Bridges, C.R., Garcia-Gomez, A., Gordin, H. (Eds.), Domestication of *Thunnus thynnus*: Proceeding of the first international Symposium held at the University of Cartagena. Spain. pp. 108–110.

Moser, H.G., 1996. The early stages of fishes in the California current Region. Calif. Coop. Fish. Invest. Atlas 33 (1), 505.

Palomera, I., Moales-Nin, B., Lleonart, J., 1988. Larval growth of anchovy, *Engraulis encrasicolus*, in the Western Mediterranean Sea. Mar. Biol. 99, 283–291.

Pauly, D., 1981. The relationships between gill surface area and growth performance in fish: a generalization of von Bertalanffy's theory of growth. Berichte der Deutschen Wissenschaftlichen Kommission fur Meeresforschung 28, 251–282.

Pauly, D., 2010. Gasping fish and panting squids: oxygen, temperature and the growth of water-breathing animals. In: Kinne, O. (Ed.), Excellence in Ecology, Book 22. International Ecology Institute, Oldendorf/Luhe.

Pepin, P., 1991. Effect of temperature and size on development, mortality, and survival rates of the pelagic early life history stages of marine fish. Can. J. Fish. Aquat. Sci. 48, 503–518.

Powell, A.B., Tucker, J.W., 1992. Egg and larval development of laboratory-reared Nassau grouper, *Epinephelus striatus* (Pisces, Serranidae). Bull. Mar. Sci. 50, 171–185.

R Core Team, 2015. R: a Language and Environment for Statistical Computing. URL. R Foundation for Statistical Computing, Vienna, Austria. https://www.R-project.org/.

Rae, G., Roman, N.S., Spinoglio, D.E., 1999. Age validation and growth of yolked larvae of *Patagonotothen tessellata* (Richardson, 1845) (Pisces: Nototheniidae) from the rocky littoral of the Beagle Channel, Argentina. Sci. Mar. 63 (SUPPL), 469–476. https://doi.org/10.3989/scimar.1999.63s1469.

Ré, P., Meneses, I., 2008. Early Stages of Marine Fishes Occurring in the Iberian Peninsula. IPIMAR/IMAR (282pp. ISBN-978-972-9372-34-6). .

Richards, W.J., Saksena, V.P., 1980. Description of larvae and early juveniles of laboratory-reared gray snapper, *Lutjanus griseous* (Linneaus) (Pisces, Lutjanaidae). Bull. Mar. Sci. 30, 515–522.

Ricker, W.E., 1979. Growth rates and models. In: Hoar, W.S., Randall, D.J., Brett, J.R. (Eds.), Fish Physiology. Vol VIII Bioenergetics and Growth. Academic Press, Inc, New York, pp. 678–719. Print. Elsevier Science, ProQuest Ebook Central. http://ebookcentral.proquest.com/lib/usf/detail.action?docID=404296.

Riley, C.M., Holt, G.J., Arnold, C.R., 1995. Growth and morphology of larval· and juvenile captive bred yellowtail snapper *Ocyuruschrysurus*. Fish. Bull. (Wash. D. C.) 93, 179–185.

Somers, I.F., 1988. On a seasonally oscillating growth function. Fishbyte 6, 8–11.

Song, Y., Oh, S.R., Seo, J.P., Ji, B.G., Lim, B.S., Lee, Y.D., Kim, H.B., 2005. Larval development and rearing of longtooth grouper *Epinephelus bruneus* in Jeju Island, Korea. J. World. Aquacult. Soc. 36, 209–216.

Song, Y.B., Lee, C.H., Kang, H.C., Kim, H.B., Lee, Y.D., 2013. Effect of water temperature and salinity on the fertilized egg development and larval development of Sevenband Grouper, *Epinephelus septemfasciatus*. Dev. Reprod. 17, 369–377. 1.2-1. https://CRAN.R-project.org/package=minpack.lm.

vonBertalanffy, L., 1938. A quantitative theory of organic growth: inquiries on growth laws II. Hum. Biol. 10, 181–213.

vonBertalanffy, L., 1951. Theoretische Biologie – Zweiter Band: Stoffwechsel, Wachstum. A. Francke Verlag, Bern.

Walters, C.J., Christensen, V., 2007. Adding realism to foraging arena predictions of trophic flow rates in Ecosim ecosystem models: shared foraging arenas and bout feeding. Ecol. Modell. 209, 342–350.

Walters, C.J., Juanes, F., 1993. Recruitment limitation as a consequence of natural selection for use of restricted feeding habitats and predation risk taking by juvenile fishes. Can. J. Fish. Aquat. Sci. 50, 2058–2070.

Zweifel, J.R., Lasker, R., 1976. Prehatch and posthatch growth of fishes - a general model. Fish Bull. U.S. 74, 609–621.